Cartilage Tissue Engineering – Comparison of Articular Cartilage Progenitor Cells and Mesenchymal Stromal Cells in Agarose and Hyaluronic Acid-Based Hydrogels

-

Tissue Engineering von Knorpel – Vergleich von Gelenkknorpel-Vorläuferzellen und mesenchymalen Stromazellen in Agarose- und Hyaluronsäure-basierten Hydrogelen

Doctoral thesis for a doctoral degree
at the Graduate School of Life Sciences,
Julius-Maximilians-Universität Würzburg,
Section Biomedicine

submitted by

Stefanie Schmidt

from

Landsberg am Lech

Würzburg, 2021

Submitted on: ……………………………………………………

Members of the Thesis Committee

Chairperson: Prof. Dr. Carmen Villmann

Primary Supervisor: Prof. Dr. Torsten Blunk

Supervisor (Second): Dr. habil. Jörg Teßmar

Supervisor (Third): Dr. Marietta Herrmann

Date of Public Defence: ………………………………………

Date of Receipt of Certificates: ………………………………

Table of contents

Summary

Articular cartilage damage caused by sports accidents, trauma or gradual wear and tear can lead to degeneration and the development of osteoarthritis because cartilage tissue has only limited capacity for intrinsic healing. Osteoarthritis causes reduction of mobility and chronic pain and is one of the leading causes of disability in the elderly population. Current clinical treatment options can reduce pain and restore mobility for some time, but the formed repair tissue has mostly inferior functionality compared to healthy articular cartilage and does not last long-term. Articular cartilage tissue engineering is a promising approach for the improvement of the quality of cartilage repair tissue and regeneration.

In this thesis, a promising new cell type for articular cartilage tissue engineering, the so-called articular cartilage progenitor cell (ACPC), was investigated for the first time in the two different hydrogels agarose and HA-SH/P(AGE-co-G) in comparison to mesenchymal stromal cells (MSCs). In agarose, ACPCs´ and MSCs´ chondrogenic capacity was investigated under normoxic (21 % oxygen) and hypoxic (2 % oxygen) conditions in monoculture constructs and in zonally layered co-culture constructs with ACPCs in the upper layer and MSCs in the lower layer. In the newly developed hyaluronic acid (HA)-based hydrogel HA-SH/P(AGE-co-G), chondrogenesis of ACPCs and MSCs was also evaluated in monoculture constructs and in zonally layered co-culture constructs like in agarose hydrogel. Additionally, the contribution of the bioactive molecule hyaluronic acid to chondrogenic gene expression of MSCs was investigated in 2D monolayer, 3D pellet and HA-SH hydrogel culture.

It was shown that both ACPCs and MSCs could chondrogenically differentiate in agarose and HA-SH/P(AGE-co-G) hydrogels. In agarose hydrogel, ACPCs produced a more articular cartilage-like tissue than MSCs that contained more glycosaminoglycan (GAG), less type I collagen and only little alkaline phosphatase (ALP) activity. Hypoxic conditions did not increase extracellular matrix (ECM) production of ACPCs and MSCs significantly but improved the quality of the neo-cartilage tissue produced by MSCs. The creation of zonal agarose constructs with ACPCs in the upper layer and MSCs in the lower layer led to an ECM production in zonal hydrogels that lay in general in between the ECM production of non-zonal ACPC and MSC hydrogels. Even though zonal co-culture of ACPCs and MSCs did not increase ECM production, the two cell types influenced each other and, for example, modulated the staining intensities of type II and type I collagen in comparison to non-zonal constructs under normoxic and hypoxic conditions. In HA-SH/P(AGE-co-G) hydrogel, MSCs produced more ECM than

ACPCs, but the ECM was limited to the pericellular region for both cell types. Zonal HA-SH/P(AGE-co-G) hydrogels resulted in a native-like zonal distribution of ECM as MSCs in the lower zone produced more ECM than ACPCs in the upper zone. It appeared that chondrogenesis of ACPCs was supported by hydrogels without biological attachment sites such as agarose, and that chondrogenesis of MSCs benefited from hydrogels with biological cues like HA.

As HA is an attractive material for cartilage tissue engineering, and the HA-based hydrogel HA-SH/P(AGE-co-G) appeared to be beneficial for MSC chondrogenic differentiation, the contribution of HA to chondrogenic gene expression of MSCs was investigated. An upregulation of chondrogenic gene expression was found in 2D monolayer and 3D pellet culture of MSCs in response to HA supplementation, while gene expression of osteogenic and adipogenic transcription factors was not upregulated. MSCs, encapsulated in a HA-based hydrogel, showed upregulation of gene expression for chondrogenic, osteogenic and adipogenic differentiation markers as well as for stemness markers. In a 3D bioprinting process, using the HA-based hydrogel, gene expression levels of MSCs mostly did not change. Nevertheless, expression of three tested genes (COL2A1, SOX2, CD168) was downregulated in printed in comparison to cast constructs, underscoring the importance of closely monitoring cellular behaviour during and after the printing process.

In summary, it was confirmed that ACPCs are a promising cell source for articular cartilage engineering with advantages over MSCs when they were cultured in a suitable hydrogel like agarose. The performance of the cells was strongly dependent on the hydrogel environment they were cultured in. The different chondrogenic performance of ACPCs and MSCs in agarose and HA-SH/P(AGE-co-G) hydrogels highlighted the importance of choosing suitable hydrogels for the different cell types used in articular cartilage tissue engineering. Hydrogels with high polymer content, such as the investigated HA-SH/P(AGE-co-G) hydrogels, can limit ECM distribution to the pericellular area and should be developed further towards less polymer content, leading to more homogenous ECM distribution of the cultured cells. The influence of HA on chondrogenic gene expression and on the balance between differentiation and maintenance of stemness in MSCs was demonstrated. More studies should be performed in the future to further elucidate the signalling functions of HA and the effects of 3D bioprinting in HA-based hydrogels.

Taken together, the results of this thesis expand the knowledge in the area of articular cartilage engineering with regard to the rational combination of cell types and hydrogel materials and open up new possible approaches to the regeneration of articular cartilage tissue.

Zusammenfassung

Gelenkknorpeldefekte, die durch Sportverletzungen, Unfälle oder graduelle Abnutzung entstehen, können zu Degeneration des Gewebes und zur Entstehung von Arthrose führen, da Knorpelgewebe nur über eine eingeschränkte Fähigkeit zur Selbstheilung verfügt. Arthrose reduziert die Beweglichkeit und verursacht chronische Schmerzen. Sie ist vor allem bei älteren Menschen einer der häufigsten Gründe für körperliche Behinderung. Die zurzeit verfügbaren operativen Behandlungsmöglichkeiten können die Symptome meist für einige Zeit lindern, aber das dabei gebildete Ersatzgewebe zeigt meistens nur eingeschränkte Funktionalität im Vergleich zu natürlichem gesunden Knorpelgewebe und bleibt nur für eine begrenzte Zeit stabil. Tissue Engineering von Gelenkknorpelgewebe ist ein vielversprechender Ansatz, um die Qualität des Ersatzgewebes und der Knorpelregeneration zu verbessern.

Diese Arbeit untersuchte einen neuen vielversprechenden Zelltyp für das Tissue Engineering von Knorpelgewebe, sogenannte Gelenkknorpel-Vorläuferzellen (ACPCs). Diese Zellen wurden erstmals in zwei verschiedenen Hydrogelen, Agarose und HA-SH/P(AGE-co-G), mit mesenchymalen Stromazellen (MSCs) verglichen. Die chondrogene Kapazität von ACPCs und MSCs in Agarose wurde unter normoxischen (21 % Sauerstoff) und hypoxischen (2 % Sauerstoff) Bedingungen in Monokultur und zonal geschichteter Kokultur untersucht. In den zonalen Kokulturen befanden sich ACPCs in einer oberen Schicht und MSCs in einer unteren Schicht. In dem neu entwickelten Hyaluronsäure (HA)-basierten Hydrogel HA-SH/P(AGE-co-G) wurde die chondrogene Differenzierung von ACPCs und MSCs ebenfalls in Monokultur und in zonal geschichteter Kokultur, wie im Agarose-Hydrogel, analysiert. Außerdem wurde der Beitrag des biologisch aktiven Moleküls Hyaluronsäure zur chondrogenen Genexpression von MSCs in 2D-, 3D-Pellet- und HA-SH-Hydrogel-Kulturen untersucht.

Diese Arbeit zeigte, dass sowohl ACPCs als auch MSCs in Agarose- und HA-SH/P(AGE-co-G)-Hydrogelen chondrogen differenzieren konnten. ACPCs produzierten im Agarose-Hydrogel ein Gewebe, das dem Gelenkknorpel ähnlicher war als das von MSCs produzierte Gewebe, da es mehr Glykosaminoglykane (GAG), weniger Typ I Kollagen und nur geringe Aktivität der Alkalinen Phosphatase (ALP) aufwies. Hypoxische Bedingungen konnten die Produktion von extrazellulärer Matrix (ECM) durch ACPCs und MSCs nicht erhöhen, aber sie verbesserten die Qualität des von MSCs produzierten Gewebes. Die Herstellung von zonalen Agarose-Konstrukten mit ACPCs in der oberen Schicht und MSCs in der unteren Schicht führte zu einer ECM-Produktion in zonalen Hydrogelen, die im Allgemeinen zwischen der ECM-Produktion

der ACPC-Monokultur und der MSC-Monokultur lag. Zonale Kokultur von ACPCs und MSCs führte zwar nicht zu einer erhöhten ECM-Produktion, allerdings beeinflussten die beiden Zelltypen sich gegenseitig und modulierten zum Beispiel die Intensitäten der Typ II und Typ I Kollagen Färbungen im Vergleich zu Monokulturen unter normoxischen und hypoxischen Bedingungen. Im HA-SH/P(AGE-co-G)-Hydrogel produzierten die MSCs mehr ECM als die ACPCs, allerdings war die Verteilung der gebildeten ECM bei beiden Zelltypen auf den perizellulären Bereich beschränkt. Zonale HA-SH/P(AGE-co-G)-Hydrogele führten zu einer zonalen Verteilung von ECM, die der natürlichen Struktur von Gelenkknorpel ähnlich war, da die MSCs in der unteren Schicht mehr ECM produzierten als die ACPCs in der oberen Schicht. Anscheinend wurde die chondrogene Differenzierung von ACPCs von Hydrogelen unterstützt, die, so wie Agarose, keine biologischen Bindestellen aufwiesen, und die Chondrogenese von MSCs profitierte von Hydrogelen mit biologischen Signalen wie HA.

Da HA ein attraktives Material für Tissue Engineering von Knorpel darstellt und das HA-basierte Hydrogel HA-SH/P(AGE-co-G) anscheinend die chondrogene Differenzierung von MSCs begünstigte, wurde der Beitrag von HA zur chondrogenen Genexpression in MSCs untersucht. Eine Hochregulation der chondrogenen Genexpression ließ sich in 2D- und 3D-Pellet-Kulturen von MSCs als Reaktion auf HA beobachten, während die Genexpression von osteogenen oder adipogenen Transkriptionsfaktoren nicht hochreguliert wurde. Der Einschluss von MSCs in einem HA-basierten Hydrogel führte zu einer Erhöhung der Genexpression von chondrogenen, osteogenen, adipogenen und Stemness-Markern. Ein 3D-Druck-Prozess mit dem HA-basierten Hydrogel veränderte die Genexpression von MSCs in den meisten Fällen nicht. Dennoch wurde die Expression von drei getesteten Genen (COL2A1, SOX2, CD168) in gedruckten im Vergleich zu gegossenen Konstrukten herunterreguliert. Dies unterstrich die Wichtigkeit einer genauen Kontrolle des Verhaltens der Zellen während und nach dem Druck-Prozess.

Zusammenfassend ließen sich ACPCs als vielversprechender neuer Zelltyp für das Tissue Engineering von Gelenkknorpelgewebe bestätigen. ACPCs haben Vorteile gegenüber MSCs, vor allem, wenn sie in einem passenden Hydrogel wie Agarose kultiviert werden. Die Leistung der Zellen war stark von den verschiedenen Hydrogelen und der Umgebung beeinflusst, die diese den Zellen darboten. Die unterschiedliche chondrogene Leistung von ACPCs und MSCs in Agarose- und HA-SH/P(AGE-co-G)-Hydrogelen zeigte deutlich die übergeordnete Relevanz der Auswahl von passenden Hydrogelen für die verschiedenen Zelltypen, die im Tissue Engineering von Gelenkknorpel Verwendung finden. Hydrogele mit einem hohen Polymergehalt,

wie das eingesetzte HA-SH/P(AGE-co-G)-Hydrogel, können die Verteilung der gebildeten ECM auf den perizellulären Bereich beschränken und sollten weiterentwickelt werden, um einen niedrigeren Polymergehalt und damit eine homogenere ECM-Verteilung durch die kultivierten Zellen zu erreichen. Der Einfluss von HA auf die chondrogene Genexpression und auf die Balance zwischen Differenzierung und Erhaltung der Stemness in MSCs ließ sich aufzeigen. In Zukunft sollten weitere Studien die Signalfunktionen von HA und den Einfluss des 3D-Drucks in HA-basierten Hydrogelen genauer zu untersuchen.

Zusammengenommen erweitern die Ergebnisse dieser Arbeit das Wissen im Bereich des Tissue Engineerings von Gelenkknorpelgewebe, vor allem in Bezug auf eine rationale Kombination von Zelltypen und Hydrogel-Materialien, und eröffnen neue Ansätze zur Knorpelregeneration.

Introduction

1 Introduction

1.1 Articular cartilage

There are three different types of cartilage in the human body: Elastic cartilage, fibrocartilage, and hyaline (articular) cartilage. Elastic cartilage contains much elastin and is a flexible sort of cartilage that can be found in non-load bearing body parts like the auricle [1]. Fibrocartilage contains thick collagen fibres and is the only cartilage that contains type I collagen additionally to type II collagen in its mature state. An example for fibrocartilage is the meniscus [2]. Hyaline articular cartilage is a connective tissue that covers articulating surfaces of bone in synovial joints, such as the knee or the hip [3,4].

1.1.1 Structure of synovial joints and function of articular cartilage

Articular cartilage covers the contacting surfaces of the two bones in synovial joints (Figure 1). The cartilage on the bones´ ends prevents friction and grinding of the bones when the joint is moved [5].
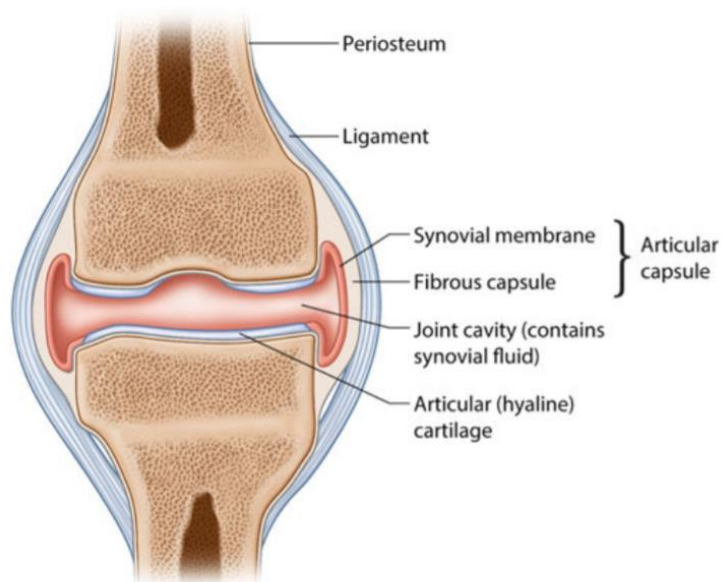
Figure 1: Synovial joint. Articular cartilage on the ends of the articulating bones acts as buffer against loads and forces that act on the joint. The articular capsule is composed of the synovial membrane and a fibrous capsule. The articular joint capsule contains synovial fluid that is produced by the cells of the synovial membrane. Reprinted by permission from Springer Nature Customer Service Centre GmbH: *Monaghan, N.G.; Wyss, J.F. Joint Pain. In Pain Management and Palliative Care: A Comprehensive Guide, Sackheim, K.A., Ed. Springer New York: New York, NY, 2015; 10.1007/978-1-4939-2462-2_19pp. 131-140.* [6] © Springer Science+Business Media New York 2015.

The joint cavity is filled with synovial fluid that is produced by cells of the synovial membrane. The synovial membrane surrounds the joint cavity and the articulating bone surfaces and keeps the synovial fluid in the joint capsule (Figure 1). Synovial fluid has two main functions. It contributes to further reduction of friction between the joint bones as it is a thick, lubricating fluid. Additionally, it provides nutrients for chondrocytes, the resident cells in articular cartilage, as cartilage does not have a blood supply [3]. The fluid is squeezed out of the tissue when the joint is loaded and flows back in with fresh nutrients when the pressure is gone. The main function of articular cartilage in a joint is to provide smooth movement of the bones´ ends against each other and to withstand and buffer the loads and forces that act on a weight-bearing joint like the knee [3,5].

1.1.2 Articular cartilage composition and structure

Hyaline articular cartilage is a tissue with low cell density. Chondrocytes, the resident cells, have no direct contact with each other and amount to only 2 % of the total cartilage volume. The tissue also has no blood or lymphatic vessels and no innervation [4,5]. Extracellular matrix (ECM) that is produced by chondrocytes makes up the largest part of articular cartilage. Its main components are water, collagens and proteoglycans. Type II collagen is with 90-95 % the main collagen in articular cartilage and forms a fibril network that is stabilized by less abundant collagens (types I, IV, V, VI, IX and XI). Proteoglycans are proteins that carry one or several chains of glycosaminoglycans (GAGs). Glycosaminoglycans are long linear chains of repeating disaccharides, for example chondroitin sulfate, keratan sulfate or hyaluronic acid. The most prominent proteoglycan in articular cartilage is aggrecan. Aggrecan carries over 100 glycosaminoglycan chains, mainly chondroitin sulfate but also keratan sulfate. This already large proteoglycan forms huge aggregates with hyaluronic acid through non-covalent bonds and the stabilizing function of the link protein. These aggregates draw water into the tissue because they contain many negatively charged residues that draw counter-ions, and they provide a hydrated gel like structure. The water is pressed out of the tissue during loading of the joint and seeps back in after relieving the load. Intertwined collagens and proteoglycans form a gel-like network that is viscoelastic and resilient and provides the tensile (type II collagen) and compressive (aggrecan) strength of cartilage tissue that is needed to withstand the continuous loads and shear forces that synovial joints are exposed to [3-5].

Another factor that is thought to be important for the long-lasting biomechanical function of cartilage tissue is its zone-like structure. Articular cartilage is composed of three different zones, the superficial zone, the middle zone, and the deep zone that form during postnatal growth from the isotropic neonatal tissue [7]. The zones differ regarding cell morphology and expression patterns and therefore also in ECM composition and arrangement.
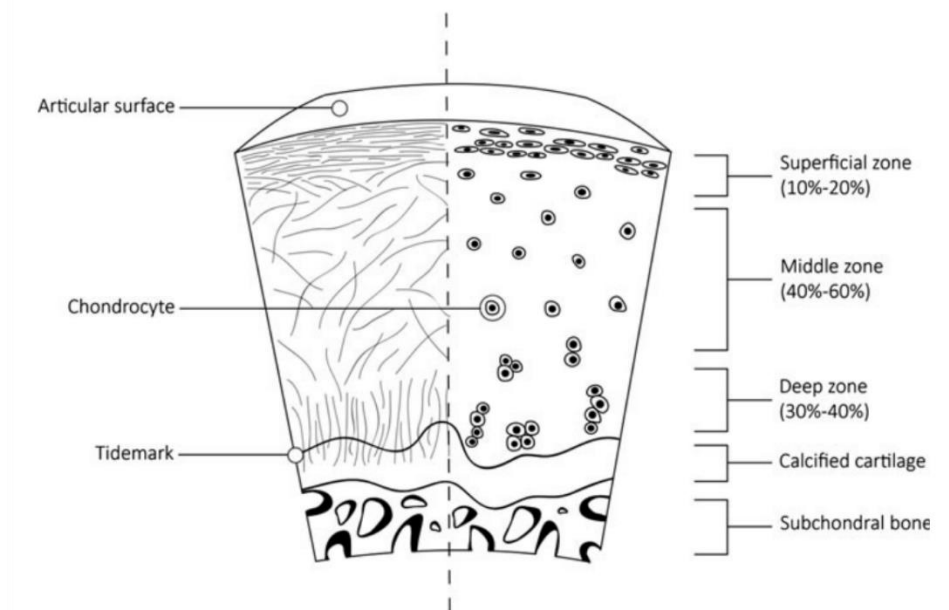
Figure 2: Schematic representation of articular cartilage and its zonal structure. The superficial zone of articular cartilage contains flattened chondrocytes that are oriented parallel to the articular surface (right half of the figure). The collagen fibres in this zone are also oriented parallel to the cartilage surface (represented by the lines in the left part of the figure). The middle zone contains round chondrocytes (right half of the figure) and randomly oriented collagen fibres (left part of the figure). The deep zone contains large round chondrocytes that are arranged in vertical columns (right half of the figure). The collagen fibres are oriented parallel to the chondrocyte columns in this zone and reach into the calcified zone (left half of the figure). The tidemark is the border between the deep zone and calcified cartilage. Calcified cartilage is a transition zone between cartilage and subchondral bone. Reprinted by permission from Springer Nature Customer Service Centre GmbH: *Ondrésik, M.; Oliveira, J.M.; Reis, R.L. Knee Articular Cartilage. In Regenerative Strategies for the Treatment of Knee Joint Disabilities, Oliveira, J.M., Reis, R.L., Eds. Springer International Publishing: Cham, 2017; 10.1007/978-3-319-44785-8_1pp. 3-20.* [8] © Springer International Publishing AG 2017.

The superficial zone contains a relatively high amount of small, flattened, elongated chondrocytes that are oriented parallel to the cartilage surface as are the collagen fibres of this zone (Figure 2). Type II collagen content is highest in this zone, while proteoglycan content is lowest. Additionally, superficial chondrocytes produce the lubricating proteoglycan 4 (PRG4) that contributes to the low-friction characteristics of articular cartilage surface. The middle zone represents 40-60 % of the total articular cartilage volume and contains round chondrocytes at a lower cell density than in the superficial zone (Figure 2). This zone has a

high content of proteoglycans and type II collagen fibres, and the collagen fibres are randomly arranged. Middle and deep zone are mainly responsible for resistance to compressive forces. The deep zone contains circa 30-40 % of total cartilage volume and has the highest concentration of proteoglycan and collagen. Chondrocytes from the deep zone are large and round and arranged in vertical columns (Figure 2). Collagen fibres are organized parallel to these chondrocyte columns, reach into the calcified layer and thereby attach cartilage to bone. The tidemark represents the border between deep cartilage and calcified layer. The calcified layer serves as a transition between cartilage and bone, and the chondrocytes it contains are hypertrophic and express hypertrophy markers like collagen type X or alkaline phosphatase (ALP) [4,5,7].

1.1.3 Articular cartilage defects and clinical treatments

Cartilage is a complex and highly specialized tissue that can withstand great mechanical forces and cyclic loading without being damaged [5,9]. However, when load limits are breached for example by a sports accident or a traumatic injury, cartilage tissue can be damaged. Another frequent cause of cartilage damage is wearing down the tissue over many years which is often the case in older patients. Due to its composition, especially the lacking blood supply, cartilage tissue has a limited capacity for self-regeneration [4,5]. Therefore, injuries mostly do not heal by themselves and can evolve into osteoarthritis (OA), a degenerative disease of cartilage that can lead to pain and disability [10,11]. OA is the most common joint disease worldwide and circa 10 % of men and 18 % of women suffer from it [12]. Hip and knee OA was even ranked one of the main contributors to global disability [13]. In the end-stage of the disease, artificial joint replacement is the last option for patients. However, there are clinical treatments for repair of beginning or less severe cartilage injuries. Additionally, much research is done with the goal to someday reproduce normal healthy articular cartilage tissue for cartilage defects.

One of the most used clinical treatments is microfracture, a bone marrow stimulation technique. Microfracture is a simple, fast and inexpensive way to treat small cartilage defects. In this minimally invasive procedure, holes are made into subchondral bone to stimulate the bone marrow to flow into the cartilage defect and form a blood clot containing mesenchymal stem cells. These cells form fibrocartilaginous tissue to close the defect. That leads to pain reduction in patients and is stable for several years, however, this tissue often is

biomechanically inferior to hyaline cartilage, and the use of microfracture is mostly limited to defects smaller than 2-4 cm^2 [14-16].

Another clinical approach for small (< 4 cm^2) cartilage defects is Osteochondral Autograft Transfer (OAT). Osteochondral plugs are harvested from non-weight bearing cartilage of the patient and transplanted directly in the defect. Donor site morbidity can be a problem with this technique because new tissue defects are being introduced [15,17].

For larger defects, Osteochondral Allograft Transfer (OCA) can be used. Instead of transplanting the patient's own tissue, fresh grafts from another person are used. Tissue availability and graft failure are main problems of this treatment. OAT and OCA provide mature cartilage tissue for the treated defect that can bear loads earlier after surgery and thereby reduce the recovery time in comparison to other surgical treatments [15,18].

PACI (particulate articular cartilage implantation) is mostly used for smaller defects. For this method, autologous or allogeneic cartilage is being crushed into small particles and then implanted into the cartilage defect. Long-term follow up data are needed for this method to rigorously evaluate its promising results [19].

A cell-based method for treating large (> 4 cm^2) cartilage defects is autologous chondrocyte implantation (ACI). For this treatment, the patient´s own chondrocytes are harvested from non-weight-bearing regions of the joint, expanded *in vitro* for four to six weeks and then re-implanted into the cartilage defect. ACI has led to hyaline-like cartilage production that was stable for several years also in larger defects. However, the biggest disadvantages are long recovery times and the two needed surgeries that lead to higher costs and increased burden for the patient [15,16,20,21].

However, none of the currently known surgical techniques can consistently and completely regenerate hyaline articular cartilage tissue. Additionally, incomplete defect filling and poor integration with the surrounding tissue can lead to failed regeneration. One step to improve the outcome of cartilage defect treatments was to introduce the use of scaffolds [16]. Scaffolds can be used in combination with cells or alone and give the implant more stability from the beginning. They provide an easier way to implant cells and can additionally promote desired cell behaviour and instruct and organize development and distribution of ECM [22]. Scaffold-plus-chondrocytes approaches are called MACT (matrix assisted chondrocyte transplantation) and are tissue engineered treatment options for the clinic. BioSeed®-C, CaReS® and NOVOCART® 3D are three examples that are already available in some European countries [19,23]. BioSeed®-C (BioTissue Technologies GmbH, Freiburg, Germany) uses expanded autologous chondrocytes like ACI. Autologous serum is used as a

stimulus for expanding cells. The scaffold is a polyglactin 910/poly-p-dioxanone fleece that is seeded with the expanded chondrocytes suspended in fibrin glue. The implant can be sutured or glued into the cartilage defect [23]. CaReS® (Arthro Kinetics Biotechnology, Krems, Austria) uses a type I collagen hydrogel as cell carrier and primary autologous chondrocytes. After cells are embedded in the hydrogel, they are cultured *in vitro* for 10-13 days. Autologous serum is used as stimulus in that time. Then the construct can be implanted [19,23]. NOVOCART® 3D (TETEC AG, Reutlingen, Germany) is a biphasic construct that is seeded with P1 autologous chondrocytes. Therefore, isolated cells are expanded in 2D until they reach confluence and are then seeded in the scaffold. One layer of the scaffold is a dense collagen-based membrane that cells cannot pass, and the other layer is a porous sponge consisting of type I collagen and chondroitin sulfate that is carrying the cells [19,23,24]. Those tissue engineered approaches showed promising results in their clinical studies, but the formed tissue was often partially fibrocartilaginous, and the results were often not consistent between individuals or studies [19,25-30].

Summing up, despite many improvements, innovations and research that have happened in the field of cartilage regeneration over the last 20 years, we are still looking for a way to restore native articular cartilage function completely. There is still a lot that we do not know, and careful, yet innovative research is still needed to improve clinical therapy. Tissue engineering still appears to be the method of choice for cartilage repair. Several important aspects that are critical for the successful engineering of cartilage tissue have been identified and are presented in the following section of the introduction. Consideration of these aspects in cartilage engineering has been suggested to lead to improvement of the regeneration of articular cartilage tissue.

1.2 Important aspects of articular cartilage tissue engineering

The combination of cells, scaffolds and additional growth factors or other signals with the aim to produce native-like cartilage tissue is the basic principle of cartilage tissue engineering [22] (Figure 3). As tissue engineering opens up so many new possibilities it has become one of the most promising methods for long-term cartilage tissue regeneration.

In the following, several important aspects that should be considered for improving cartilage tissue engineering are presented.
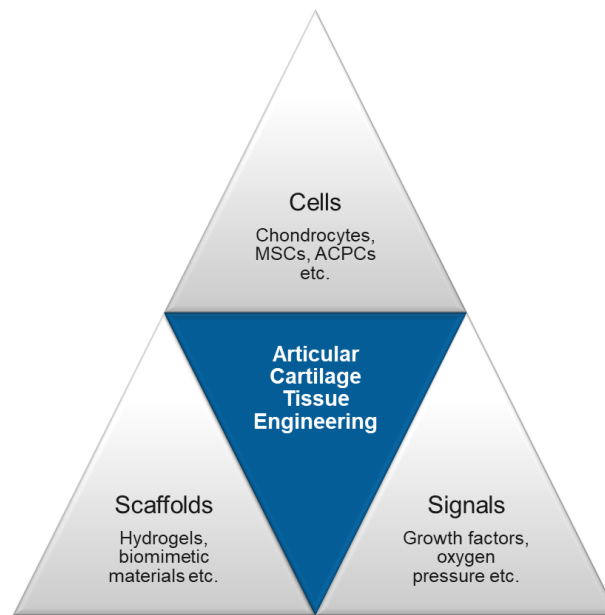
Figure 3: Triad of articular cartilage engineering. Cells, scaffolds, and additional signals form the triad of articular cartilage engineering. These three factors and their interplay are the basic principle of tissue engineering.

1.2.1 Different cell sources

Chondrocytes

One particularly important point for articular cartilage tissue engineering is the choice of cell type. The obvious choice would be chondrocytes, as those are the cells that are resident in normal healthy cartilage and that can produce proper articular cartilage ECM in the defect. Most of the above-described cell-based clinical therapies are using chondrocytes. However, there are two main problems regarding the use of these cells. For one, when autologous chondrocytes are employed, a new defect has to be created in order to harvest suitable cells. Those new defects are introduced into non-weight bearing parts of the tissue,

but the risk of donor site morbidity is still an issue [31]. Only small parts of cartilage can be harvested to avoid too much damage, and therefore, the harvested chondrocytes have to be expanded *in vitro* in 2D culture. This results in the second problem, as chondrocytes tend to dedifferentiate when they are expanded in 2D [32,33]. When chondrocytes dedifferentiate, they lose their ability to produce and maintain healthy articular cartilage ECM. This results often in the production of biomechanically inferior fibrocartilage. It has been shown that chondrocytes can maintain their chondrogenic phenotype better when they are cultured in 3D [32,34], but then harvested cells cannot be expanded as much as in 2D culture.

MSCs

Mesenchymal stromal cells (MSCs) on the other hand can be differentiated into chondrocyte-like cells *in vitro* [35-37]. They can be expanded in 2D without losing their chondrogenic differentiation potential like chondrocytes. Therefore, MSCs are a promising alternative cell source for articular cartilage repair strategies. MSCs can be isolated from different tissues, for example bone marrow, adipose tissue, synovium or umbilical cord blood [38,39]. Human MSCs have to fulfil at least three minimal criteria, according to The International Society for Cellular Therapy: They have to adhere to plastic surfaces, carry the surface antigens CD73, CD90 and CD105, while they do not carry the surface antigens CD14, CD19, CD34, CD45 and HLA-DR, and they have to be able to differentiate in the chondrogenic, adipogenic and osteogenic direction [40].

In recent years, MSCs have received increasing attention in cartilage regenerative medicine. Autologous and allogeneic MSCs have been used for injection into the joint with or without additional substances [41-56] especially for the treatment of osteoarthritis. The results of these studies were promising regarding pain relief in patients but were controversial regarding regeneration of articular cartilage [54,55]. More standardized studies and comparisons would be needed to fully reveal the potential of injected MSCs [54,57]. Recently, several studies could show that extracellular vesicles, so-called exosomes, that are produced by MSCs are responsible for the positive effects on injured and inflamed cartilage tissue, and that the main course of action of injected MSCs in the joint is a paracrine one [58-60]. This is a promising application for MSCs and their exosomes in cartilage regeneration, additionally to their use in cartilage tissue engineering. MSCs also have been implanted into cartilage defects with or without a scaffold in several studies [53-56,61-69]. Nejadnik et al. could, for example, show that the implantation of MSCs led to similar results as common ACI with chondrocytes [61]. However, the results differed between the studies. Most showed improvement compared to controls, but the quality of the formed tissue varied

between fibrocartilage and hyaline-like cartilage [56]. For this treatment, as for the injection of MSCs into the joint, more comparable studies, also long-term follow-ups, are needed to evaluate the full potential of these therapeutical approaches.

MSC-based articular cartilage tissue engineering is additionally limited. Several studies have shown that especially MSCs from the bone marrow (BMSCs) that are often used for cartilage regeneration tend to form hypertrophic cartilage when differentiated in common *in vitro* chondrogenic culture systems [35,70,71]. That can lead to endochondral ossification of the tissue. It has been proposed that these bone-marrow-derived MSCs follow a natural line of differentiation and form only transient cartilage tissue that then progresses towards the formation of bone [70,72], similar to the longitudinal growth of long bones or bone fracture healing. However, in the regeneration of cartilage tissue, this process is highly undesirable as bone tissue of course cannot fulfil the functions of healthy articular cartilage. Common markers for hypertrophy and endochondral ossification are type X collagen, alkaline phosphatase (ALP), matrix metalloproteinase 13 (MMP13), runt-related transcription factor II (RUNX2) and increased volume of the cells [71,73,74]. There are several approaches to control the differentiation of MSCs and to steer it towards a more stable chondrogenic phenotype, for example by co-culture with chondrocytes [75-78], low oxygen tension (hypoxia) [79-82], scaffolds [83-85], inhibition or activation of signalling pathways [86-88] or changes in *in vitro* differentiation protocols [89,90].

Due to the difficulties with chondrocytes and MSCs for articular cartilage tissue engineering, there is an ongoing search for alternative promising cell sources. Induced pluripotent stem cells (iPSCs) or embryonic stem cells (ESCs) have been used, but high costs, tumorigenicity and the ethical problems associated with ESCs have limited their use in cartilage regeneration so far [19,72,91].

ACPCs

However, some years ago, chondroprogenitor cells were detected in articular cartilage [92,93]. These cells, also called articular cartilage progenitor cells (ACPCs), are a subpopulation of chondrocytes that reside mostly in the superficial layer of articular cartilage [93]. ACPCs can differentiate into chondrogenic, osteogenic and adipogenic direction [92,94]. Alsalameh et al. isolated them from cartilage tissue by selecting cells that were positive for CD105 and CD166. The co-expression of these two surface markers was proposed to define a bone-marrow-derived mesenchymal stem cell population [92,95]. Dowthwaite et al. isolated ACPCs from the superficial layer of articular cartilage using differential adhesion to serum fibronectin and a high colony forming efficiency after an initially low cell seeding

density [93]. Other isolation methods of cartilage progenitor cells have also been used after their discovery by different groups [96-99]. Unfortunately, it has not been possible to define one specific marker for ACPC identification yet, and differently isolated progenitor cells are probably not the same cell populations [100]. The present work focuses mostly on ACPCs that were identified, isolated and characterized in the way the Archer group established in their previous work [93,94,101].

Interestingly, when *in vitro* monolayer expansion of ACPCs and normal chondrocytes was compared, it was found that ACPCs could still form cartilage in high-density pellet culture after 30 population doublings, while chondrocytes were defined as dedifferentiated after only 21 population doublings. Additionally, ACPCs showed longer telomere-length at 22 population doublings than chondrocytes at 21 population doublings. Telomerase activity in ACPCs was 2,6-fold higher than in freshly isolated chondrocytes, while dedifferentiated chondrocytes showed no detectable telomerase activity at all [101]. The maintenance of telomere length indicated the stem cell or progenitor character of ACPCs [94]. Clonally derived ACPCs also maintained SOX9 expression after monolayer expansion of up to 45 population doublings, while chondrocytes usually lose SOX9 expression due to dedifferentiation after only a few population doublings [94,101]. Several studies have also shown that ACPCs seem to form cartilage tissue without tendencies towards hypertrophy or endochondral ossification [94,102,103]. These findings make ACPCs a promising cell type for cartilage tissue engineering, as they can be expanded in 2D culture to achieve enough cells, do not lose their chondrogenic potential during monolayer expansion, and form stable cartilage tissue without the risk of endochondral bone formation. There have been several animal studies and even one pilot clinical study in humans to test performance of ACPCs in cartilage tissue repair [94,98,104-106]. The number of studies is of course still limited, and no final conclusion can be drawn from them. However, the first results were promising as it could be shown that ACPCs were able to repair a cartilage lesion in a goat model with similar results as the current gold-standard chondrocytes [94], that autologous ACPCs outperformed fibrin-only constructs in an equine cartilage defect model [104] and that ACPC-scaffold constructs formed cartilage-like tissue without chondrogenic induction when they were implanted subcutaneously into nude mice [105]. In the latter study, the compare-group with bone marrow derived stem cells became vascularized after six weeks [105]. In another study, allogeneic ACPCs were injected intraarticularly together with hyaluronic acid, using a rabbit knee model. This treatment had no adverse effects but did not yield better results than a treatment with hyaluronic acid only [106]. In the pilot clinical study in humans,

ACPC implantation (MACT procedure) was performed in 15 patients. The results were promising, as no graft failures occurred and after one year, all patients reported good quality of life and no moderate or severe limitations. The study results were judged by the authors to be similar or better than previously reported results from chondrocyte implantations [98]. The number of studies comparing chondrogenesis of ACPCs and MSCs directly in hydrogels for cartilage tissue engineering is also limited [103,107]. Levato et al. compared ACPC-hydrogel constructs for the first time with MSC- and chondrocyte-hydrogel constructs. The used hydrogel was gelatin methacryloyl (GelMA), derived from porcine gelatin. Cells were chondrogenically differentiated as monocultures or zonally layered co-cultures in the hydrogel. ACPCs outperformed chondrocytes but not MSCs regarding cartilage ECM production but showed significantly lower levels of type X collagen than the other cell types. Co-culture of MSCs and ACPCs yielded the highest glycosaminoglycan amount in comparison to the other co-cultures [103]. Mouser et al., from the same research group, tested chondrogenesis of ACPCs, MSCs and chondrocytes against each other in two GelMA-based hydrogels: GelMA/gellan and GelMA/gellan/HAMA [107]. The results were similar to the previous study [103] with ACPCs outperforming chondrocytes but not MSCs. A zonally layered construct with ACPCs in the upper and MSCs in the lower zone was 3D bio-printed and successfully chondrogenically differentiated, but the printing process decreased the quality of the formed ECM [107]. However, these studies show only the beginning use of ACPC in cartilage repair. There is still a lot that we do not know about this promising cell type, and further research studies are needed to fully characterize the potential of ACPCs in articular cartilage tissue engineering.

1.2.2 Oxygen partial pressure

As was described before, articular cartilage does not have a blood supply. Oxygen is usually transported to the organs in the body via vasculature, and the oxygen partial pressure is specifically adapted to the needs of the specific organs [108,109]. The levels of oxygen in the body are lower than those in the air (21 %) [109]. Cartilage tissue gets oxygen the same way it gets nutrients, via the synovial fluid that is pressed out and flows into the tissue when the joint is loaded and unloaded. Synovial fluid itself is relatively hypoxic, and therefore, physioxia (the physiological oxygen partial pressure) in cartilage tissue lies between 1 and 5 % [110-112]. This chronically low oxygen pressure strongly influences development and integrity of native articular cartilage [113,114]. Cells can sense the level of oxygen in their

surroundings and can respond to it with different actions. This is mediated mainly by the hypoxia inducible factors (HIFs) HIF-1α and HIF-2α. When oxygen pressure is high, HIF-α subunits are hydroxylated by specific prolyl hydroxylases that need oxygen for this procedure. As result of this hydroxylation, HIF-α subunits are degraded by the proteasome. However, when oxygen levels are low, hydroxylation is inhibited by the lack of oxygen and HIF-α is not degraded. Instead, it forms heterodimers with the constitutively expressed HIF-β. These heterodimers translocate to the nucleus and activate the transcription of specific hypoxia responsive elements (HREs) that can, for example, regulate survival and metabolism in cartilage [115,116].

Despite the important roles of hypoxia in native cartilage, many *in vitro* tissue engineering studies are performed under 21 % oxygen that represent hyperoxic conditions for normal articular cartilage and chondrocytes and can influence the results in unwanted ways [109]. Therefore, oxygen partial pressure that is relevant for *in vivo* situations is an aspect in cartilage tissue engineering that should be considered. It has been shown that using hypoxic (for cartilage physioxic) oxygen partial pressure (1-5 %) instead of normoxic air conditions (21 %) can have beneficial effects on the performance of the cells restoring cartilage tissue. There are several studies that report an increase in matrix deposition and a downregulation of catabolic factors in isolated and passaged (dedifferentiated) chondrocytes by hypoxia in contrast to normoxic air conditions [115,117-121].

Additionally, low oxygen tension can have beneficial effects on the differentiation of MSCs towards cartilage tissue. An increase in chondrogenic gene expression and matrix deposition in hypoxia-differentiated MSCs (in pellets or scaffolds) has been reported several times [81,122-128]. However, there are also studies that found no effect of hypoxia on chondrogenic gene expression [129] or matrix production [130-132]. It was suggested by Anderson et al. [133] that donor variability might play a role in these contradictory results. They found that MSCs with low chondrogenic capacity in normoxia showed a stronger reaction to hypoxia with upregulation of chondrogenic markers than MSCs with initially high chondrogenic capacity in normoxia [133].

When MSCs are chondrogenically differentiated, hypoxia can steer their phenotype to a more permanent articular cartilage by inhibiting hypertrophy and thereby avoiding the more growth plate-like cartilage phenotype that can result in endochondral ossification in the tissue. Several studies have shown downregulation of hypertrophy markers in MSC derived cartilage tissue formed under hypoxic compared to normoxic conditions [81,82,130,134]. There are hints that this could be a similar process than in embryonic limb development as

there is an oxygen gradient with lower oxygen levels where permanent articular cartilage is developing and higher oxygen levels (because of beginning vascularisation) where transient cartilage is undergoing hypertrophy and endochondral ossification [81].

Considering the possible modulating influences of hypoxic cell culture, it becomes clear that the oxygen partial pressure is an important factor that should be considered in cartilage tissue engineering.

1.2.3 Zonal structure

Native articular cartilage contains three distinct zones, the superficial zone, the middle zone and the deep zone, as was described before. Cell morphology and gene expression as well as matrix composition are distinct between the zones. The biomechanical function of articular cartilage is strongly correlated with its zonal architecture [5,135,136]. The lack of this specific zonal structure in repair tissue is suggested to be one of the main reasons for insufficient cartilage regeneration of most treatments currently available [137,138]. Therefore, research has been trying to recapitulate a zonal organization that is similar to native articular cartilage structure. The aim was to mimic some of the properties that make native zonal cartilage more stable than non-zonal repair tissue [136,137]. Several approaches have been employed to isolate chondrocytes from distinct zones and to use them to build up tissue engineered zonal constructs [136,139-142]. Compared to constructs with non-zonal, full-thickness isolated chondrocytes, zonal constructs showed similar or higher matrix production and biomechanical properties [141,142]. However, the use of zonally isolated chondrocytes for reconstruction of zonal constructs is limited because it is difficult to isolate clinically relevant cell numbers and to obtain pure zonal chondrocyte populations with the current methods [136]. Different other cell types (for example MSCs or ACPCs) were suggested and used for the generation of different zones in combination with or as alternative for chondrocytes [103,107,136-138]. Similar to general tissue engineering of articular cartilage, approaches with and without scaffolds and materials were investigated, each with their own advantages and disadvantages [137]. Other approaches are working with different materials and physical or chemical gradients that can influence the encapsulated cells or have zonal properties in themselves [137,143-146]. The layered osteochondral structure may also be reproduced by zonal tissue engineering [136,147,148].

Biofabrication and 3D bioprinting have established themselves in the generation of zonal tissue engineered constructs as they provide the possibility to deposit different materials

and/or cells as specific structures and layer by layer. Even complex, personalized implant structures may be produced this way [103,136,137,149,150]. However, the effects of the printing process on the used cells should be evaluated as cells are exposed to shear forces when they are printed. At high shear forces, cells can be harmed and killed. However, when cells survive the printing process, they can still be changed afterwards. For example, it has been shown before that the 3D bioprinting process can alter the gene expression profile of MSCs [107]. Therefore, it has to be made sure that the printing process does not affect the used cells in unwanted ways.

In principle, zonal tissue engineering for articular cartilage is a promising approach for better functional repair tissue but much research is still needed to find the optimal conditions to produce a tissue that mimics native zonal structure and function of cartilage.

1.2.4 Scaffold material

One main aspect of tissue engineering is the material that is used to encapsulate or carry the cells. General requirements for materials that are used in tissue engineering are biocompatibility, biodegradability, suitable mechanical properties and permeability so that oxygen, nutrients and waste can diffuse in and out of the scaffold [151,152]. Not all materials that are used in *in vitro* experiments for tissue engineering fulfil all these requirements but for an application *in vivo* they are very important. The used material determines the microenvironment and the mechanical, physicochemical and biological conditions that the cells experience in the tissue engineered construct. As cells are strongly influenced by their surroundings, it is important to choose a suitable material for the used cells and the intended purpose. In the case of articular cartilage tissue engineering, this may be achieved by using materials that mimic natural articular cartilage [153]. Scaffolds for cartilage engineering have been made of natural, synthetic or hybrid (natural/synthetic) materials, and they have been used as microporous scaffolds or hydrated polymeric networks (hydrogels) [151,153]. Hydrogels are often used for engineering cartilage tissue because they can provide the cells with an environment of high-water content that is similar to native articular cartilage [154]. Nature-derived materials are for example agarose, alginate, hyaluronic acid, chitosan or collagen. Agarose and alginate are natural polysaccharides. Agarose can be obtained from red seaweed and alginate from brown algae [155]. Agarose is used as thermo-responsive hydrogel that gels at low temperatures and is fluid at higher temperatures. Alginate hydrogels can be formed by the addition of divalent cations, such as Ca^{2+} [156]. Agarose and

alginate do not have any biological cues like integrins or other binding sites for cells and are therefore called inert hydrogels [157]. However, they still provide the cells with an environment that is similar to articular cartilage matrix and support the spherical shape of mature chondrocytes. This is thought to be beneficial for the development of articular cartilage [32,157,158]. Other natural materials like hyaluronic acid, chondroitin sulfate, chitosan or collagen are based on molecules that naturally occur in cartilage tissue as part of the ECM. These materials are used to improve chondrogenicity of encapsulated cells by mimicking their natural environment or by providing biological cues for chondrogenic differentiation [151,153,157]. Chitosan, a derivative of chitin, is a polysaccharide that is not part of the human native cartilage but is chemically similar to GAG and can enhance the deposition of cartilage ECM [151,159]. Collagen is a main component of cartilage ECM, and different scaffolds and hydrogels are derived from it, for example gelatin or GelMA but also constructs consisting of type I, type II and/or type III collagen [153,160]. Gelatin is obtained through hydrolysis of collagen, and GelMA is methacrylated gelatin [155,161]. Collagens can contribute to cell adhesion, proliferation and differentiation and have integrin binding sites all of which can be beneficial for cartilage ECM formation [152,155,162]. Chondroitin sulfate is a GAG that naturally occurs in human cartilage tissue and can be used in scaffolds for articular cartilage engineering [153,163]. Hyaluronic acid (HA) is an abundant polysaccharide in articular cartilage tissue and has important functions as signalling molecule for the cells. It has been shown that addition of HA to scaffolds can enhance the production of articular cartilage ECM [164,165]. Modification and/or mixture and blending of different hydrogel materials is often performed to achieve better biological, biomechanical or crosslinking properties.

In addition to natural materials, synthetic polymers like polyethylene glycol (PEG), polylactic acid (PLA), polycaprolactone (PCL) or polyglycidol (PG) have been used in cartilage tissue engineering [150,152,153,161,166]. They have more clearly defined characteristics, are easy to produce and their properties can be fine-tuned more easily than in natural materials. Chemical modifications can easily be introduced for different crosslinking modes or to attach biological factors [152,166-168]. PCL is often used together with natural materials to enhance and tailor mechanical stiffness and to increase shape stability in 3D bioprinting approaches [149,164,169]. PEG, PG and their derivatives are often used as hydrogels, and crosslinking with natural polymers like hyaluronic acid increases cartilage ECM production in hybrid hydrogels in comparison to pure synthetic hydrogels [164,165].

Hybrid hydrogels that combine the best characteristics of natural materials and of synthetic materials are currently thought to be the most promising approach for cartilage tissue engineering and 3D bioprinting. However, the matching of the used cells to the appropriate material is a step of paramount importance on the way to a successfully engineered articular cartilage construct.

1.3 Hyaluronic acid

One very interesting biomaterial that is used in cartilage tissue engineering is hyaluronic acid (HA). As mentioned above, it has been shown that HA can have beneficial effects on the cells when it is used as part of a hydrogel or scaffold in cartilage engineering [164,165]. As it is part of the natural ECM of cartilage, it seems to mimic this environment and its signals for the cells in the tissue engineered construct. In the following, structure, occurrence and function of HA in the human body and its application in articular cartilage tissue engineering are highlighted in more detail.

1.3.1 Characteristics and functions of HA in the human body

Hyaluronic acid (HA) is a non-sulfated, linear glycosaminoglycan that is ubiquitously expressed in all vertebrates. It is composed of repeating disaccharides, N-acetyl-D-glucosamine and D-glucuronic acid (Figure 4) and can reach molecular weights of several megadalton (MDa) in the human body.
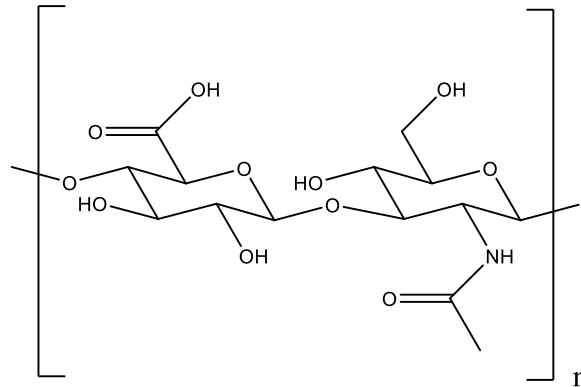
Figure 4: Structure of hyaluronic acid. HA is a polysaccharide with repeating disaccharides: N-acetyl-D glucosamine and D-glucuronic acid.

HA is, for example, expressed in embryonic tissues, synovial fluid, the vitreous body of the eye, umbilical cord and the ECM of soft connective tissue and cartilage [170-172]. As HA carries carboxyl and hydroxyl groups, it is negatively charged and highly hydrophilic. Therefore, it can draw huge amounts of water and forms viscous networks which gives it the ability to bear compressive forces in tissues and joints [170,173,174]. However, in addition to its role as structural component, HA has multiple other biological functions, for

example in cell and organ development, cell migration and proliferation, cancer, inflammation and tissue injury [174]. It is fascinating that this molecule with a relatively simple structure is present in so many tissues and has so many different functions. However, the biology of HA is much more complex than it was thought at first. Garantziotis and Savani wrote in their review from 2019: "The HA matrix can be best viewed as a canvas that is continually woven, unraveled, and decorated by dynamic patterns of hyaladherins which help shape HA-specific effects." [174]. This sentence describes the important balance between HA anabolism and catabolism and its many binding partners, the hyaladherins. Other factors that additionally expand HA function are its molecular weight, chemical modifications, macromolecular structure, microenvironment and its downstream signalling [174].

HA synthesis and degradation is performed constantly in the body and disruption of this delicate balance is associated with pathologies like inflammation or cancer [175,176]. HA is synthesized by three different hyaluronic acid synthases (HAS) that are located in the cell membrane. The three HAS are thought to produce HA of different length [170,177,178]. HA is degraded by hyaluronidases (HYAL) and reactive oxygen species (ROS) or internalised and degraded by cells [171,174,175,179]. When HA is newly synthesized or degraded, its molecular weight distribution changes in this specific area. The molecular weight (MW) of HA is an important factor for the different functions of HA. However, high and low MW HA are often defined differently in different studies.

For example, high MW HA has been found to act anti-inflammatory, while low MW fragments and oligosaccharides increase the expression of proinflammatory chemokines [174,180,181]. HA also can have opposing functions in cancer as low MW HA supports cell migration, invasion and angiogenesis while very high MW HA has been linked to cancer resistance [170,182,183]. Accumulation of HA in various tumours has been associated with poor prognosis [184,185], and HA metabolism has been suggested as a target for cancer therapies [176,186].

The versatile functions of HA are also controlled by HA binding partners, the hyaladherins. Aggrecan, versican, link protein and TSG-6 (tumour necrosis factor-stimulated gene 6) are examples for matrix hyaladherins, and CD44 (cluster of differentiation 44), CD168 (also called RHAMM: Receptor for hyaluronan mediated motility), TLR2,4 (toll-like-receptor 2,4), HARE (hyaluronan receptor for endocytosis), and LYVE-1 (lymphatic vessel endothelial hyaluronan receptor 1) are cell surface receptors for HA [187]. Aggrecan and link protein, for example, bind to HA in cartilage ECM to form huge networks of proteoglycans and glycosaminoglycans and thereby contribute greatly to the structure and biomechanical

functions of cartilage ECM. CD44 and CD168 are the main cell surface receptors of HA. Through them, HA can act as signal transductor and activate diverse signalling pathways in the cells. These signals are again dependent on the cell type, the identity, timing, amount and location of receptors, the amount, structure and MW of the binding HA and other influencing factors [174]. CD44 has almost as variable functions as HA itself and is present in almost all human cells [178,188]. In addition to HA, it can also bind to other ECM components, like fibronectin, osteopontin and collagen [189] and has several different isoforms as it is subject to alternative splicing [190]. The receptor is involved in cell adhesion, motility, growth, development and survival, tumorigenesis, inflammation and wound healing. It tethers HA to the cell surface and is responsible for its internalisation [178,183,191]. Signalling pathways that are known to be activated by CD44 include PI3K/PDK1/Akt, Ras/RAF1/MEK/ERK1/2, PLCϵ-Ca^{2+} signalling and SMAD signalling for BMP7 activation [178,192]. Ezrin, merlin and erbB1,2 have been described to form a complex with Hsp90 and cytosolic CD44 domain [178,193].

CD168 is also subject to alternative splicing and has several isoforms that determine the location of the HA-receptor. CD168 can be found on the cell membrane, in the cytoplasm, in mitochondria and in the nucleus [178,194]. CD168 is involved in cell motility, wound healing, cancer, inflammation and mitotic spindle formation [195]. It is not a transmembrane protein, and it can act as co-receptor for HA on the cell surface together with integral membrane proteins [178]. It can, for example, associate with CD44 and protein tyrosine kinase receptors like PDGFR (platelet-derived growth factor receptor) to regulate HA- and growth factor-induced MAPK/ERK1,2 signalling that can lead to motility and invasion in cancer cells [196,197]. Other signalling factors CD168 can influence are for example Ras (Ras: short for rat sarcoma), FAK (focal adhesion kinase), PKC (protein kinase C), c-Src (Src: short for sarcoma), NF-κB (nuclear factor kappa-light-chain-enhancer of activated B cells) and PI3K (phosphatidylinositol kinase) [178].

Even though the known HA signalling and functions are already very versatile and complex, research will probably discover many more in the future.

1.3.2 Applications of HA in articular cartilage tissue engineering

Hydrogels that mimic biological cues of the natural microenvironment of the used cells are thought to direct the differentiation and development of the cells in specific directions. Hyaluronic acid, the multifunctional component of many different tissues, has been used for

different tissue engineering strategies, for example for the engineering of fat tissue, cancer models, heart valves and cardiac repair, neural tissue and especially for cartilage tissue [173,198,199]. As described before, HA is a main component of articular cartilage tissue, and contributes greatly to the biomechanical functions of cartilage by forming highly hydrated networks with aggrecan. Additionally, it has many different functions as signalling molecule [5,178]. HA is important in embryonic development of cartilage and bone. During the early stage of limb bud development before condensation of cells, HA is thought to separate cells from each other and to increase cell migration and division. However, in later stages the HA amount decreases, probably because it is internalised through CD44 and degraded by the cells [200]. When cartilage matures postnatally, HA is again expressed in higher amounts together with the other ECM molecules [4]. In mature cartilage, HA forms huge networks and is attached to chondrocytes that regulate its degradation and synthesis and receive extracellular signals via HA receptors [178]. HA has been implied in signalling pathways that are important for chondrogenesis, for example TFGβ and BMP signalling [201-204]. TGFβ and sonic hedgehog signalling can, for example, increase expression of hyaluronan synthase 2 [205,206] which leads to increased expression of HA. Wnt signalling that is involved in cartilage development and maintenance can also be influenced by HA and its receptors [207,208]. These examples demonstrate the involvement and importance of HA in native biological processes in cartilage even if the exact mechanisms of HA as biomimetic material in tissue engineering have not been intensely studied so far. However, there are several studies that have directly demonstrated the beneficial effects of HA-scaffolds on cells and developing cartilage ECM [164,165,209,210]. Additionally, blocking of HA receptors with antibodies has been shown to decrease chondrogenesis in HA hydrogels [211]. The disadvantage of HA is that is has poor mechanical properties and degrades rapidly in its natural form. This can be prevented through chemical modification and crosslinking with other natural or synthetic polymers [212]. The possibility to easily modify HA, its biocompatibility and biological activity are some of the reasons why it is so frequently used in tissue engineering. There are a multitude of different combinations and modifications for HA, and some of them were reviewed by Burdick et al. [198] and Highley et al. [213].

HA has also been used as bioink material for 3D bioprinting [164,169,214,215]. 3D bioprinting of cells and hydrogel materials allows for the construction of complex tissue engineering constructs [155]. A 3D bioprinter can deposit cell/hydrogel suspension in predefined patterns and on top of each other, layer by layer. Therefore, personalized implants, complex tissues with several different cells or materials or for example zonally layered

cartilage constructs can be produced by 3D bioprinting. However, not all materials have suitable properties for the use as bioink material. As HA has versatile functions and can easily be modified, it is a popular bioink material for 3D bioprinting approaches [150,216]. In the following, the HA hydrogels that were used in the present work will be introduced. The used HA was modified with thiol-groups. HA-SH$_{11.7\,kDa}$ and HA-SH$_{410\,kDa}$ were modified on the carboxyl-group of glucuronic acid (Figure 5). HA-SH/P(AGE-co-G) hydrogel from HA-SH$_{11.7\,kDa}$ and allyl-modified polyglycidol was crosslinked through a UV-induced radical thiol-ene coupling with Irgacure I2959 as photo-initiator [164]. HA-SH$_{410\,kDa}$ was crosslinked in a two-step procedure, first via Michael addition with PEGDA and then with PEG-allyl via UV-induced radical thiol-ene coupling with the photo-initiator Irgacure I2959 (Hauptstein et al., manuscript in preparation).
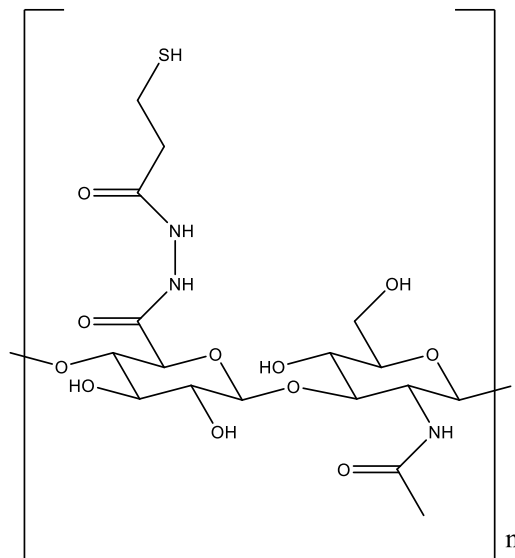
Figure 5: Structure of modified hyaluronic acid. HA is a polysaccharide with repeating disaccharides: N-acetyl-D glucosamine and D-glucuronic acid. HA was modified with a thiol-group on the carboxyl-group of D-glucuronic acid. The modified HA was called HA-SH.

Modifications of HA have several advantages for tissue engineering, including the possibility to crosslink it to other components. However, lately the question has arisen if the modifications can interfere with the binding of cell receptors to HA and thereby reduce the biological activity of HA. The binding of HA to CD44 is mainly mediated by hydrogen bonds and van der Waals forces. Binding HA lies in a shallow groove on the CD44-surface, and 13 amino acid residues of CD44 are the main contacts that recognize HA. However,

also the rest of the groove contributes to HA binding. Most important for HA recognition are the carboxyl group of glucuronic acid and the N-acetyl-group of N-acetyl-glucosamine, but also the hydroxyl groups on C6 of N-acetyl-glucosamine and on C3 and C2 of glucuronic acid are involved [217]. These groups are also the sites where most modifications are introduced to HA.

It has been shown that deacetylation and/or sulfation (on C6-OH) of N-acetyl-glucosamine in HA lead to decreased binding of CD44 to HA [218]. Kwon et al. demonstrated that it is important for CD44-HA interaction where a modification is introduced, how high the degree of modification is and what kind of modification is attached to HA. They showed that increased degree of modification (circa 40 %) generally decreases CD44-HA binding and chondrogenesis in HA hydrogels. Adhesion of CD44 to a HA hydrogel was decreased especially with a bulky and hydrophobic modification (norbornene) on the carboxyl group [219].

These studies show that it is important to consider the consequences on biological functions when a hydrogel material is altered or modified. The possibilities for HA modifications and applications are manifold but it is important to consider that changed materials can have changed effects on the employed cells.

1.4 Goals of the thesis

Articular cartilage has limited capacity for self-healing and repair as it is a tissue without blood supply [4,5]. Different clinical treatments are employed to repair damage to articular cartilage, but those approaches mostly yield biomechanically inferior repair tissue. The complete regeneration of native articular cartilage is still a challenge, but techniques like tissue engineering and 3D-bioprinting are promising to improve the repair of cartilage defects. However, more studies on different cell sources, biomaterials and cell signals for improving cartilage tissue engineering are needed to enhance the quality of cartilage repair in the future.

Therefore, one aim of this thesis was to evaluate a new promising cell source for articular cartilage engineering, articular cartilage progenitor cells (ACPCs), in comparison to mesenchymal stromal cells (MSCs). Two different hydrogels were employed for this comparison, the widely used agarose and a hyaluronan (HA)-based hydrogel consisting of thiol-modified HA (HA-SH) crosslinked with allyl-modified polyglycidol (HA-SH/P(AGE-co-G)). Additionally, the effects of low oxygen tension and zonal layering were investigated. HA can be used as scaffold for tissue engineering but has also been shown to transmit biological signals to different cells and to enhance chondrogenesis in MSCs [164,165,173,212,220] Therefore, the second goal of this thesis was to evaluate the contribution of the signalling molecule HA to the chondrogenic gene expression of MSCs. Gene expression levels of HA cell surface receptors and important factors for differentiation were investigated in response to HA in the culture medium and HA as part of a cell-encapsulating hydrogel.

1.4.1 Comparison of chondrogenesis of ACPCs and MSCs in different hydrogels

ACPCs have been detected in the superficial layer of articular cartilage several years ago [92,93]. It has been proposed that they could represent a promising cell source for articular cartilage engineering. They do not lose their chondrogenic capacity after a few population doublings like chondrocytes [94,101], and they do not tend to form hypertrophic cartilage like MSCs [94,102,103]. However, the number of studies that compare ACPCs directly to MSCs in hydrogels are limited [103,107], and studies in agarose, a widely used hydrogel for articular chondrogenesis, are completely missing. Different oxygen tension and zonal structure are two important factors when articular cartilage formation is considered that have not extensively been investigated so far for ACPCs. A previous study [103] has shown

promising results for layered constructs with ACPCs in the upper layer and MSCs in the lower layer of a hydrogel construct.

Therefore, ACPCs and MSCs were seeded into agarose hydrogel, and both monoculture and layered co-culture constructs were produced. ACPCs were seeded into the upper layer and MSCs into the lower layer. ACPCs and MSCs were chondrogenically differentiated for 28 days in chondrogenic medium containing TGFβ1 and under 21 % oxygen or 2 % oxygen. Chondrogenic differentiation and formation of extracellular matrix (ECM) were analysed with immunohistochemical stainings, biochemical assays and qRT-PCR (see section 4.1.1.).

As HA is an attractive material for cartilage engineering and it has been shown that cells can perform differently in different hydrogels [157], the chondrogenesis of ACPCs and MSCs was compared in a second, HA-based, hydrogel. This HA-SH/P(AGE-co-G) hydrogel was developed at the Department for Functional Materials in Medicine and Dentistry, University of Würzburg, within the framework of the EU research project HydroZONES (Bioactivated hierarchical hydrogels as zonal implants for articular cartilage regeneration) and has previously been shown to support chondrogenesis of MSCs [164]. Zonal constructs consisting of ACPCs in an upper layer and MSCs in a lower layer in this hydrogel were used in the HydroZONES project for a long-term *in vivo* cartilage regeneration study in horses. The evaluation of ECM production and chondrogenesis of ACPCs, MSCs and their zonal constructs in the HA-SH/P(AGE-co-G) hydrogel that was performed in this thesis served additionally as an *in vitro* evaluation for the *in vivo* animal study.

For this comparison, ACPCs and MSCs were encapsulated in HA-SH/P(AGE-co-G) hydrogel and monoculture and zonally layered co-culture constructs were produced. They were chondrogenically differentiated for 28 days in chondrogenic medium with TGFβ1. Chondrogenic differentiation and formation of extracellular matrix (ECM) were analysed with immunohistochemical stainings and biochemical assays (see section 4.1.2.). Additionally, the differences in ECM production and chondrogenesis of the same cells in the two different hydrogels agarose and HA-SH/P(AGE-co-G) were evaluated (see section 4.1. and especially 4.1.3.).

1.4.2 Evaluation of the contribution of hyaluronan to chondrogenic gene expression of MSCs

It is known that HA has many different functions as signalling molecule [170,174,193,194]. HA is a natural component of articular cartilage tissue and has been shown to support chondrogenesis in tissue engineering approaches [164,165]. For the generation of hydrogels, HA mostly has to be modified with functional groups that can be used to crosslink the polymer to stable constructs [213]. However, such modifications can change the binding of HA to the cells and its effect on them [218,219]. It is of great interest to evaluate how unmodified HA and the modified and crosslinked HA in the hydrogels affect chondrogenic gene expression of MSCs. Additionally, it is interesting if and how the processing of HA hydrogels, such as in 3D bioprinting, influences gene expression and HA signalling in HA-based hydrogels.

Therefore, the effect of unmodified HA on the gene expression of MSCs in 2D monolayer or 3D pellet culture was investigated, and the gene expression of MSCs encapsulated in a HA-based hydrogel was analysed in cast and 3D-bioprinted constructs for seven days. HA cell surface receptors, transcription factors (chondrogenic, osteogenic and adipogenic), differentiation markers and stemness markers were investigated by qRT-PCR (see section 4.2.).

Material

2 Material

2.1 Instruments

Table 1: Overview of used instruments

Instrument	Manufacturer	Headquarters
Accu-jet® pro	Brand	Wertheim, Germany
Analytical scale Pioneer™ (readability 0.001g)	OHaus	Parsippany, NJ, USA
Analytical scale CP224S (readability 0.0001 g)	Sartorius	Göttingen, Germany
Cellink plus 3D printer	Cellink Life Sciences	Gothenburg, Sweden
Centrifuge Rotina 420 R	Hettich	Tuttlingen, Germany
Centrifuge SIGMA 1-14	SIGMA Laborzentrifugen GmbH	Osterode, Germany
Centrifuge Multifuge 3SR	Heraeus	Hanau, Germany
Centrifuge Biofuge fresco	Kendro Laboratory products (now Thermo Fisher Scientific)	Langenselbold, Germany
CO_2 incubator	ibs technomara GmbH	Fernwald, Germany
CO_2 incubator	Heraeus	Hanau, Germany
CO_2 incubator Binder CB150 (with O_2 regulation)	Binder	Neckarsulm, Germany
Cryostat CM 3050S	Leica Biosystems	Wetzlar, Germany
Drying and heating chamber	Binder	Neckarsulm, Germany
FACSCanto flow cytometer	BD Biosciences	Franklin Lakes, NJ, USA
Freezers (-20 °C)	Liebherr	Bulle, Switzerland
Ultra-deep freezer TTS 500 (-80 °C)	Thalheimer Kühlung	Ellwangen, Germany
Fridges	Liebherr	Bulle, Switzerland
Glass rings, Ø 5 mm, custom-made	Department for Functional Materials in Medicine and Dentistry (FMZ), Chair: Prof. Jürgen Groll, University of Würzburg (collaboration)	Würzburg, Germany
HandyStep® dispenser	Brand	Wertheim, Germany
Hemocytometer Neubauer	Paul Marienfeld GmbH	Lauda, Germany
Laminar flow box Herasafe Typ-HS18	Heraeus	Hanau, Germany
Mastercycler® Gradient	Eppendorf	Hamburg, Germany
Magnetic stirrer	VWR	Darmstadt, Germany
Microscope BX51/DP71 camera	Olympus	Hamburg, Germany
Microscope IX51/XC30 camera	Olympus	Hamburg, Germany

Microtome	pfm medical	Cologne, Germany
Microwave Micromat 1000W	AEG	Frankfurt am Main, Germany
Multimode microplate reader Tecan GENios pro	Tecan	Männedorf, Switzerland
Nanodrop 2000c spectrophotometer	Thermo Fisher Scientific	Waltham, MA, USA
Orbital shaker Unimax 1010	Heidolph	Schwabach, Germany
PCR-cycler primus 96 advanced	PEQLAB Biotechnologie (now part of VWR)	Erlangen, Germany (now: Darmstadt, Germany)
pH-meter HI2210	Hanna Instruments	Kehl am Rhein, Germany
Pipettes Research® Plus	Eppendorf	Hamburg, Germany
Pipette multistep	Brand	Wertheim, Germany
Pipette displacement Microman™	Gilson	Middleton, USA
Pipette Multipette E3/E3x	Eppendorf	Hamburg, Germany
Real-Time PCR Detection System CFX96 Touch	Biorad	München, Germany
Roll mixer RM5	A. Hartenstein	Würzburg, Germany
Silicon molds, cylindrical, Ø 6 mm, custom-made	FMZ, Chair: Prof. Jürgen Groll, University of Würzburg (collaboration)	Würzburg, Germany
Teflon molds, cylindrical, Ø 6 mm, custom-made	Research group of Jos Malda, UMC Utrecht (collaboration)	Utrecht, Netherlands
TissueLyser	Qiagen	Hilden, Germany
Thermomixer MHR 23	DITABIS	Pforzheim, Germany
UV irradiation hand lamp (365 nm/254 nm)	Vilber	Collégien, France
Vortex 2	IKA	Staufen, Germany
Vortex-centrifuge CombiSpin	A. Hartenstein	Würzburg, Germany
Water bath	Memmert	Schwabach, Germany

2.2 Consumables

Table 2: Overview of used consumables

Consumable	Manufacturer	Headquarters
Amplitube PCR reaction stripes 8 x 0.2 ml	Simport	Bernard-Pilon, Canada
Cartridges, plastic	Nordson EFD	Westlake, OH, USA
Cellstar cell culture plates 6-, 12-, 24-, 48-, 96-well	Greiner Bio-one	Frickenhausen, Germany
Cellstar suspension culture plates 24-, 48-well	Greiner Bio-one	Frickenhausen, Germany

Chamber-slides 8-well, removable	ibidi	Gräfelfing, Germany
Combitips® advanced 0.5 ml	Eppendorf	Hamburg, Germany
Coverslip 24x40 mm / 24x50 mm	Paul Marienfeld	Lauda-Königshofen, Germany
Coverslip 24x60 mm	ibidi	Gräfelfing, Germany
Coverslip Ø 13 mm/14 mm	Paul Marienfeld	Lauda-Königshofen, Germany
Cryovials CryoPure 2.0 ml	Sarstedt	Nümbrecht, Germany
Dispenser tips 12.5 ml/25 ml	Nerbe plus	Winsen, Germany
Eppendorf Tubes®, 5 ml	Eppendorf	Hamburg, Germany
FACS tubes (75x12 mm)	A. Hartenstein	Würzburg, Germany
Falcon cell strainer (100 µm)	pluriSelect	Leipzig, Germany
Hardshell PCR plates, 96-well, thin wall	Bio-Rad	Hercules, CA, USA
Microseal® ´C´ Film	Bio-Rad	Hercules, CA, USA
Micro test plate (analytical) 96 well	Nerbe plus GmbH	Winsen, Germany
Microtome blades (N35)	Feather	Osaka, Japan
Nalgene™ Rapid-Flow™ bottle-top filter, pores: 0.2 µm	Thermo Fisher Scientific	Waltham, MA, USA
Parafilm	Pechiney	Chicago, IL, USA
PAP pen liquid blocker	Science Services	Munich, Germany
PCR plate, 96-well, skirted, 0.2 ml	Thermo Fisher Scientific	Waltham, MA, USA
pH indicator paper	Carl Roth	Karlsruhe, Germany
Pipette filter tips	Sarstedt	Nümbrecht, Germany
Pipette tips	Nerbe plus	Winsen, Germany
Pipettes serological	Greiner Bio-one	Frickenhausen, Germany
Pistons, beige, plastic	Nordson EFD	Westlake, OH, USA
Plate 96-well, black	Thermo Fisher Scientific	Waltham, MA, USA
Polypropylene tubes 15 ml/50 ml	Greiner Bio-one	Frickenhausen, Germany
SafeSeal micro tubes 1.5 ml/2.0 ml	Sarstedt	Nümbrecht, Germany
Scalpels	Feather	Osaka, Japan
Stainless steel beads, Ø 5 mm	Qiagen	Hilden, Germany
Steel nozzle orange, Ø 330 µm	Nordson EFD	Westlake, OH, USA
SuperFrost® Plus adhesion slides	R. Langenbrinck	Emmendingen, Germany
Syringe Filter ReliaPrep™, pores: 0.2 µm	Ahlstrom-Munksjö	Helsinki, Finland
Syringes	BD Biosciences	Franklin Lakes, NJ, USA
Tissue culture flasks (T175)	Greiner Bio-one	Frickenhausen, Germany

2.3 Chemicals

If not stated otherwise, chemicals were purchased from Sigma Aldrich/Merck (Darmstadt, Germany) or Carl Roth (Karlsruhe, Germany).

Table 3: Overview of used chemicals

Chemical	Manufacturer	Headquarters
Acetone, 99.5 %	AppliChem	Darmstadt, Germany
Antibody diluent, Dako REAL™	Dako	Hamburg, Germany
Aqua ad iniectabilia	B. Braun	Melsungen, Germany
Ethanol absolute, 99.8 %, for molecular biology	AppliChem	Darmstadt, Germany
FACS clean solution	BD Biosciences	Franklin Lakes, NJ, USA
FACS sheath solution	BD Biosciences	Franklin Lakes, NJ, USA
FACS shutdown solution	BD Biosciences	Franklin Lakes, NJ, USA
bFGF (basic fibroblast growth factor)	Biolegend	London, UK
CIAP (calf intestinal alkaline phosphatase)	Thermo Fisher Scientific (Invitrogen)	Waltham, MA, USA
Collagenase II	Worthington	Lakewood, USA
DAPI, IS mounting medium	Dianova	Hamburg, Germany
DMEM/F12 (Dulbecco's Modified Eagle´s Medium: Nutrient Mixture F-12)	Thermo Fisher Scientific (Gibco®)	Waltham, MA, USA
DMSO	Thermo Fisher Scientific	Waltham, MA, USA
Dulbecco´s phosphate-buffered saline (DPBS), (no $CaCl_2$, no $MgCl_2$)	Thermo Fisher Scientific (Gibco®)	Waltham, MA, USA
Distilled water (DNase/RNase free)	Thermo Fisher Scientific (Gibco®)	Waltham, MA, USA
FCS (fetal calf serum)	Thermo Fisher Scientific (Gibco®)	Waltham, MA, USA
Formaldehyde, 37 %	Th. Geyer	Renningen, Germany
Hoechst 33258 dye	Polysciences	Warrington, PA, USA
Hyaluronic acid sodium salt (0.6-1.0 MDa)	Carbosynth	Compton, UK
ImProm-II™ Reverse Transcription System Kit	Promega	Madison, WI, USA
ITS™+ Premix	Corning™	Corning, NY, USA
Life/Dead cell staining kit II	PromoKine	Heidelberg, Germany
MESA GREEN qPCR MasterMix Plus for SYBR® Assay No ROX	Eurogentec	Seraing, Belgium

NEAA (non-essential amino acids)	Thermo Fisher Scientific (Gibco®)	Waltham, MA, USA
Papain	Worthington	Lakewood, NJ, USA
Penicillin/streptomycin (100 U/ml penicillin, 0.1 mg/ml streptomycin)	Thermo Fisher Scientific (Gibco®)	Waltham, MA, USA
Phosphate buffered saline (Dulbecco A) tablets	Thermo Fisher Scientific	Waltham, MA, USA
2-propanol	VWR international, part of Avantor (VWR chemicals BDH)	Poole, UK
Proteinase K (Ready to use)	Dako	Hamburg, Germany
Terralin Liquid® disinfectant	Schülke	Norderstedt, Germany
TGFβ1 (transforming growth factor β 1)	Biolegend	London, UK
Tissue-Tek® O.C.T.compound	Sakura Finetek	Zoeterwonde, The Netherlands
TRIzol® Reagent	Thermo Fisher Scientific (Ambion)	Waltham, MA, USA
Trypsin-EDTA 0.25 %	Thermo Fisher Scientific (Gibco®)	Waltham, MA, USA
Ultra-Streptavidin HRP Kit (Multi-Species, diaminobenzidine) Antibody	Biolegend	London, UK
Xylene	VWR international, part of Avantor (VWR chemicals BDH)	Poole, UK

2.4 Hydrogel components

Table 4. Overview of used hydrogel components

Chemical	Characteristics	Manufacturer/Provider
Agarose	Low melt	Sigma Aldrich/Merck, Darmstadt, Germany
Hyaluronic acid, thiol-modified (HA-SH)	11.7 kDa, 34 % modified	FMZ, Chair: Prof. Jürgen Groll, University of Würzburg, Würzburg, Germany (collaboration Simone Stichler, Verena Schill)
Hyaluronic acid, thiol-modified (HA-SH)	410 kDa, 43 % modified	FMZ, Chair: Prof. Jürgen Groll, University of Würzburg, Würzburg, Germany (collaboration Leonard Forster)
Irgacure 2959	Photoinitiator	BASF, Ludwigshafen, Germany

Polyglycidol, allyl-modified (P(AGE-co-G))	5.21 kDa, 9.8 % modified		Kind gift of PolyVation, Groningen, Netherlands
Polyethylene glycol diacrylate (PEGDA)	6 kDa		FMZ, Chair: Prof. Jürgen Groll, University of Würzburg, Würzburg, Germany (collaboration Leonard Forster)
Polyethylene glycol, allyl-modified (PEG-Allyl)	6 kDa, 2-arm		FMZ, Chair: Prof. Jürgen Groll, University of Würzburg, Würzburg, Germany (collaboration Leonard Forster)

2.5 Antibodies

Table 5: Overview of used antibodies

Antibody	Source/Type	Application/Dilution	Manufacturer
Anti-aggrecan	Mouse monoclonal	IHC: 1:300	Thermo Fisher Scientific, Waltham, MA, USA
Anti-CD168 (ab170527)	Rabbit polyclonal	FACS: 1:100 IHC: 1:100	Abcam, Cambridge, UK
Anti-CD44 (ab119348)	Rat monoclonal	FACS: 1:100	Abcam, Cambridge, UK
Anti CD44 (Clone BJ18)	Mouse monoclonal	IHC: 1:100	Biolegend, London, UK
Anti-type I collagen (ab34710)	Rabbit polyclonal	IHC: 1:200	Abcam, Cambridge, UK
Anti-type II collagen (ab34712)	Rabbit polyclonal	IHC: 1:200	Abcam, Cambridge, UK
Anti-type VI collagen (ab6588)	Rabbit polyclonal	IHC: 1:200	Abcam, Cambridge, UK
Alexa Fluor 488 anti-rabbit	Goat	FACS: 1:400 IHC: 1:400	Jackson ImmunoResearch Laboratories, West Grove, PA, USA
Alexa Fluor 488 anti-mouse	Goat	IHC: 1:400	Jackson ImmunoResearch Laboratories, West Grove, PA, USA
Fluorescein (FITC)-conjugated AffiniPure IgG anti-rat	Goat	FACS: 1:400 IHC: 1:400	Jackson ImmunoResearch Laboratories, West Grove, PA, USA
ChromPure Rabbit IgG, whole molecule	Rabbit isotype control	FACS: 1:100	Jackson ImmunoResearch Laboratories, West Grove, PA, USA

ChromPure Rat IgG, whole molecule	Rat isotype control	FACS: 1:100	Jackson ImmunoResearch Laboratories, West Grove, PA, USA

2.6 Primers

Table 6: Overview of used primers

Target gene	Sequence (5´-> 3´) /Assay ID	Manufacturer
ACAN (aggrecan)	qHsaCID0008122	Bio-Rad, Hercules, CA, USA
CD44 (cluster of differentiation 44)	qHsaCID0013679	Bio-Rad, Hercules, CA, USA
COL2A1 (α1 chain, type II collagen)	qHsaCED0001057	Bio-Rad, Hercules, CA, USA
GAPDH (glyceraldehyde 3-phosphate dehydrogenase)	qHsaCED0038674	Bio-Rad, Hercules, CA, USA
HMMR (hyaluronan mediated motility receptor; CD168; RHAMM)	qHsaCED0036330	Bio-Rad, Hercules, CA, USA
Nanog (nanog)	qHsaCED0043394	Bio-Rad, Hercules, CA, USA
POU5F1 (POU domain, class 5, transcription factor 1; OCT4)	qHsaCED0038334	Bio-Rad, Hercules, CA, USA
PPARG (peroxisome proliferator-activated receptor gamma)	qHsaCID0011718	Bio-Rad, Hercules, CA, USA
RUNX2 (runt-related transcription factor 2)	qHsaCID0006726	Bio-Rad, Hercules, CA, USA
SOX2 ((sex determining region Y)-box 2)	qHsaCED0036871	Bio-Rad, Hercules, CA, USA
SOX5 ((sex determining region Y)-box 5)	qHsaCED0037871	Bio-Rad, Hercules, CA, USA
SOX6 ((sex determining region Y)-box 6)	qHsaCID0012146	Bio-Rad, Hercules, CA, USA
SOX9 ((sex determining region Y)-box 9)	qHsaCED0044083	Bio-Rad, Hercules, CA, USA
ACAN (aggrecan), equine	F: aatgggaaccagcctacacg R: gctctcct tg tgctgcact	Biomers, Ulm, Germany
COL1A1 (α1 chain, type I collagen), equine	F: agggtgagacaggcgaaca R: gggaccttgttcaccaggag	Biomers, Ulm, Germany
COL2A1 (α1 chain, type II collagen), equine	F: acctcgtggcagagatgga R: tgggcagcaaagtttccac	Biomers, Ulm, Germany

CXCL-12 (C-X-C motif chemokine ligand 12), equine	F: gccagagccaacatcaaac R: tcagtttcgggtcaatgcac	Biomers, Ulm, Germany
GLUT1 (glucose transporter 1), equine	F: ccctgcaccagttgagtgtc R: gggaggaaggtgatgctcag	Biomers, Ulm, Germany
HPRT1 (hypoxanthin-guanin-phosphoribosyl-transferase 1), equine	F: aagcttgctggtgaaaag R: gcatatcctacgacaaact	Biomers, Ulm, Germany
PGK1 (phosphoglycerate kinase 1), equine	F: ggaagaagggaagggcaaag R: ggaaagtgaagctcggaaggt	Biomers, Ulm, Germany
PRG4 (proteoglycan 4), equine	F: cttcccatttattgttgctg R: tagaatacccttcccacat	Biomers, Ulm, Germany
STC1 (stanniocalcin 1), equine	F: atgaggcggagcagaatgat R: ttgaggcagcgaaccactt	Biomers, Ulm, Germany

2.7 Cell culture media

Table 7: Overview of used cell culture media

Medium	Composition
Proliferation medium for equine MSCs	DMEM – high glucose 10 % FCS 1 % penicillin/streptomycin 1 ng/ml bFGF
Proliferation medium for human MSCs	DMEM/F12 10 % FCS 1 % penicillin/streptomycin 3 ng/ml bFGF
Proliferation medium for equine ACPCs	DMEM – high glucose 10 % FCS 1 % penicillin/streptomycin 1 % NEAA 0.2 mM L-ascorbic acid 2-phosphate sequi-magnesium salt hydrate 5 ng/ml bFGF
Chondrogenic differentiation medium for equine MSCs and ACPCs	DMEM – high glucose 1 % penicillin/streptomycin 1 % ITS+ Premix 0.1 µM dexamethasone 0.2 mM L-ascorbic acid 2-phosphate sequi-magnesium salt hydrate 10 ng/ml TGFβ1
Basic chondrogenic medium for human MSCs (without TGFβ1)	DMEM – high glucose 1 % penicillin/streptomycin 1 % ITS+ Premix 0.1 µM dexamethasone

	0.2 mM L-ascorbic acid 2-phosphate sequi-magnesium salt hydrate 40 µg/ml L-proline
Basic serum-free medium	DMEM/F12 1 % penicillin/streptomycin
Basic serum-containing medium	DMEM/F12 10 % FCS 1 % penicillin/streptomycin
Cryoconservation medium	DMEM/F12 10% FCS 1 % penicillin/streptomycin 5 % DMSO

2.8 Cells

Table 8: Overview of used cells

Cell type	Source	Provider
MSCs	Human femoral heads (of patients undergoing elective hip arthroplasty) [166]	Klinik König-Ludwig-Haus Würzburg; Direktor: Maximilian Rudert, collaboration. Isolation in the Blunk lab, as described by Böck et al. [166]
MSCs	Equine bone marrow aspirate from the sternum [103,221]	Research group of Jos Malda, UMC Utrecht, Netherlands, collaboration. Isolation as described by Visser et al. [221]
ACPCs	Equine articular cartilage (metacarpophalangeal joint) [94,103]	Research group of Jos Malda, UMC Utrecht, Netherlands, collaboration. Isolation as described by Levato et al. [94,103]

2.9 Buffers and Solutions

Table 9: Overview of used buffers and solutions and their composition

Buffer/Solution	Composition
Basic FGF stock solution	10 µg/ml bFGF 1 % BSA PBS
Blocking solution (IHC)	1 % BSA PBS

Buffered formalin	3.7 % formalin (37 % stock solution) PBS
Chloramine T solution	15.67 mg/ml chloramine T 88.89 % citric acid buffer 11.11 % 2-propanol
Chondroitin sulfate stock solution	100 µg/ml chondroitin sulfate 0.85 mg/ml L-cysteine PBE
Citric acid buffer (pH 6 buffer)	33.33 mg/ml citric acid monohydrate 80 mg/ml sodium acetate trihydrate 22.67 mg/ml NaOH 0.8 % glacial acid 20 % 2-propanol pH 6.0 store at 4 °C
DAB (p-dimethylaminobenzaldehyde) solution	174.42 mg/ml DAB 69.77 % 2-propanol 30.23 % (perchloric acid 60 %)
Dexamethasone stock solution	1 mM dexamethasone Absolute ethanol
DMMB (dimethylmethylene blue) solution	0.5 % (3.2 mg/ml DMMB in absolute ethanol) 3.04 g/l glycine 2.37 g/l NaCl ddH$_2$O pH 3.0
FACS buffer	1 % BSA PBS
Fast green staining solution (0.02 %)	0.2 mg/ml fast green ddH$_2$O
Hoechst 33258 stock solution	1 mg/ml Hoechst 33258 dye ddH$_2$O
Hydroxyproline stock solution	1 mg/ml Hydroxyproline 0.85 mg/ml L-cysteine PBE
ITS+ premix (ready-to-use)	0.625 mg/ml human recombinant insulin 0.625 mg/ml human transferrin 0.625 µg/ml selenous acid 0.125 g/ml BSA 0.535 mg/ml Linoleic acid
L-ascorbic acid 2-phosphate sequi-magnesium salt hydrate stock solution	50 mg/ml L-ascorbic acid 2-phosphate sequimagnesium salt hydrate PBS Sterile filtered
L-proline stock solution	40 mg/ml L-proline PBS Sterile filtered
MPER buffer (mammalian protein extraction reagent buffer)	6.057 g/l Tris 8.766 g/l NaCl 0.2922 g/l EDTA

	0.3803 g/l EGTA 1 % Triton X-100 ddH2O pH 7.6
Papain digestion buffer	0.85 mg/ml L-cysteine 3 U/ml papain PBE buffer
PBE buffer (phosphate buffered extraction buffer)	6.53 g/l Na_2HPO_4 6.48 g/l NaH_2PO_4 EDTA ddH2O pH 6.5
PBE/Cysteine buffer	0.85 mg/ml L-cysteine PBE buffer
PBS (phosphate buffered saline)	10 PBS (Dulbecco A) tablets 1 l ddH_2O
Picrosirius red staining solution (0.1 %)	1 mg/ml direct red 80 Saturated aqueous solution of picric acid
pNPP solution (p-Nitrophenyl phosphate solution)	SIGMAFAST p-Nitrophenyl phosphate tablets in indicated amounts of water, resulting in: 1 mg/ml pNPP 0.2 M Trizma buffer 5 mM magnesium chloride ddH_2O
Safranin O staining solution (0.1 %)	1 mg/ml safranin O ddH_2O
TEN buffer (Tris-EDTA-NaCl buffer)	0.1 M NaCl 1 mM EDTA 10 mM Tris ddH_2O pH 7.4
TGFβ1 stock solution	10 µg/ml TGFβ1 1 % BSA PBS Sterile filtered

2.10 Software

Table 10: Overview of used software

Software	Supplier	Headquarters
CellSense™ 1.16	Olympus	Hamburg, Germany
CFX Manager™ software version 3.1.	Biorad	Hercules, CA, USA
Chemdraw 20.0	PerkinElmer	Waltham, MA, USA
FlowJo v.10.0.7	Treestar	San Carlos, CA, USA

GraphPad Prism Version 6.0	GraphPad Software	LaJolla, CA, USA
Inkscape 0.92.4	The Inkscape Project	-
Microsoft 365	Microsoft	Redmond, WA, USA

Methods

3 Methods

3.1 Cell culture

3.1.1 Cell isolation

Bone marrows were recovered, after informed consent, from the explanted femoral heads of patients undergoing elective hip arthroplasty. The procedure was approved by the local Ethics Committee of the University of Würzburg (186/18). Human bone marrow-derived mesenchymal stromal cells (MSCs) were isolated as previously described [166]. Briefly, bone debris and marrow were washed in PBS several times and the resulting solution was centrifuged to pellet the cells. They were seeded on tissue culture plastic and the non-adherent cells were removed after two days [166].

Equine MSCs were isolated from equine bone marrow aspirate from the sternum as described by Visser et al. [221]. The cells were kindly provided by the research group of Prof. Jos Malda (UMC Utrecht) for a collaboration project and the present work. Briefly, a Ficoll-Paque density gradient was used to isolate the mononuclear cell fraction and cells were subsequently seeded on tissue culture plastic [103,221].

Equine ACPCs were isolated from equine articular cartilage from the metacarpophalangeal joint as described by Levato et al. [103] and Williams et al. [94]. The cells were kindly provided by the research group of Prof. Jos Malda (UMC Utrecht) for a collaboration project and the present work. Cartilage tissue was harvested with a scalpel under sterile conditions, minced and digested for 2 h in 0.2 % pronase solution (0.2 wt% pronase in DMEM (with GlutaMAX™ and pyruvate), 10 µl/ml HEPES buffer, 1 µl/ml gentamicin) at 37 °C. Then, pronase solution was removed and cartilage was incubated for 12 h in 0.075 % collagenase II solution (0.075 wt% collagenase II in DMEM (with GlutaMAX™ and pyruvate), 10 µl/ml HEPES buffer, 1 µl/ml gentamicin, 50 µl/ml FCS) at 37 °C for further digestion. After that, the digested tissue was sieved through a 70 µm cell strainer and the resulting cell suspension was centrifuged for 5 min at 300 x g. The cells were counted, resuspended in serum-free medium and plated on fibronectin coated 6-well plates (10 µg/ml fibronectin in PBS+Ca+Mg for 1 h at 37 °C). The cell density was 500 cells/cm^2. After 20 min, medium was removed, and plates were washed with PBS+Ca+Mg to remove non-adherent cells. The adherent cells were cultured for 6 days (DMEM (high glucose, GlutaMAX™, pyruvate), 10 % FCS, 1 % PS, 0.2 mM ascorbic acid-2-phosphate, 5 ng/ml bFGF).

After 6 days, colonies with more than 32 cells were harvested individually, pooled and then expanded further in 2D culture.

3.1.2 2D cell expansion

Circa $1*10^6$ human MSCs were seeded per T175 flask in 25 ml of proliferation medium for human MSCs (see Table 7, pp. 44-45). Equine ACPCs and MSCs were seeded at $4*10^5$ cells per T175 flask in 22 ml of their respective proliferation medium (see Table 7, pp. 44-45). Medium was exchanged every two to three days and cells were cultured to 80-90 % confluency in an incubator (37 °C, 5 % CO_2, 21 % O_2, humidified). For passaging and harvest of cells, a 0.25 % trypsin-EDTA solution was used.

3.1.3 Treatment of cells in 2D monolayer with HA

50000 human MSCs per well were seeded in 6-well plates in basic serum-containing medium (see Table 7, pp. 44-45) to allow cell attachment to the plastic surface. 2 ml medium per well were used. After one day cells were washed once with DPBS and medium was exchanged with basic serum-free medium (see Table 7, pp. 44-45) to starve the cells for one day. After one day, medium was exchanged to basic serum-free medium with or without the supplementation of HA (1 mg/ml; 0.6-1.0 MDa). After two days, cells were harvested for qRT-PCR analysis.

3.1.4 Treatment of cells in 3D pellet culture with HA

$2*10^5$ cells per well were seeded in a 96-well plate with V-shaped bottom. The 96-well plate was centrifuged for 5 min at 500 x g to pellet the cells at the bottom of the wells. For 3D pellet culture of human MSCs, pellets were cultured in basic serum-containing medium (see Table 7, pp. 44-45) for one day to allow condensation and formation of pellets. After one day, pellets were washed once with DPBS and then the medium was exchanged with basic serum-free medium (see Table 7, pp. 44-45) for one day to starve the cells. Then, basic serum-free medium with or without the supplementation of HA (2 mg/ml; 0.6-1.0 MDa) was added to the pellets. Pellets were harvested for qRT-PCR analysis after one day with or without HA supplementation and three pellets were pooled for one sample.

3.1.5 3D agarose hydrogel culture

40 mg per ml (4 %) low melt agarose in DPBS were heated up with a microwave until agarose was dissolved completely. The solution was then slowly cooled down in a thermo-mixer to 40 °C and mixed 1:1 with a cell solution at a concentration of $40*10^6$ cells per ml. This resulted in a 2 % agarose gel with $20*10^6$ cells per ml. 55 µl of this gel were cast into custom made silicone or Teflon molds (Ø 6 mm). The molds with the cast gel were shortly put into a fridge to cool the gel down below 25 °C to solidify the hydrogel around the encapsulated cells. The solid cylindrical constructs were then collected with a small spoon and put in 24- or 48-well plates (suspension culture). Equine MSCs and ACPCs in agarose were cultured for one, 14 and 28 days in their respective chondrogenic differentiation medium (see Table 7, pp. 44-45). Two to three ml medium per well were used. Cells were cultured in either a normal incubator (37 °C, 5 % CO_2, 21 % O_2, humidified) or a hypoxia incubator (37 °C, 5 % CO_2, 2 % O_2, humidified). Medium was exchanged every two to three days.

3.1.6 3D HA-SH hydrogel culture

3.1.6.1 HA-SH/P(AGE-co-G) hydrogels

5 wt% P(AGE-co-G) were dissolved in DPBS by vortexing and sterile filtered through a 0.2 µm syringe filter. The needed amount of HA-SH$_{11.7 \text{ kDa}}$ (5 wt%) was irradiated with an UV hand lamp at 254 nm for 10 min to sterilize the material. Then, 0.05 wt% photoinitiator Irgacure2959 and 5 wt% HA-SH$_{11.7 \text{ kDa}}$ were added and dissolved by vortexing. The mixture was protected from light and pH was adjusted to 7.4. A cell pellet was resuspended in the resulting 10 wt% hydrogel precursor solution so that the end-concentration was $20*10^6$ cells/ml. 55 µl per construct of precursor solution with cells were cast into custom made silicone or Teflon molds (Ø 6 mm). For crosslinking of the hydrogel precursor solution, it was irradiated with an UV hand lamp at 365 nm for 10 min. Afterwards, hydrogel constructs were put into 24- or 48-well plates (suspension culture) with two to three ml of chondro-genic differentiation medium (see Table 7, pp. 44-45) per well and cultured in an incubator (37 °C, 5 % CO_2, 21 % O_2, humidified). Medium was exchanged every two to three days. Equine ACPCs and MSCs were cultured for one and 28 days.

3.1.6.2 HA-SH /PEGDA/PEG-allyl/Irgacure2959 hydrogels

To produce a hydrogel precursor solution of 0.5 wt% HA-SH, 0.5 wt% PEGDA, 1 wt% PEG-allyl and 0.05 wt% Irgacure I2959 and PBS, stock solutions of the components were prepared. 4 wt% PEGDA, 4 wt% PEG-allyl and 0.5 wt% Irgacure were dissolved in DPBS. 1 wt% HA-SH was dissolved in 154 mM HEPES buffer (pH 7.6) shortly before it was used to resuspend the cell pellet of human MSCs. HA-SH$_{410 kDa}$ was used for the formation of HA-SH/PEGDA/PEG-Allyl/Irgacure2959 hydrogels. Calculated amounts of PEGDA, PEG-allyl and Irgacure stock solution and PBS were mixed and added to the HA-SH/cell suspension so that final concentrations were 0.5 wt% HA-SH, 0.5 wt% PEGDA, 1 wt% PEG-allyl, 0.05 wt% Irgacure and $20*10^6$ cells/ml. The crosslinking reaction (Michael addition) was started the moment that HA-SH and PEGDA were put together. The hydrogel precursor solution was incubated at 37 °C for 60 min (predetermined). The vial was mixed gently every 10 min to avoid sedimentation of cells. After that time, the solution had become viscous enough to keep its shape when it was pipetted with a displacement pipette or when it was bioprinted. The now "printable" hydrogel precursor solution was then either cast into glass rings (Ø 5 mm) or extruded through a 330 µm steel nozzle with 50 kPa by the bioprinter Cellink plus (40 µl per construct). The printed hydrogel precursor was collected in a tube and subsequently cast into glass rings (Ø 5 mm). Once the solution was in the glass rings, it was irradiated with an UV hand lamp at 365 nm for 10 min. The resulting hydrogels were cultured in 48-well plates in 1 ml chondrogenic differentiation medium for human MSCs without TGFβ1 for one, four and seven days. Medium was exchanged on day two, day four and day six.

3.1.7 Preparation of zonal hydrogels

Zonal hydrogels were prepared with either HA-SH/P(AGE-co-G) or with agarose hydrogels. For agarose hydrogels, the first/lower layer of the construct was cast into a mold (custom made silicone or Teflon molds (Ø 6 mm) and the agarose was cooled down shortly to get a semi-solid hydrogel. When the second/upper layer was cast on the first layer, the first layer was not disrupted but could also still attach to the second layer, as it was not completely solid yet. A similar mechanism was used for zonal HA-SH/P(AGE-co-G) hydrogels. The first/lower layer was irradiated only for 5 min at 365 nm so that not all functional groups were crosslinked, then the second/upper layer was cast on top and the complete hydrogel was irradiated again for 5 min at 365 nm to complete the crosslinking. In both zonal agarose

and HA-SH/P(AGE-co-G) hydrogels the lower, MSC containing layer had a volume of 35 µl and the upper ACPC containing layer had a volume of 20 µl.

3.2 Staining of cells and tissue sections

3.2.1 Cell viability assay

To investigate viability of cells that were encapsulated in hydrogels, constructs were washed once in PBS and then incubated in PBS with 0.1 % calcein acetoxymethyl ester (calcein-AM) (green) and 0.05 % ethidium homodimer III (red) (Life/Dead cell staining kit II, Promokine) for 30-45 min at RT. After incubation, constructs were washed once with PBS and then images were taken with an inverse fluorescent microscope (Olympus IX51/XC30). Cell viability was assessed on d1 after cell encapsulation and on d7.

3.2.2 Sectioning of 3D constructs

3.2.2.1 Cryo-sectioning

After harvesting of 3D hydrogel constructs, they were fixed with 3.7 % buffered formalin overnight at 4 °C. They were then washed with PBS and embedded in Tissue-Tek® O.C.T.compound overnight at RT in a wet chamber. On the next day, the constructs were flash-frozen with liquid nitrogen in Tissue-Tek® O.C.T.compound and stored at -20 °C. Cryo-sectioning was performed with a cryostat (Leica CM 1850) at -24 °C. Sections were cut to be 6 µm thick, collected on SuperFrost® Plus adhesion glass slides and stored at -20 °C until they were stained.

3.2.2.2 Paraffin sectioning

3D hydrogel constructs were harvested and then fixed with 3.7 % buffered formalin overnight at 4 °C. On the next day, they were incubated for 1 h in 70 % ethanol, then for 2 h in two changes of 96 % ethanol. Next, they were incubated in 100 % ethanol for 1 h and then in fresh 100 % ethanol overnight at RT. On the next day, samples were incubated in two changes of xylene for 4 h. Afterwards, samples were put into hot liquid paraffin for 2-3 h, were then embedded in paraffin, cooled down and solidified on a cold plate overnight. Samples were stored at RT until they were sectioned. Paraffin sectioning was performed with a

microtome and sections were cut to be 1 µm thick. They were put in a warm water bath and collected on adhesion glass slides. Afterwards, sections on glass slides were incubated at 60 °C overnight and stored at room temperature (RT) until they were stained.

3.2.3 Safranin O staining

Paraffin sections needed to be deparaffinized before staining could begin. First, they were incubated in two changes of xylene for 10 min. Then, they were incubated in two changes of 100 % ethanol for 6 min. Afterwards, sections were incubated in 80 %, 70 % and 50 % ethanol for 1 min each. After this, cryo-sections and paraffin sections were stained the same way. Sections were incubated in ddH$_2$O for 1 min, then in Weigert´s hematoxylin for 6 min. Then they were shortly rinsed with ddH$_2$O and 0.5 % hydrochloric acid in ethanol. Subsequently, sections were rinsed for 5 min under running tap water and then they were incubated in 0.02 % Fast Green solution (see Table 9, pp. 45-47) for 4 min. Then, sections were rinsed in 1 % acetic acid and were stained for 6 min in 0.1 % Safranin O solution (see Table 9, pp. 45-47). They were incubated in 100 % ethanol for 1 min, in 2-propanol for 2 min and in xylene for 2 min before they were covered in entellan and coverslips. Samples were dried under a fume hood for 2 days and images were taken with a microscope (Olympus BX51/DP71).

3.2.4 Picrosirius red staining

Paraffin sections were deparaffinized as described for Safranin O staining (in 3.2.3.) Then, deparaffinized sections and cryo-sections were stained the same way. They were incubated in Weigert´s Hematoxylin for 8 min, rinsed under running tap water for 10 min and then incubated in 0.1 % picrosirius red (see Table 9, pp. 45-47) for 60 min. Afterwards, sections were incubated in two changes of 0.5 % acetic acid for 5 min, then in 100 % ethanol for 1 min, in 100 % 2-propanol for 2 min and in xylene for another 2 min. They were covered in entellan and coverslips and were dried under a fume hood for 2 days. Images were taken with a microscope (Olympus BX51/DP71).

3.2.5 Immunohistochemistry

Paraffin sections were deparaffinized as described in 3.2.3. Afterwards, they were washed three times with PBS for 5 min and sections were circled with a PAP-pen. For antigen retrieval, sections were first incubated in a 0.1 % pronase solution in PBS for 30 min at 37

56

°C. Then, sections were washed three times for 5 min with PBS and incubated in a 1 % hyaluronidase solution in PBS for 30 min at 37 °C. Subsequently, they were again washed three times with PBS for 5 min and then incubated in blocking solution (1 % BSA in PBS) for 30 min at RT. Sections were then incubated with a primary antibody overnight at RT in a wet chamber. Dilutions used for the respective antibodies can be found in Table 5 (pp. 42-43). For cryo-sections and formalin-fixed 2D cell culture, antigen retrieval was performed by incubation with proteinase K for 10 min at 37 °C instead of pronase and hyaluronidase. The other steps were the same for all samples. On the next day, sections/cells were washed three times for 5 min with PBS and incubated with a secondary antibody (Table 5, pp. 42-43) for 60 min at RT in the dark. Afterwards, sections were washed three times for 5 min with PBS and mounted with DAPI mounting medium. Fluorescent images were taken with a microscope (Olympus BX51/DP71).

For immunohistochemical staining with diaminobenzidine chromogen and peroxidase enzyme, Ultra-Streptavidin HRP Kit (Multi-Species, diaminobenzidine) Antibody from Biolegend was used according to the manufacturer's instructions. Used primary antibodies and dilutions can be found in Table 5 (pp. 42-43) and antigen retrieval was performed as described above.

3.3 Biochemical assays

3.3.1 Papain digestion

Before biochemical assays could be performed with harvested 3D samples, they had to be digested using papain. Wet weight of hydrogels was determined directly after harvesting. Hydrogels or pellets were transferred to 2 ml SafeSeal micro tubes and a defined amount of PBE/cysteine buffer (500µl or 200 µl) (see Table 9, pp. 45-47) and one stainless steel bead per tube were added. Samples were homogenized using a TissueLyser at 25 Hz for 5 min. Afterwards, the same amount of PBE/cysteine buffer as before was added to the homogenized samples, containing papain. The end concentration of papain in the samples was 3 U/ml. Samples were shaken at 60 °C in a thermomixer for 16 -20 h and then stored at -20 °C until biochemical assays were performed.

3.3.2 DNA assay

To determine the amount of DNA present in the samples, a fluorescence assay with DNA intercalating dye Hoechst 33258 was performed [222]. 200 µl dye solution (1 µl Hoechst 33258 stock solution per 10 ml TEN buffer) (see Table 9, pp. 45-47) were added to 10 µl digested sample (pure or diluted in PBE/cysteine buffer). Quantification of DNA amount was performed by a Tecan microplate reader (excitation: 360 nm, emission: 460 nm) and salmon testis DNA was used as a standard.

3.3.3 Glycosaminoglycan assay

For determination of glycosaminoglycan (GAG) amount in the samples, a dimethyl-methylenblue (DMMB) assay was performed [223]. 200 µl of DMMB (see Table 9, pp. 45-47) were added to 50 µl of sample (mostly diluted between 1:5 to 1:50 in PBE/cysteine buffer) and measured with a Tecan microplate reader at 525 nm. Bovine chondroitin sulfate was used as a standard.

3.3.4 Hydroxyproline assay

Collagen content of samples was determined by a hydroxyproline assay. 10-100 µl sample were added to 100 µl of 37 % hydrochloric acid (fuming hydrochloric acid). Samples were heated to 105 °C in a thermomixer for 16-20 h. On the next day, SafeSeal micro tubes with samples were opened and HCl fumes could evaporate under a fume hood for 2 h. The dried samples were dissolved in 500 µl ddH$_2$O and 100 µl of this solution were added to 50 µl of chloramine T solution (see Table 9, pp. 45-47). Samples were incubated for 20 min at RT. Then 50 µl of DAB solution (see Table 9, pp. 45-47) was added to each well and incubated for 30 min at 65 °C in a drying chamber. The quantification of hydroxyproline was performed by a Tecan microplate reader at 560 nm, with L-hydroxyproline as standard. The amount of total collagen was calculated using a hydroxyproline to collagen ratio of 1:10 [224,225].

3.3.5 Alkaline phosphatase activity assay

For investigation of alkaline phosphatase (ALP) activity in hydrogel samples, no papain digestion was performed. Constructs were harvested, wet weights were determined, and samples were put directly in MPER buffer on ice to preserve enzyme activity of ALP. Then, small steel beads were added, and samples were homogenized using a TissueLyser at 15 Hz

for 2 min. Homogenized samples were stored at -80 °C or were directly analysed. Whenever possible, samples were stored on ice. ALP activity assay was performed using the substrate pNPP (p-nitrophenyl phosphate). pNPP solution was prepared using SIGMAFAST™ p-Nitrophenyl phosphate tablets, according to manufacturer's instructions (see Table 9, pp. 45-47). 25 µl sample were added to 50 µl pNPP solution and a kinetic measurement was performed by a Tecan microplate reader. Dephosphorylation of pNPP by ALP resulted in the production of a yellow compound that was detected at 405 nm. Readings at 655 nm were subtracted to correct for non-specific background values. The kinetic protocol run for 30 min with a reading every two minutes and shaking in between. Calf intestinal alkaline phosphatase was used as standard [226].

3.4 Quantitative real-time PCR analysis

For quantitative real-time PCR analysis, one sample was one complete hydrogel, three pellets or one 6-well full of 2D cultured cells. For pellets and hydrogels, samples were homogenized by a TissueLyser and stainless-steel beads at 25 Hz for 5 min before RNA extraction with TRIzol® reagent. cDNA was transcribed from total RNA with ImProm-II™ Reverse Transcription System Kit and MESA GREEN qPCR MasterMix Plus for SYBR® Assay No ROX was used for qPCR (quantitative polymerase chain reaction). Analysis was performed with a Real-Time PCR Detection System CFX96 Touch. Used primers (see Table 6, pp. 43-44) were obtained from two different sources: Ready to use primers from Bio-Rad and self-designed primers from Biomers. Cycling protocol for Bio-Rad primers was: 5 min at 95 °C for initial denaturation, then 40 cycles of 15 sec at 95 °C, 30 sec at 60 °C and 30 sec at 70 °C. Cycling protocol for Biomer primer was: 6 min at 95 °C for initial denaturation, then 40 cycles of 15 sec at 95 °C, 30 sec at 60 °C and 30 sec at 72 °C. A melting curve analysis for PCR product integrity was performed (0.5 °C increments from 65 °C to 95 °C). Software CFX Manager™ (software version 3.1.) was used to process the raw data and the relative expression levels were normalized to the housekeeper genes GAPDH or HPRT1 and determined using the $2^{-\Delta\Delta CT}$ method. Whenever useful, samples were additionally normalized to a d1, d0 or untreated sample value.

3.5 Flow cytometry

Flow cytometry was used to analyse the existence and quantity of cell surface receptors CD44 and CD168 on human MSCs. Therefore, cells were harvested with 0.25 % Trypsin-EDTA from an 80-90 % confluent 2D culture and stained with respective antibodies. Cells were transferred to FACS tubes and centrifuged for 7 min at 400 x g and 4 °C. Cells were blocked with 5 % goat serum in FACS buffer for 20 min at 4 °C. For permeabilization of cells, 0.3 % Triton X-100 was added to the blocking solution. Cells were washed two times with FACS buffer, then they were incubated with the primary antibodies (see Table 5, pp. 42-43) for 25 min at 4 °C. Afterwards, cells were washed two times with FACS buffer and incubated with the secondary (goat) antibody (see Table 5, pp. 42-43) for 20 min at 4 °C in the dark. Subsequently, cells were washed twice with FACS buffer and kept on ice in FACS buffer until measured. One tube of unstained cells was used to adjust the settings of the FACSCanto flow cytometer. The resulting data from the measurement were processed using FlowJo v.10.0.7.

3.6 Statistical analysis

Graph Pad Prism 6.0 (GraphPad Software, La Jolla, CA, USA) was used for statistical analysis. Statistical significance was determined with Student´s t-test (Figures 16, 31 A-D, 32 A-F, 33 A-F, 34 A-D, 35 A-D), one-way ANOVA (Figures 9, 10, 11, 13, 14, 18, 19, 24, 28, 31 E-F, 32 G-I, 33 G-I, 34 E-F, 35 E-F) or two-way ANOVA (Figures 17, 21, 22, 25). Tukey´s post-hoc test was used in conjunction with one-way and two-way ANOVA.

Results and Discussion

4 Results and discussion

4.1 Articular cartilage tissue engineering with ACPCs and MSCs

Tissue engineering is a promising approach in articular cartilage repair. Additionally, it allows for versatile research on cartilage development, function and structure which is essential knowledge to develop successful treatments for cartilage defects. Chondrocytes harvested from cartilage or stem cells that can be differentiated into chondrocytes are used to produce tissue with the aim that it will be as similar to native articular cartilage as possible. If the right combination of cell type, scaffold and other stimuli is used, cartilage similar to native tissue can be produced.

MSCs are considered as potential cell source for cartilage repair as they can differentiate into chondrocytes and do not lose this chondrogenic potential when they are expanded in 2D culture in contrast to chondrocytes [35-37]. However, they also tend to produce fibrocartilage rather than articular cartilage and can undergo terminal differentiation and hypertrophy [35,70,71]. This can lead to endochondral ossification and decreased functionality of cartilage tissue. ACPCs are a relatively new, promising cell source for cartilage repair that have been found in the upper layer of articular cartilage [92,93]. They have the same advantage over chondrocytes as MSCs because they can be expanded without losing their ability to differentiate chondrogenically [101]. In previous studies, a high chondrogenic potential and no tendency to differentiate terminally was detected [94,102]. Therefore, ACPCs are considered as promising alternative cell source for cartilage engineering. Animal models and even one pilot clinical study in humans have been used to test the suitability of ACPCs for cartilage repair [94,98,104,105]. However, only two studies have compared the chondrogenesis of MSCs and ACPCs directly in hydrogels [103,107]. As the dependence of cell performance on hydrogel composition has not been completely resolved yet, additional studies in other hydrogels are needed to critically evaluate chondrogenesis of ACPCs in comparison to MSCs.

One important factor for articular cartilage function is its zonal structure. At the moment, it cannot be restored by clinical treatments and therefore, tissue engineering has developed several strategies to produce tissue with zones similar to native cartilage. One approach uses different cell types for different zonal layers. In previous studies, a combination of ACPCs in the upper layer and MSCs in the lower layer showed promising results [103,107].

Additionally, co-culture of chondrocytes and MSCs has been reported to improve chondrogenesis [227].

Therefore, here, ACPCs and MSCs were chondrogenically differentiated in 3D agarose or HA-SH/P(AGE-co-G) hydrogel constructs for 28 days, and their produced tissue was examined and compared with the aim to determine advantageous conditions for articular cartilage regeneration. Figure 6 shows a schematic depiction of the hydrogel constructs that were produced for the experiments.
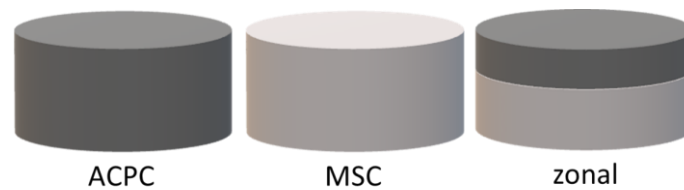

Figure 6: Schematic depiction of the structure of zonal (co-culture) and non-zonal (monoculture) constructs. This figure has been published in the International Journal of Molecular Sciences (MDPI) and was reproduced from Schmidt et al. [228].

4.1.1 Chondrogenesis of ACPCs and MSCs in agarose hydrogel

Cartilage engineering works best when the cells can experience a 3D environment. Hydrogels are often used as 3D cell carrier material as they can provide the encapsulated cells with an environment of high water content similar to the conditions in native cartilage [154]. Agarose hydrogel is known as chondro-permissive material that has been well-characterized in several cartilage tissue engineering studies [229-231]. It has been shown that this hydrogel can prevent the loss of phenotype or morphology in 3D culture of chondrocytes [32]. As described above, chondrogenesis of ACPCs and MSCs in hydrogels was only compared in two other studies so far [103,107], and none of them used the "gold-standard" hydrogel agarose. Additionally, knowledge of ACPCs reaction to low oxygen pressure in hydrogels is limited. Oxygen levels in the microenvironment of native articular cartilage (1-5 %) lie below the atmospheric oxygen levels (21 %) and therefore it is important to test *in vitro* cartilage development also under this hypoxic (also called physioxic) condition [109,232].

In the present study, ACPCs, MSCs and zonal constructs (Figure 6) were cultured in 3D agarose hydrogel under normoxic and hypoxic conditions with the aim to produce articular cartilage tissue. Survival of cells, ECM quality and quantity as well as the influence of zonal

layering and hypoxic conditions were tested. The ECM of the resulting tissues was analysed using biochemical assays, histology, immunohistochemistry and qRT-PCR.

Figure 7 shows a chronological experimental workflow for the experiments with ACPCs, MSCs and zonal agarose constructs and indicates the different harvest time points for constructs under hypoxic (2 % oxygen pressure) or normoxic (21 % oxygen pressure) conditions.
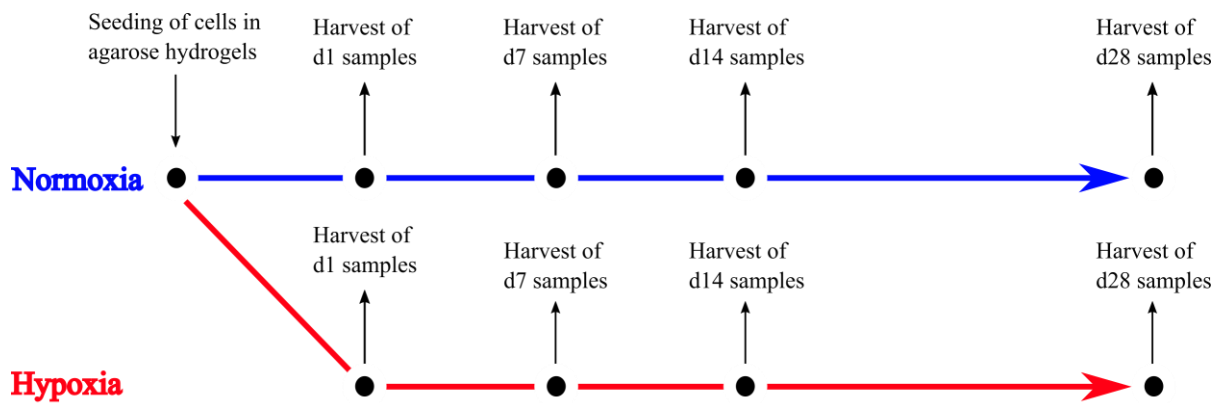

Figure 7: Experimental workflow for cartilage tissue engineering experiments in agarose hydrogels seeded with ACPCs, MSCs or zonal constructs. Medium was exchanged every two to three days.

4.1.1.1 Comparison of chondrogenesis of ACPCs and MSCs in normoxia

As a first experiment, the survival of ACPCs and MSCs in agarose hydrogels was investigated. Figure 8 shows Live/Dead staining of ACPC, MSC and zonal constructs at day 1 and at day 7 under normoxic conditions.
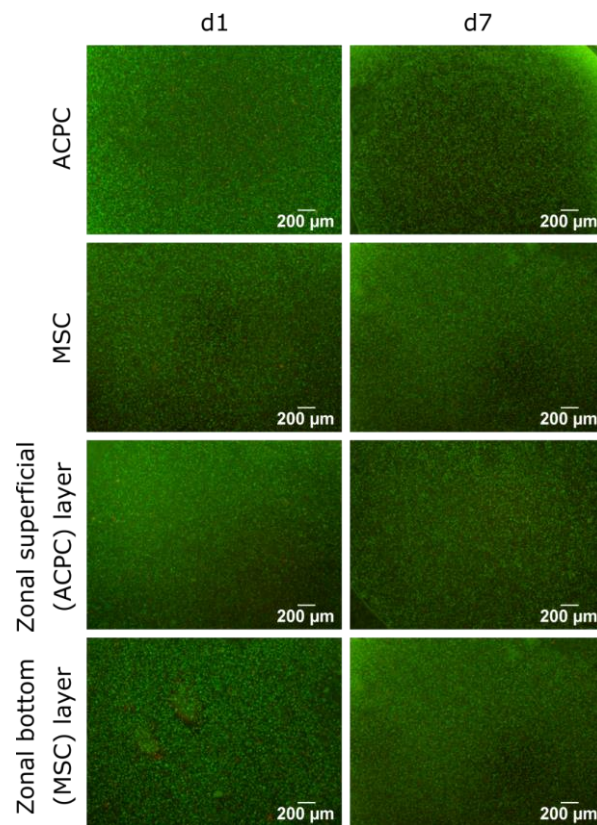
Figure 8: Staining of live and dead cells in agarose hydrogel constructs under normoxic conditions. Constructs were seeded with 20.0 x 10^6 cells ml^{-1} and stained after 1 and 7 days of chondrogenic differentiation under normoxic conditions. ACPCs and MSCs were either cultured alone or in zonally layered co-culture constructs. This figure was published as part of another figure in the International Journal of Molecular Sciences (MDPI) and was adapted from Schmidt et al. [228].

Living cells were stained with calcein-AM and were coloured green, while dead cells were stained with ethidium homodimer III and appeared red in Figure 8. The green cells strongly outnumbered the red cells in this experiment which means that most of the cells survived the seeding and change from 2D into 3D environment, and only a small amount died from the procedure. After seven days, the staining showed similar ratios of live and dead cells as on d1. From these results it can be assumed that the culture conditions were favourable for the survival of the cells. There seemed to be no significant difference in the number of dead cells between MSCs and ACPCs. The staining showed similar ratios of green and red

staining for ACPCs and MSCs. Therefore, one can assume that the survival of the different cells was not affected differently by the culture conditions.

Proliferation is, next to survival, an important factor that can affect the number of seeded cells over the course of the experiments. As different cell types can have different proliferation rates in different environments, the amount of DNA was measured at the beginning, during and at the end of the experiments (Figure 9). DNA amount can be directly correlated with the number of cells [222].
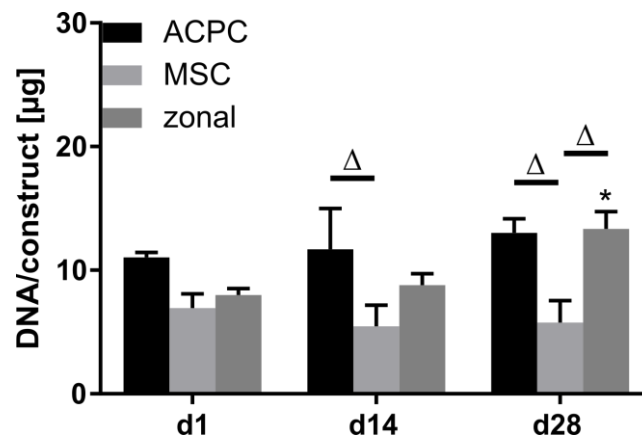
Figure 9: DNA content in ACPC, MSC, and zonal constructs under normoxic conditions. Biochemical analysis of DNA amount in agarose hydrogel constructs, seeded with 20.0×10^6 cells ml^{-1}, after 1, 14, and 28 days of chondrogenic differentiation under normoxic conditions. ACPCs and MSCs were either cultured alone or in zonally layered co-culture constructs. Data are presented as means ± standard deviation (n=3 biological replicates). (*) indicates statistically significant differences between a d14 or d28 value and the corresponding d1 value of the same group ($p < 0.05$). (Δ) indicates statistically significant differences between groups. This figure was published as part of another figure in the International Journal of Molecular Sciences (MDPI) and was adapted from Schmidt et al. [228].

A quantitative biochemical DNA assay revealed that ACPC constructs showed significantly higher amounts of DNA than MSCs at d14 and d28 (Figure 9). DNA amount of MSCs did not change significantly over time. Zonal constructs at d28 had significantly higher amounts of DNA than MSCs. Zonal constructs at d28 were also the only group that showed significantly higher DNA levels than the same group at d1 (Figure 9). These results suggested that although ACPCs did not grow significantly more from d1 to d28, the changes in cell numbers still led to significantly different cell numbers in ACPC and MSC constructs. Only co-culture in zonal constructs led to significant increase in cell numbers. Since the zonal layers were not analysed separately, it is hard to say which cells proliferated in the zonal constructs. However, co-culture between MSCs and chondrocytes increased proliferation of chondrocytes through MSC-secreted factors in previous studies [77,233-235]. As ACPCs

are a subpopulation of chondrocytes, it can be assumed that ACPCs were the cells that proliferated in zonal co-culture constructs, and that the proliferation was due to factors secreted by MSCs.

As GAGs (glycosaminoglycans) are a major component of articular cartilage, they are a good indicator for successful chondrogenesis. In this study, the amount of produced GAG was analysed using a quantitative GAG assay and histological safranin O staining (Figure 10).
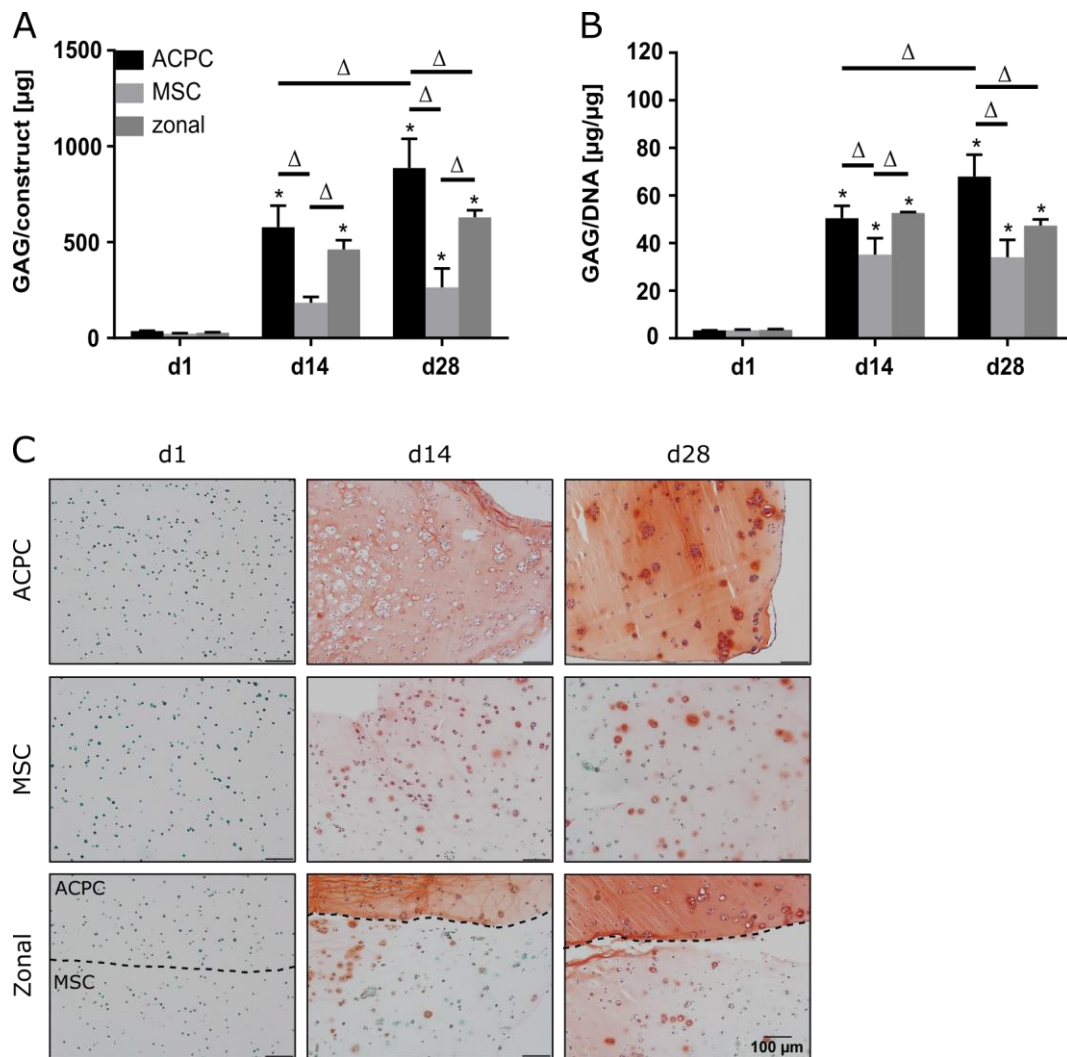

Figure 10: GAG production in ACPC, MSC, and zonal constructs under normoxic conditions. Biochemical and histological analysis of GAG in agarose hydrogel constructs, seeded with 20.0×10^6 cells ml^{-1}, after 1, 14, and 28 days of chondrogenic differentiation under normoxic conditions. ACPCs and MSCs were either cultured alone or in zonally layered co-culture constructs. **(A)** Production of total GAG (GAG/construct) and **(B)** GAG normalized to DNA (GAG/DNA). Data are presented as means ± standard deviation (n=3 biological replicates). (*) indicates statistically significant differences between a d14 or d28 value and the corresponding d1 value of the same group ($p < 0.05$). (Δ) indicates statistically significant differences between groups, or within a group between time points ($p < 0.05$). **(C)** Histological safranin-O staining for visualization of produced GAG. In zonal constructs, the upper layer contained ACPCs and the lower layer MSCs (indicated by

the dashed line). This figure has been published in the International Journal of Molecular Sciences (MDPI) and was reproduced from Schmidt et al. [228].

Figure 10 A shows the amount of GAG per one construct, and Figure 10 B shows the amount of produced GAG per DNA. The normalisation "per DNA" includes the information from Figure 9 (p. 67) and is used for better comparability between the constructs of different cell types with different amounts of cells. Figures 10 A and B show that all three constructs (ACPC, MSC, zonal) produced significant amounts of GAG over the time of the experiment. However, ACPCs produced significantly more GAG than MSCs up to d14 and d28. On d28, the amount of GAG in ACPC constructs was even significantly higher than the amount in zonal constructs. GAG amount of ACPC constructs also increased significantly from d14 to d28 contrary to MSC and zonal constructs. Zonal constructs contained significantly more GAG than MSC constructs on d14 and d28 except for d28 in Figure 10 B. The difference in GAG production between ACPCs and MSCs was also clearly visible in the histological safranin O staining (Figure 10 C). The signal for MSC constructs was much weaker than the signal for ACPC constructs at d14 and d28. While ACPCs seemed to spread their GAG evenly through the whole construct with a stronger staining around the cells, MSCs mainly showed staining around the cells with only very faint staining in the rest of the gel. These trends were reflected in zonal constructs where the two layers can be distinguished easily by staining of the contained GAG. The upper layer with ACPCs was stained more intensely than the lower MSC layer. The mixture of the ACPC layer that contained high levels of GAG and the less GAG containing MSC layer in zonal constructs could explain GAG levels of zonal constructs in Figure 10 A and B that lay between the levels of ACPCs and MSCs. These results suggested that ACPCs produced more GAG in agarose gel than MSCs. A direct effect of the co-culture of ACPCs and MSCs in zonal gels on the production of GAG could not be detected.

Collagen is another important component of articular cartilage tissue. As chondrogenesis of ACPCs and MSCs was compared in this study, the production of total collagen was analysed using a quantitative hydroxyproline assay and picrosirius red staining of the hydrogels (Figure 11). The amount of total collagen per construct significantly increased in all three constructs (ACPC, MSC, zonal) from d1 to d14 and from d14 to d28 (Figure 11 A). The levels of total collagen per construct in the different constructs were similar at the different time points (Figure 11 A). However, when collagen was normalised to the amount of DNA in the constructs, MSCs showed significantly higher levels of collagen than ACPCs and

zonal constructs on d14 and d28 (Figure 11 B). Except for ACPCs on d14, all constructs significantly increased their collagen per DNA levels in comparison to d1 and MSC constructs showed a significantly higher amount of collagen per DNA on d28 compared to d14 (Figure 11 B). Staining of total collagen showed higher intensity for MSC than for ACPC constructs. However, differences were not as prominent as in the safranin O staining for GAG (Figure 10 C, p. 68). Zonal co-culture constructs showed similar staining signal for both layers at d28 and more intense signal for the ACPC layer than the MSC layer on d14. These results suggested that MSCs produced more collagen per cell than ACPCs but the total amount of collagen in the hydrogels was similar because of the higher cell number of ACPCs.
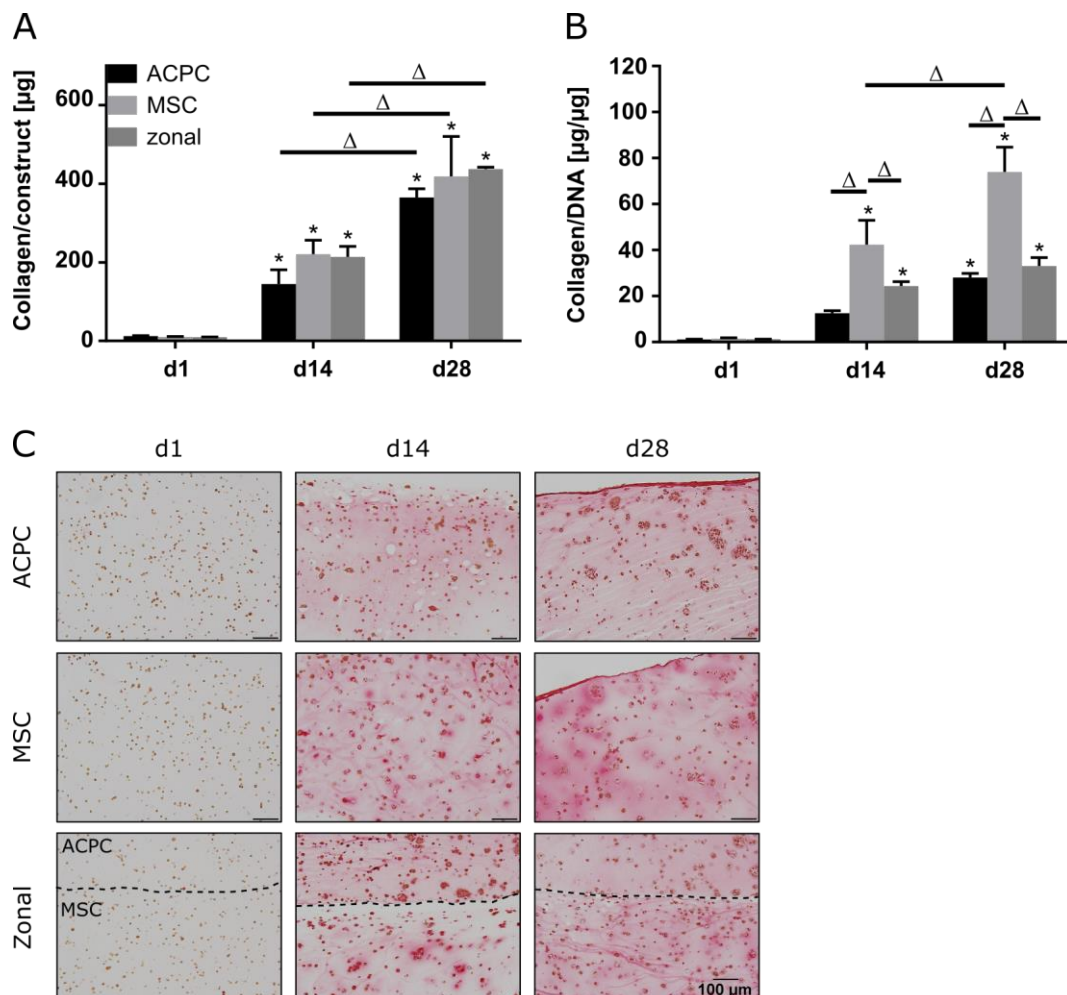
Figure 11: Collagen production in ACPC, MSC, and zonal constructs under normoxic conditions. Biochemical and histological analysis of collagen in agarose hydrogel constructs, seeded with 20.0 x 10^6 cells ml^{-1}, after 1, 14, and 28 days of chondrogenic differentiation under normoxic conditions. ACPCs and MSCs were either cultured alone or in zonally layered co-culture constructs. **(A)** Production of total collagen (collagen/construct) and **(B)** collagen normalized to DNA (collagen/DNA). Data are presented as means ± standard deviation (n=3 biological replicates). (*) indicates statistically significant differences between a d14 or d28

value and the corresponding d1 value of the same group (p < 0.05). (Δ) indicates statistically significant differences between groups, or within a group between time points (p < 0.05). **(C)** Histological picrosirius red staining for visualization of produced collagen. This figure was published as part of another figure in the International Journal of Molecular Sciences (MDPI) and was adapted from Schmidt et al. [228].

There are many different types of collagen, and different (cartilage) tissues contain different types and amounts of them. Articular cartilage contains mostly type II collagen, while type I collagen is more common in fibrocartilage [2-4]. Type VI collagen is concentrated pericellularly around the cells in normal articular cartilage [236,237]. Therefore, the produced collagen was analysed further using immunohistochemistry to distinguish the different collagen types that were present. Type II collagen staining increased over time for ACPC and MCS constructs. They were similarly intense at d14 as well as at d28 (Figure 12 A). This was reflected in the zonal constructs except for the upper ACPC layer at d14. This layer seemed to be more intensely stained in co-culture constructs than in monoculture ACPC constructs (Figure 12 A). Type I collagen was strongly stained in MSC hydrogels at d14 and d28, whereas staining was distinctly weaker in ACPC hydrogels. Zonal constructs showed similar tendencies, but type I collagen seemed to be more intense in the upper ACPC layer of co-culture constructs than in monolayer ACPC constructs (Figure 12 B). Type VI collagen was located mainly pericellularly around the cells on d14 and d28 for both MSCs and ACPCs (Figure 12 C). This distribution was similar to type VI collagen in native articular cartilage [237]. Zonal constructs showed similar staining. As the production of type II collagen appeared to be similar between ACPCs and MSCs but MSCs produced distinctly more type I collagen (Figure 12), the higher total amount of collagen produced by MSCs per cell (Figure 11, p. 70) seemed to be due to a higher expression of type I collagen. However, it also had to be considered that ACPC constructs contained more cells then MSC constructs (Figure 9, p. 67) and therefore it was difficult to compare the levels of type II collagen per cell between ACPCs and MSCs. The distinctly lower type I collagen level in ACPC constructs despite a higher cell number suggested that ACPCs probably produced markedly less type I collagen per cell than MSCs. In articular cartilage, type I collagen is usually not present. It is an indicator for formation of fibrocartilage that is not desirable in articular cartilage regeneration because it is less stable and cannot fulfil the functions of articular cartilage long-term [238-241].
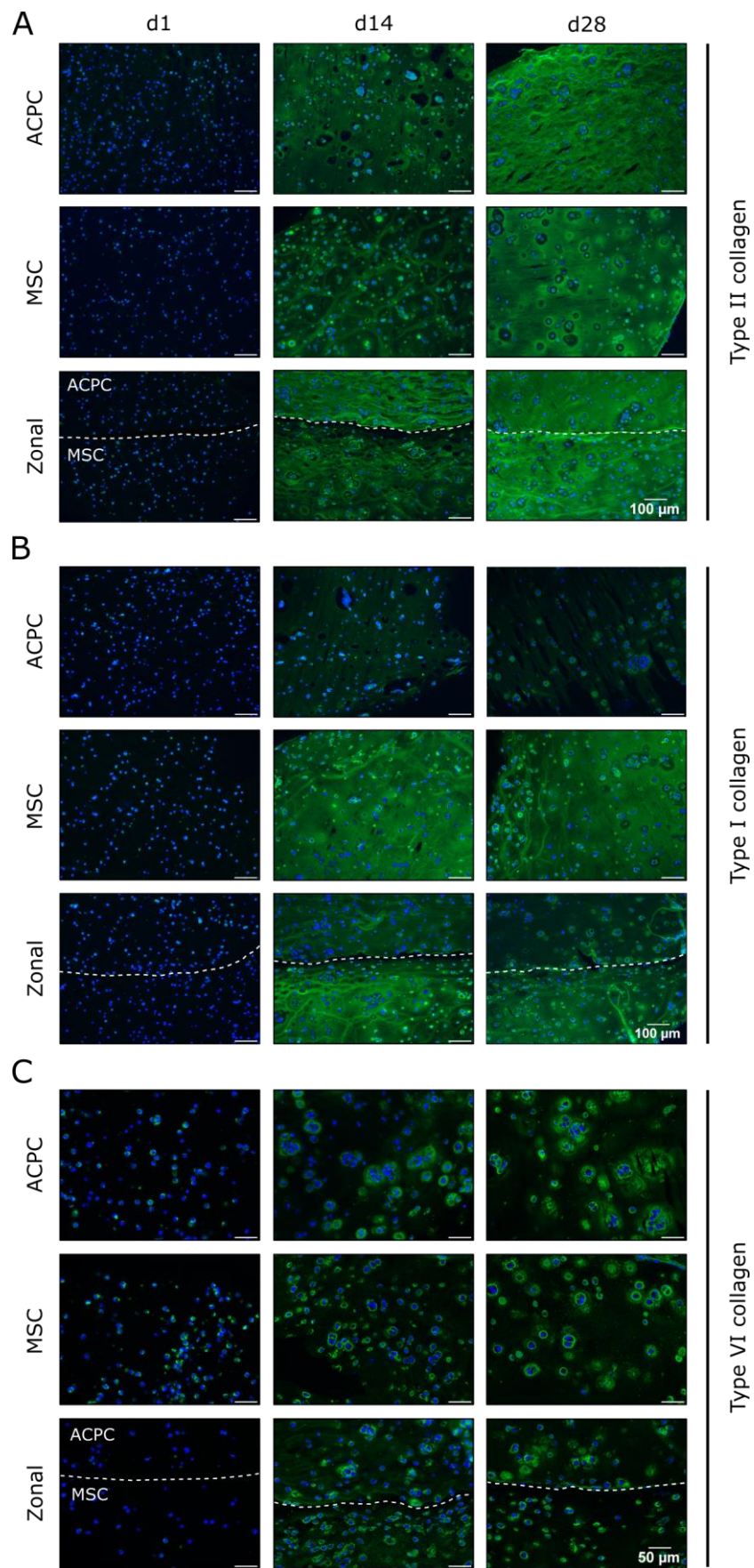
Figure 12: Staining of ACPC, MSC, and zonal constructs cultured under normoxic conditions for type II, I and VI collagen. Immunohistochemical staining for type II, I and VI collagen in agarose hydrogel constructs, seeded with 20.0 x 10^6 cells ml^{-1}, after 1, 14 and 28 days of chondrogenic differentiation under

normoxic conditions. ACPCs and MSCs were either cultured alone or in zonally layered co-culture constructs. **(A)** Immunohistochemical staining for type II collagen. **(B)** Immunohistochemical staining for type I collagen. **(C)** Immunohistochemical staining for type VI collagen. In zonal constructs, the upper layer contained ACPCs and the lower layer MSCs (indicated by the dashed line). This figure has been published as part of another figure in the International Journal of Molecular Sciences (MDPI) and was adapted from Schmidt et al. [228].

Zonal layering and co-culture of ACPCs and MSCs also seemed to influence the expression of the different collagen types. The more intense type I collagen staining of ACPCs in co-culture was not a desirable outcome but is interesting, nonetheless. However, ACPCs also seemed to have a more intense type II collagen staining in co-culture than in monoculture on d14 (Figure 12 A). This effect has also been observed in a different study, where gene expression of ACPC and MSC co-culture was analysed [107].

To further analyse chondrogenesis of ACPCs and MSCs, the relative gene expression of ACAN, PRG4, COL2A1 and COL1A1 was determined (Figure 13). Similar trends as in biochemical assays and stainings were detected.
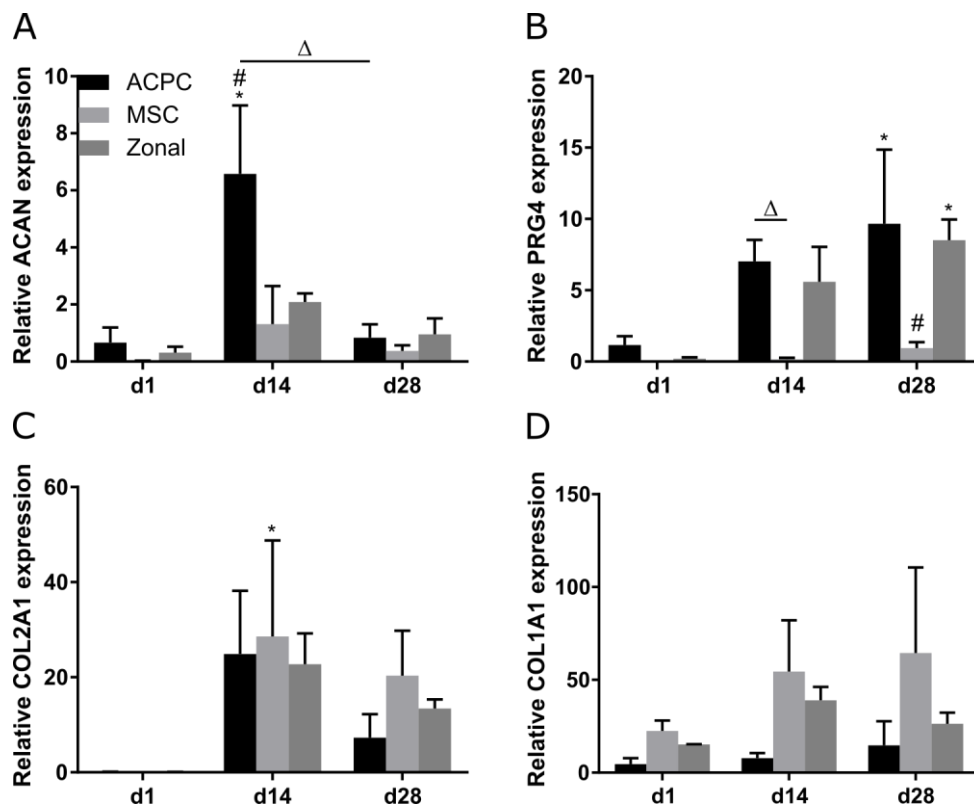

Figure 13: Relative gene expression in ACPC, MSC, and zonal agarose constructs under normoxic conditions. Gene expression as determined by qRT-PCR in agarose hydrogel constructs, seeded with 20.0×10^6 cells ml^{-1}, after 1, 14, and 28 days of chondrogenic differentiation under normoxic conditions. ACPCs and MSCs were either cultured alone or in zonally layered co-culture constructs. Relative expression of **(A)** ACAN (encoding aggrecan), **(B)** PRG4 (lubricin), **(C)** COL2A1 (type II collagen), and **(D)** COL1A1 (type I collagen). Data are presented as means ± standard deviation (n=3 biological replicates). (*) indicates statistically

The genes encoding the proteoglycans aggrecan (ACAN) and lubricin (PRG4) showed significantly higher expression levels in ACPCs than in MSCs (Figure 13 A, B) except for ACAN at d28. This corresponded to the higher GAG expression of ACPCs compared to MSCs (Figure 10, p. 68) as GAGs are part of proteoglycans in cartilage tissue [3].

The reduced ACAN expression level of ACPCs at d28 could be the result of a beginning back-steering mechanism when enough aggrecan has been produced and the formed neo-cartilage passes over into a more balanced and mature state. ACAN expression in zonal constructs was similar to the expression in MSC constructs at d14 and also stayed low at d28. In contrast, PRG4 expression levels in zonal constructs were more similar to ACPC constructs and therefore distinctly higher than in MSC constructs (Figure 13 A, B). As the different zones of layered constructs were not analysed separately in this study, it was difficult to determine how exactly the different cells in co-culture were affected by one another. The expression levels of COL2A1 (type II collagen) and COL1A1 (type I collagen) did not differ significantly between ACPC, MSC or zonal constructs (Figure 13 C, D). However, COL1A1 gene expression in ACPCs was clearly decreased on d14 and d28 in comparison to MSCs (Figure 13 D) which corresponded to the less intense type I collagen staining of ACPCs compared to MSCs (Figure 12 B, p. 72).

Terminal differentiation and hypertrophy that can lead to endochondral ossification of cartilage tissue are a serious problem for the regeneration of functional articular cartilage [70]. Therefore, the activity of alkaline phosphatase (ALP), a marker for terminal differentiation, was analysed in the different constructs in this study (Figure 14). ALP activity is important in the mineralization and development of bone, but mineralization in articular cartilage tissue leads to decreased functionality of the tissue [70].
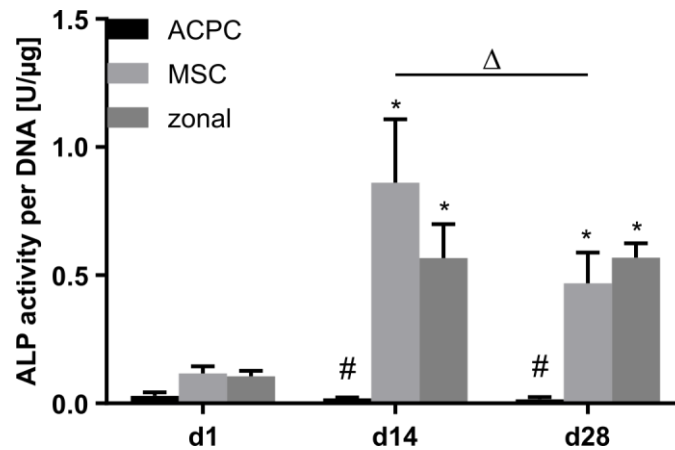
Figure 14: Alkaline phosphatase activity in ACPC, MSC, and zonal agarose constructs under normoxic conditions. ALP activity in agarose hydrogel constructs, seeded with 20.0×10^6 cells ml^{-1}, after 1, 14, and 28 days of chondrogenic differentiation under normoxic conditions. ACPCs and MSCs were either cultured alone or in zonally layered co-culture constructs. Data are presented as means $\pm$ standard deviation (n=3 biological replicates). (*) indicates statistically significant differences between a d14 or d28 value and the corresponding d1 value of the same group (p < 0.05). (#) indicates statistically significant differences of this group compared to the other two groups that share the same time point (p < 0.05). (Δ) indicates statistically significant differences between groups, or within a group between time points (p < 0.05). The data of this figure were published as part of another figure in the International Journal of Molecular Sciences (MDPI) and this figure was adapted from Schmidt et al. [228].

Figure 14 clearly shows low levels of ALP in ACPC constructs on all days, while MSC and zonal constructs showed significantly increased ALP activity levels on d14 and d28 and in comparison to ACPCs on both days. While the activity in MSC constructs seemed to significantly decrease from d14 to d28, it did not change in zonal constructs (Figure 14). MSCs are known for their tendency to differentiate terminally [35,70,71], but previous studies on co-culture between MSCs and chondrocytes reported reduction of hypertrophy in the co-cultured constructs [75-78]. As ACPCs are a subpopulation of chondrocytes, a similar effect could have been expected. However, zonal co-culture constructs in the present study showed ALP activity akin to that of MSC constructs. Other previous studies indicated that direct contact between co-cultured cells was an essential prerequisite for reduction of hypertrophy in the constructs [242,243]. In the present study, ACPCs and MSCs did have only limited contact to each other in zonal constructs. This might have been the reason why hypertrophy was not reduced in co-culture constructs in the present work.

In summary, both ACPCs and MSCs were able to produce neo-cartilage tissue in agarose hydrogel under normoxic conditions. Zonal constructs mostly reflected the respective monocultures. ACPCs produced a more articular cartilage-like tissue than MSCs as ACPC constructs contained more GAG, less type I collagen and little ALP activity and therefore seemed to be a suitable promising alternative cell source for articular cartilage regeneration.

75

4.1.1.2 Influence of hypoxia on chondrogenesis of ACPCs and MSCs

The survival of ACPCs and MSCs that were seeded into agarose hydrogel and were then cultured under hypoxic conditions (2 % oxygen) was tested in the same way as the samples from normoxic conditions (21 % oxygen). Living cells were stained with calcein-AM (green), and the nuclei of dead cells were stained with ethidium homodimer III (red) (Figure 15). As in normoxia, green living cells were much more abundant than red dead cells (Figure 15). No differences could be detected between the stainings of d1 and d7 or between MSCs and ACPCs. This suggests that both cell types survived the seeding and the following culture under hypoxic conditions well, and few cells died in the process, similar to the findings for cells cultured under normoxic conditions.
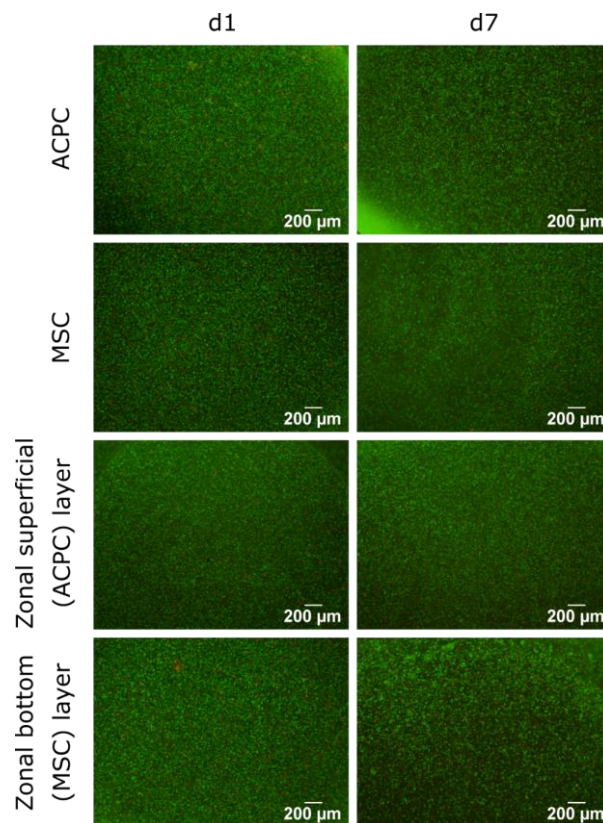

Figure 15: Staining of live and dead cells in agarose hydrogel constructs under hypoxic conditions. Constructs were seeded with 20.0 x 10^6 cells ml^{-1} and stained after 1 and 7 days of chondrogenic differentiation under hypoxic conditions. ACPCs and MSCs were either cultured alone or in zonally layered co-culture constructs. This figure was published as part of another figure in the International Journal of Molecular Sciences (MDPI) and was adapted from Schmidt et al. [228].

As a next step, it was proven that the hypoxic conditions in this study really induced a hypoxic environment for the cell laden constructs. Therefore, relative gene expression levels of phosphoglycerate kinase 1 (PGK1), glucose transporter 1 (GLUT1), C-X-C motif

chemokine ligand 12 (CXCL12) and stanniocalcin 1 (STC1) were analysed. These are genes that are known to be upregulated by hypoxia inducible factors (HIFs) as reaction to low oxygen tension [244,245]. For all tested genes, relative expression was upregulated under hypoxic conditions in comparison to normoxic conditions in both ACPCs and MSCs (Figure 16). STC1 gene expression was the only one that was not upregulated significantly but with a strong upward trend. This demonstrated that the conditions used in this study were able to provide a hypoxic environment for the cells and that they reacted to this environment in the expected manner with upregulation of HIF target genes.
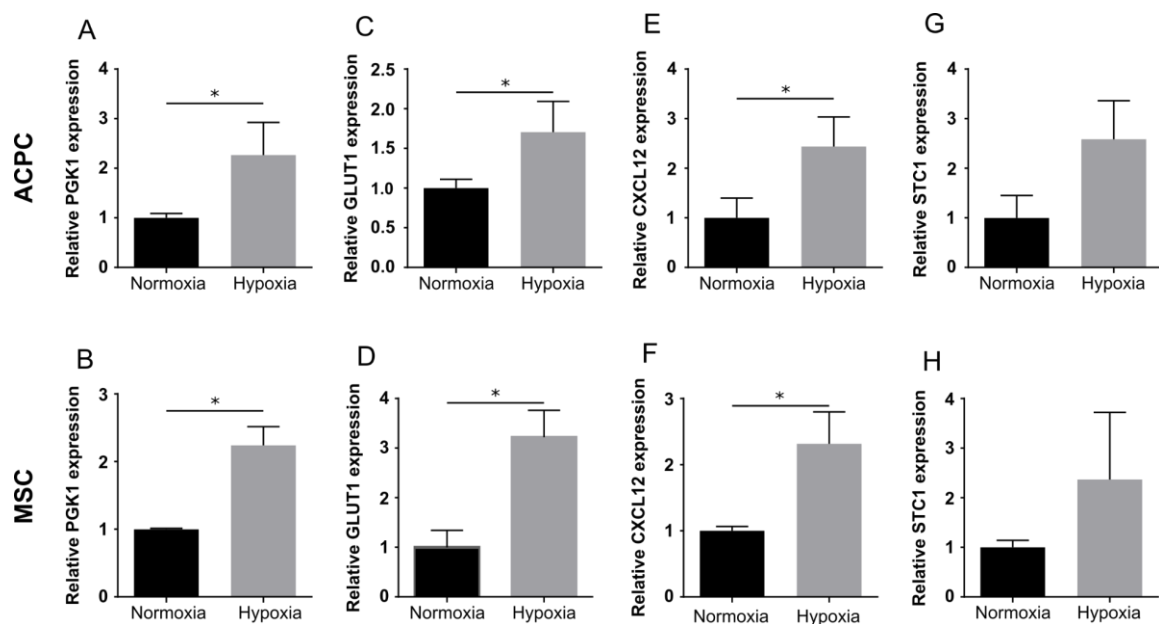

Figure 16: Relative gene expression of HIF target genes in ACPC and MSC agarose constructs. Gene expression as determined by qRT-PCR in agarose hydrogel constructs, seeded with 20.0×10^6 cells ml^{-1}, after 7 days of chondrogenic differentiation under hypoxic (2 % O_2) and normoxic (21 % O_2) conditions. Relative expression of PGK1 in **(A)** ACPC constructs and **(B)** MSC constructs. Relative expression of GLUT1 in **(C)** ACPC constructs and **(D)** MSC constructs. Relative expression of CXCL12 in **(E)** ACPC constructs and **(F)** MSC constructs. Relative expression of STC1 in **(G)** ACPC constructs and **(H)** MSC constructs. Data are presented as means ± standard deviation (n=3 biological replicates). (*) indicates statistically significant differences between two values ($p < 0.05$). Gene expression levels of HIF target genes were normalized to the gene expression of the housekeeping gene HPRT1 and to the gene expression levels of the respective normoxia values. This figure has been published in part in the International Journal of Molecular Sciences (MDPI) and was adapted from Schmidt et al. [228].

The DNA amount of constructs cultured in normoxia or hypoxia was compared to identify if cells grew differently in different oxygen environment. Figure 17 shows the different DNA amounts of constructs at d1, d14 and d28 under hypoxic or normoxic conditions. Normoxia samples are shown as striped columns because they were already discussed before (Figure 9, p. 67) and are shown only as comparison to hypoxic samples. It was

determined that DNA amounts in hypoxia treated samples were similar to the amounts of normoxia treated samples (Figure 17). The most prominent difference was the reduced DNA amount of zonal constructs at d28 in hypoxia compared to normoxia. Zonal constructs at d28 were the only samples in normoxia that showed a significantly higher DNA amount compared to d1. This difference was gone in hypoxia. This could mean that the effect of MSC-secreted factors on ACPCs that led to an increased cell growth in zonal constructs in normoxia [77,233-235] was inhibited by the hypoxic environment.
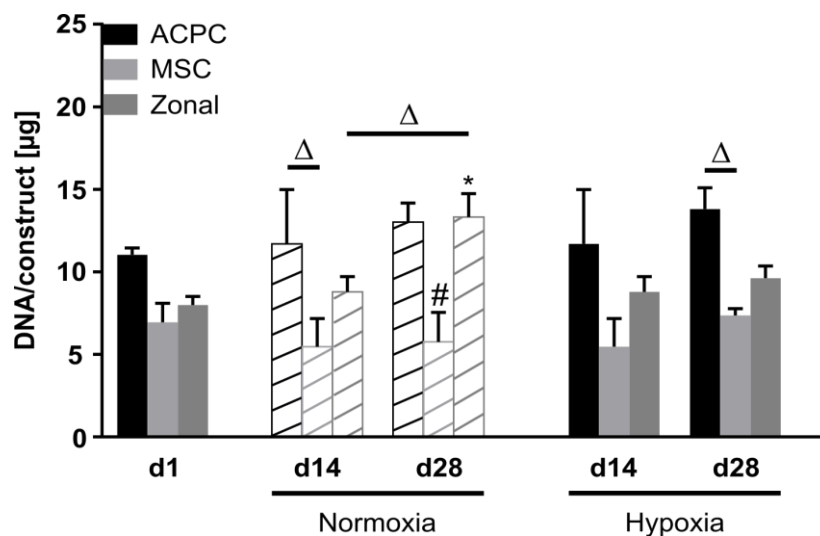

Figure 17: DNA content in ACPC, MSC, and zonal agarose constructs under normoxic and hypoxic conditions. Biochemical analysis of DNA amount in agarose hydrogel constructs, seeded with 20.0×10^6 cells ml^{-1}, after 1, 14, and 28 days of chondrogenic differentiation under normoxic (21 % O_2) or hypoxic (2 % O_2) conditions. ACPCs and MSCs were either cultured alone or in zonally layered co-culture constructs. Normoxia values are shown as striped columns because they were already discussed before (Figure 9, p. 67). Data are presented as means ± standard deviation (n=3 biological replicates). (*) indicates statistically significant differences between a d14 or d28 value and the corresponding d1 value of the same group (p < 0.05). (#) indicates statistically significant differences of this group compared to the other two groups that share the same time point and oxygen condition (p < 0.05). (Δ) indicates statistically significant differences between groups, or within a group between time points (p < 0.05). The data of this figure were published in the International Journal of Molecular Sciences (MDPI) and this figure was adapted from Schmidt et al. [228].

In the following, the ECM content of ACPC, MSC and zonal constructs under hypoxic conditions is described. First, GAG content was analysed like in normoxic samples. The biochemical GAG assay showed that all constructs produced significant amounts of GAG over 28 days (Figure 18 A, B). ACPC and zonal constructs produced significantly more GAG than MSC constructs on d14 and d28 (Figure 18 A, B). This was the case for total GAG per construct (Figure 18 A) as well as for GAG per DNA (Figure 18 B). When GAG per construct was measured, ACPCs showed a significant increase of GAG from d14 to d28 and a significantly higher value for ACPCs on d28 than for zonal constructs (Figure 18 A).

These differences were not significant when GAG was normalized to DNA (Figure 18 B). The slightly higher DNA amount of ACPCs on d28 compared to d14 (Figure 17, p. 78) is probably the reason for the lower GAG/DNA value on d28 (Figure 18 B). The results of the quantitative GAG assay were very similar to GAG values under normoxic conditions (Figure 10, p. 68), both in the range and in the differences between the groups. Safranin O staining reflected the findings made in the quantitative assay (Figure 18 C) and was therefore also comparable to the staining of normoxia samples (Figure 10, p. 68).
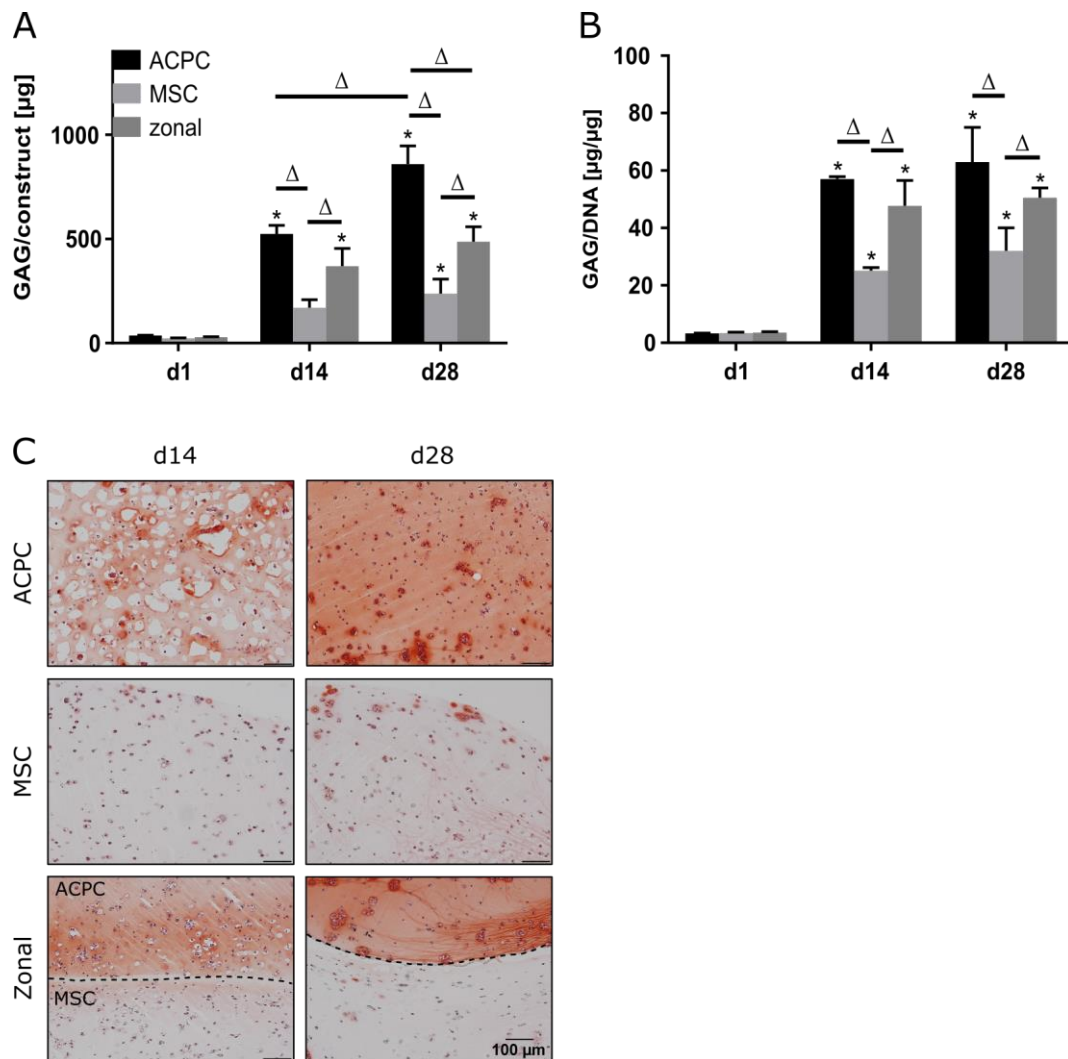

Figure 18: GAG production in ACPC, MSC, and zonal agarose constructs under hypoxic conditions. Biochemical and histological analysis of GAG in agarose hydrogel constructs, seeded with 20.0 x 10^6 cells ml^{-1}, after 1, 14, and 28 days of chondrogenic differentiation under hypoxic conditions. ACPCs and MSCs were either cultured alone or in zonally layered co-culture constructs. **(A)** Production of total GAG (GAG/construct) and **(B)** GAG normalized to DNA (GAG/DNA). Data are presented as means ± standard deviation (n=3 biological replicates). (*) indicates statistically significant differences between a d14 or d28 value and the corresponding d1 value of the same group ($p < 0.05$). (Δ) indicates statistically significant differences between groups, or within a group between time points ($p < 0.05$). **(C)** Histological safranin O staining for visualization of GAG produced under hypoxic conditions. In zonal constructs, the upper layer contained

ACPCs and the lower layer MSCs (indicated by the dashed line). This figure was published in the International Journal of Molecular Sciences (MDPI) and was reproduced from Schmidt et al. [228].

The production of collagen was analysed next. The quantitative assay revealed that all groups produced distinct levels of collagen in agarose hydrogel under hypoxic conditions (Figure 19 A, B).
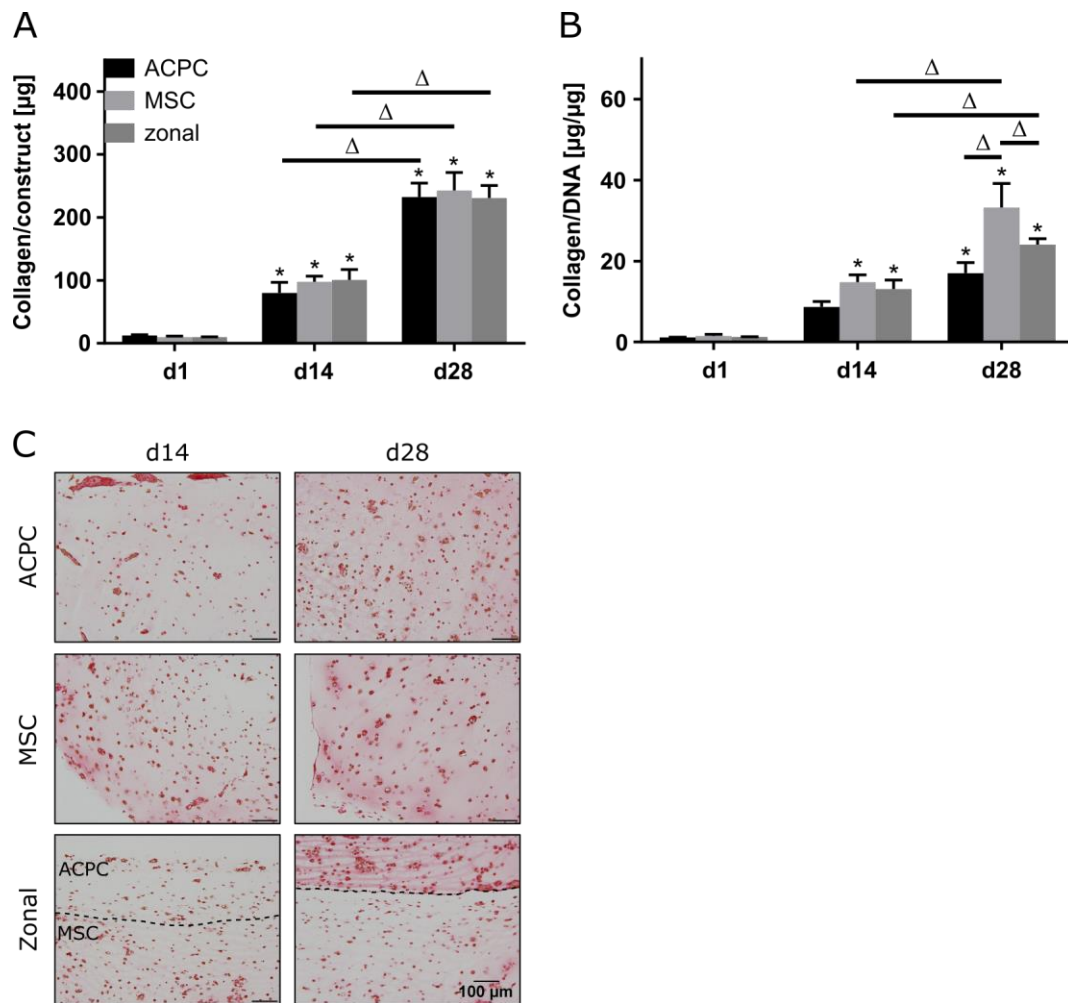

Figure 19: Collagen production in ACPC, MSC, and zonal agarose constructs under hypoxic conditions. Biochemical and histological analysis of collagen in agarose hydrogel constructs, seeded with 20.0×10^6 cells ml^{-1}, after 1, 14, and 28 days of chondrogenic differentiation under hypoxic conditions. ACPCs and MSCs were either cultured alone or in zonally layered co-culture constructs. **(A)** Production of total collagen (collagen/construct) and **(B)** collagen normalized to DNA (collagen/DNA). Data are presented as means ± standard deviation (n=3 biological replicates). (*) indicates statistically significant differences between a d14 or d28 value and the corresponding d1 value of the same group ($p < 0.05$). (Δ) indicates statistically significant differences between groups, or within a group between time points ($p < 0.05$). **(C)** Histological picrosirius red staining for visualization of produced collagen under hypoxic conditions. In zonal constructs, the upper layer contained ACPCs and the lower layer MSCs (indicated by the dashed line). This figure was published as part of another figure in the International Journal of Molecular Sciences (MDPI) and was adapted from Schmidt et al. [228].

The amount of collagen per construct increased significantly from d1 to d14 and from d14 to d28 (Figure 19 A). The same was true for samples that were cultured under normoxic conditions (Figure 11 A, p. 70), however, in hypoxia, all values were only approximately half of the respective values under normoxic conditions (Figure 19 A). When collagen was normalized to DNA (Figure 19 B), MSC and zonal constructs significantly increased their collagen content from d1 to d14 and from d14 to d28. ACPC constructs on d28 were significantly higher than on d1. MSCs produced significantly more collagen than ACPCs and zonal constructs on d28. Collagen/DNA values were, like total collagen values, approximately half as high in hypoxia (Figure 19 B) as in normoxia (Figure 11 B, p. 70). This effect was also visible in the picrosirius red stainings (Figure 19 C) that were weaker than picrosirius red stainings under normoxic conditions (Figure 11 C, p. 70). Altogether, hypoxia reduced collagen production in all three groups in agarose hydrogel.

The production of different types of collagen (type I, II and VI) was analysed under hypoxic conditions (Figure 20) to get an insight on how it was changed by low oxygen pressure and which of the different collagens was affected by the decrease of total collagen in hypoxia (Figure 19, p. 80). Type II collagen (Figure 20 A) was stained more intensely in ACPC monoculture constructs compared to MSC constructs and zonal constructs showed a more intense staining for ACPCs in the upper layer than in monoculture (Figure 20 A). ACPC constructs displayed distinctly less intense staining for type I collagen (Figure 20 B) than MSC constructs. However, type I collagen staining was considerably weaker in the zonal lower layer with MSCs than in the MSC monoculture (Figure 20 B). MSCs and ACPCs showed distinctly weaker staining for type II collagen in hypoxia (Figure 20 A) compared to normoxia (Figure 12 A, p. 72). This decrease was more pronounced in MSCs and also visible in the lower layer of zonal constructs (Figure 20 A). Type VI collagen (Figure 20 C) staining was very similar to the staining of normoxia samples (Figure 12 C, p. 72) as it was mostly pericellular around the cells for both ACPCs and MSC and monocultures as well as zonal co-cultures. This type VI collagen localisation was similar to the distribution in native articular cartilage [237].
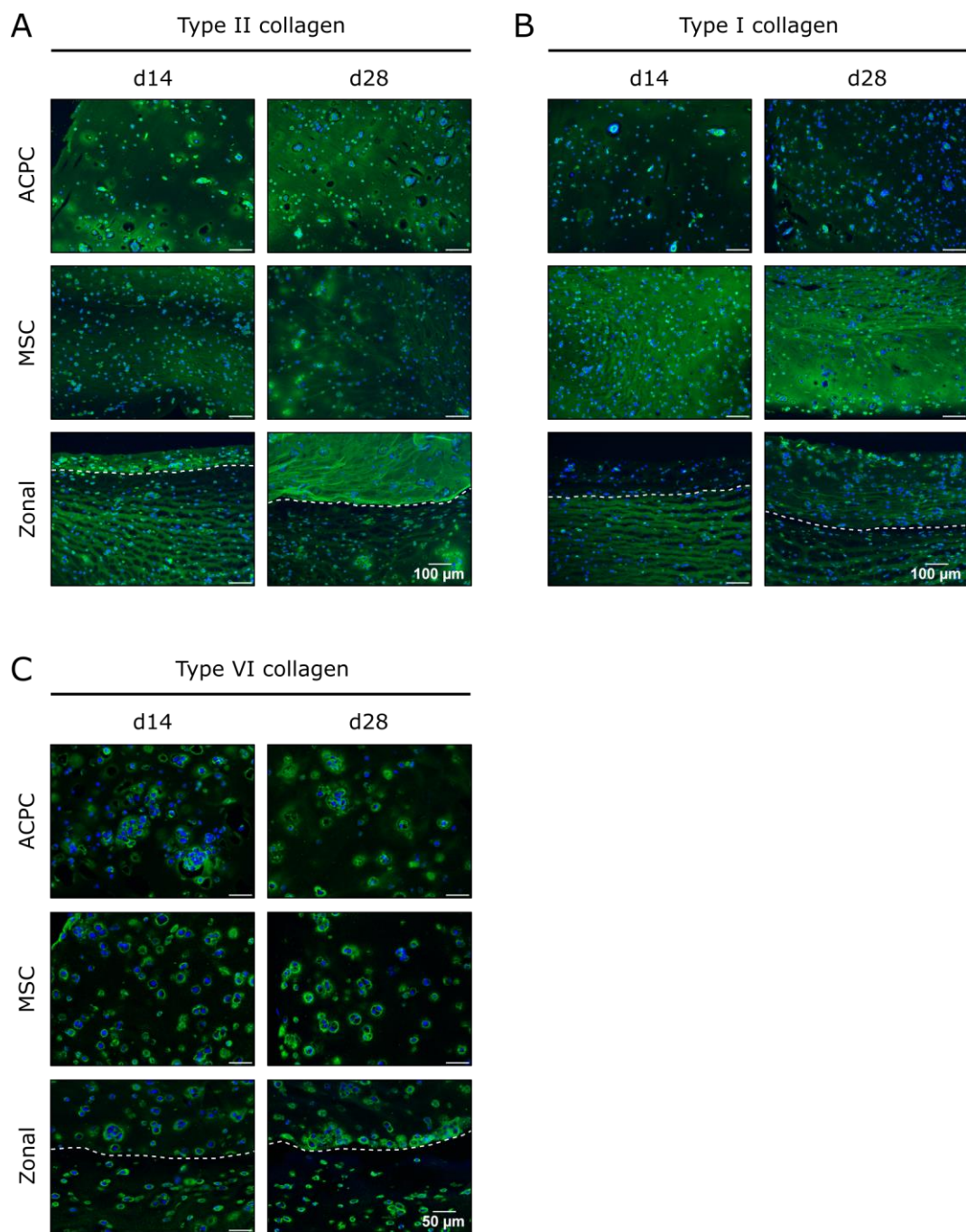
Figure 20: Staining of ACPC, MSC, and zonal agarose constructs cultured under hypoxic conditions for type II, I and VI collagen. Immunohistochemical staining for type II, I and VI collagen in agarose hydrogel constructs, seeded with 20.0×10^6 cells ml^{-1}, after 14 and 28 days of chondrogenic differentiation under hypoxic conditions. ACPCs and MSCs were either cultured alone or in zonally layered co-culture constructs. **(A)** Immunohistochemical staining for type II collagen. **(B)** Immunohistochemical staining for type I collagen. **(C)** Immunohistochemical staining for type VI collagen. In zonal constructs, the upper layer contained ACPCs and the lower layer MSCs (indicated by the dashed line). This figure was published as part of another figure in the International Journal of Molecular Sciences (MDPI) and was adapted from Schmidt et al. [228].

The combination of co-culture and hypoxia seemed to be favourable for the production of more hyaline cartilage tissue as it increased production of type II collagen in ACPCs and reduced type I collagen production in MSCs. Co-culture and hypoxia have both been

described as conditions that can improve chondrogenesis [77,115]. Interestingly, in this study, hypoxic conditions seemed to only have positive influence on collagen production when combined with co-culture. By the reduction of type I collagen production, it directed MSCs towards production of a more hyaline type of cartilage. Otherwise, however, ECM quantity and quality did not increase due to low oxygen pressure. There are previous studies that also showed no improvement of MSCs´ total ECM production by hypoxia [129,131,132]. The knowledge about ACPCs reaction to hypoxic conditions in hydrogels is limited. In one study, ACPCs were exposed to low oxygen pressure in self-organized constructs on fibronectin-covered membranes [232]. In contrast to tested articular chondrocytes, ACPCs showed, similar to the present study, only minor reactions to the hypoxic conditions [232].

Relative gene expression of COL1A1 was generally higher in MSCs than in ACPCs, while COL2A1 was more similar between ACPCs and MSCs (Figure 21 C, D). Hypoxic conditions seemed to reduce the expression of COL1A1 in all constructs by trend (Figure 21 D) in comparison to normoxic conditions. COL2A1 expression seemed to be the same between high and low oxygen tension (Figure 21 C). ACAN expression was significantly higher in ACPC constructs than in MSC or zonal constructs both on d14 and d28. A difference to the normoxic values was ACAN expression in ACPC constructs on d28 as it was not downregulated as under normoxic conditions (Figure 21 A). PRG4 expression was significantly higher in ACPCs under low oxygen tension compared to high oxygen tension. It was also significantly higher than the PRG4 expression of MSC and zonal constructs as the expression of zonal constructs was significantly lower in hypoxia than in normoxia (Figure 21 B). At 21 % oxygen, zonal constructs expressed similar amounts of PRG4 than ACPC constructs. However, although PRG4 expression in ACPC hydrogels did increase at 2 % oxygen, it decreased significantly in zonal hydrogels (Figure 21 B). Interestingly, hypoxia appeared to be able to suppress PRG4 expression in zonal constructs. This might not have been a favourable effect of hypoxia, but it was a second hint that co-cultures of ACPCs and MSCs had different effects in hypoxia than in normoxia. A reason for that might be that MSCs secreted different factors under high or low oxygen tension with different effects on the co-cultured ACPCs and vice versa. It has been shown, for example, that exosomes derived from hypoxia preconditioned MSCs differed in their effect from exosomes derived from MSCs without preconditioning [246,247].
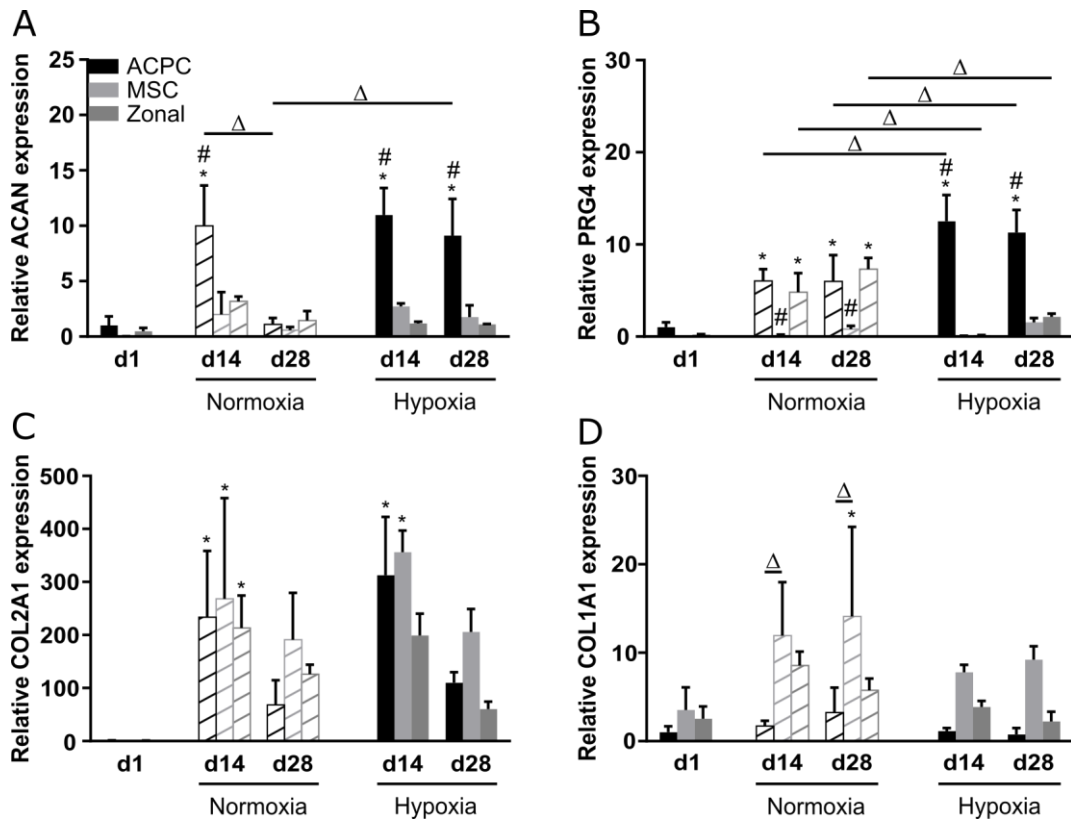
Figure 21: Relative gene expression in ACPC, MSC, and zonal agarose constructs. Gene expression as determined by qRT-PCR in agarose hydrogel constructs, seeded with 20.0×10^6 cells ml^{-1}, after 1, 14, and 28 days of chondrogenic differentiation under normoxic or hypoxic conditions. ACPCs and MSCs were either cultured alone or in zonally layered co-culture constructs. Relative expression of **(A)** ACAN (encoding aggrecan), **(B)** PRG4 (lubricin), **(C)** COL2A1 (type II collagen), and **(D)** COL1A1 (type I collagen). Normoxia values are shown as striped columns because they were already discussed before (Figure 13, p. 73). Data are presented as means ± standard deviation (n=3 biological replicates). (*) indicates statistically significant differences between a d14 or d28 value and the corresponding d1 value of the same group ($p < 0.05$). (#) indicates statistically significant differences of this group compared to the other two groups that share the same time point and oxygen condition ($p < 0.05$). (Δ) indicates statistically significant differences between groups, or within a group between time points ($p < 0.05$). Gene expression levels were normalized to the gene expression of the housekeeping gene HPRT1 and to the gene expression of ACPCs on d1. The data of this figure were published in the International Journal of Molecular Sciences (MDPI) and this figure was adapted from Schmidt et al. [228].

Even though hypoxia did not increase the production of cartilage ECM and even seemed to reduce the production of type II collagen especially in MSCs, the increase of PRG4 expression in ACPC constructs and the decrease by trend of COL1A1 expression in all constructs were positive effects of hypoxic conditions on the development of a more hyaline cartilage tissue that could lead to better functional properties of the tissue.

Several previous studies have revealed that hypoxic conditions can reduce hypertrophy and endochondral ossification especially in MSC chondrogenesis [79-82]. Therefore, analysis of ALP activity, marker for endochondral ossification, was especially interesting in this study. As in normoxia, ACPCs showed very low levels of ALP activity compared to MSC

and zonal constructs. However, ALP activity of MSC and zonal constructs was significantly reduced by hypoxia both on d14 and d28 (Figure 22). These findings were in concert with reports from the literature [80,81,102]. Together with the downregulation of COL1A1 expression, the reduction of ALP activity in MSCs showed that hypoxia had positive effects on the quality of cartilage tissue formed by MSCs. However, ACPC constructs displayed exceptionally low ALP activity under all conditions, which appeared to make them, when combined with agarose gels, more suitable for the formation of stable hyaline cartilage tissue.
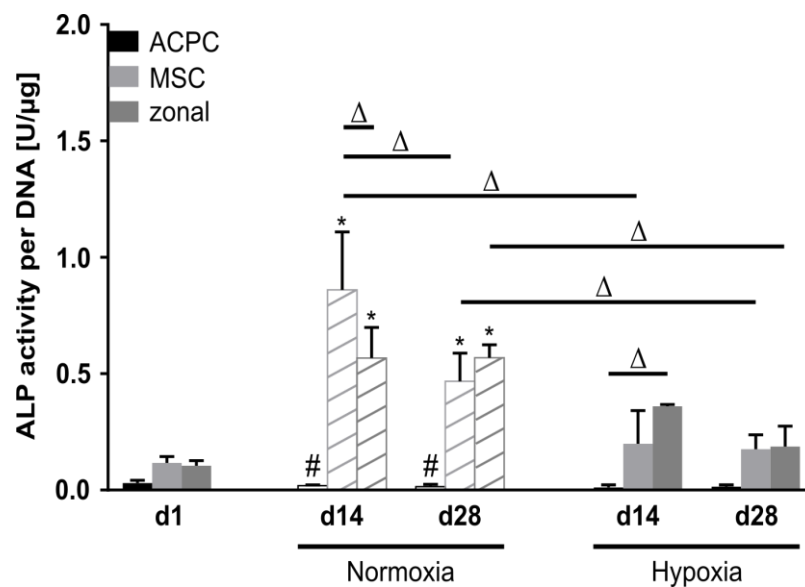

Figure 22: Alkaline phosphatase activity in ACPC, MSC, and zonal agarose constructs. ALP activity in agarose hydrogel constructs, seeded with 20.0 x 10^6 cells ml^{-1}, after 1, 14, and 28 days of chondrogenic differentiation under normoxic and hypoxic conditions. ACPCs and MSCs were either cultured alone or in zonally layered co-culture constructs. Normoxia values are shown as striped columns because they were already discussed before (Figure 14, p. 75). Data are presented as means ± standard deviation (n=3 biological replicates). (*) indicates statistically significant differences between a d14 or d28 value and the corresponding d1 value of the same group (p < 0.05). (#) indicates statistically significant differences of this group compared to the other two groups that share the same time point and oxygen condition (p < 0.05). (Δ) indicates statistically significant differences between groups, or within a group between time points (p < 0.05). The data of this figure were published in the International Journal of Molecular Sciences (MDPI) and this figure was adapted from Schmidt et al. [228].

4.1.1.3 Summary of chondrogenesis of ACPCs and MSCs in agarose hydrogel

In the present study, three different constructs were tested: Agarose hydrogels laden with ACPCs, MSCs or both, in zonal layers with ACPCs on top and MSCs in the lower layer. They were compared in their ability to differentiate chondrogenically and produce cartilage neo-tissue similar to hyaline articular cartilage under normoxic (21 % oxygen) and hypoxic (2 % oxygen) conditions. All three constructs were able to produce distinct amounts of cartilage ECM in all conditions, however, quality and quantity of the formed tissue were different between the three groups. ACPCs produced in general more GAG and proteoglycans than MSCs, while MSCs produced more total collagen. Values for zonal constructs mostly lay in between those of ACPCs and MSCs. When collagen content was analysed further, it was shown that ACPCs produced much less type I collagen than MSCs under both normoxic and hypoxic condition. ACPCs also had very low levels of ALP activity compared to MSCs. Hypoxia reduced production of collagen in general but especially in MSCs, and significantly decreased ALP activity in MSC and zonal constructs. Gene expression of PRG4 in ACPCs was increased by low oxygen pressure, and gene expression of type I collagen was decreased by trend in all groups. Hypoxia in combination with co-culture seemed to increase production of type II collagen in ACPCs and reduced type I collagen production in MSCs while co-culture alone seemed to increase type I and type II collagen production in ACPCs. Hypoxia also decreased relative PRG4 gene expression in zonal constructs. Taken together, hypoxia appeared, despite the reduction of type II collagen production, to improve the cartilage tissue formed by MSCs by reducing type I collagen gene expression and ALP activity. The resulting tissue was less fibrocartilaginous and less hypertroph than the tissue produced by MSCs under normoxic conditions. Zonal co-cultures appeared to have influence on the type II collagen/type I collagen ratio and were affected differently by hypoxia than monocultures. It is possible that factors secreted by MSCs (or ACPCs) that are responsible for the different effects in co-culture also differ between normoxia and hypoxia. This could explain differences between mono- und co-culture in hypoxia and normoxia. It has been shown, for example, that exosomes derived from hypoxia preconditioned MSCs differed in their effect from exosomes derived from MSCs without preconditioning [246,247]. That would be an interesting topic to explore in further experiments.

Taken together, in agarose hydrogels, ACPCs outperformed MSC as well as zonal constructs, as they produced more GAG and proteoglycans and similar levels of type II collagen, while their type I collagen content was much lower. Additionally, ACPCs showed only little tendency towards terminal differentiation (shown by ALP activity), regardless of

oxygen tension. ACPCs produced cartilage tissue that was more similar to hyaline cartilage tissue in both normoxia and hypoxia. Therefore, in this study in agarose hydrogels, they appeared to be a better choice for cartilage tissue engineering than MSCs.

4.1.2 Chondrogenesis of ACPCs and MSCs in a HA-based hydrogel

Biomimetic hydrogels/scaffolds can combine two aspects of the triad of articular cartilage engineering (Figure 3, p. 15): "scaffolds" and "signals". They are cell carrier materials that consist of molecules that are naturally occurring in the ECM of different tissues [151]. ECM molecules can interact with cells and influence cell shape, function and differentiation. When these natural ECM molecules are used in tissue engineering, one hopes that they provide an environment that influences the cells positively and directs them towards producing the desired tissue [151]. ECM molecules that are used for biomimetic cartilage tissue engineering either as porous scaffolds or hydrogels are for example collagen, hyaluronic acid (HA) or chondroitin sulfate [153]. To adjust the physicochemical characteristics of hydrogels, synthetic polymers like poly(ethylene-glycol) (PEG) or poly(glycidol) (PG) are used in combination with natural polymers [153]. In the following experiments, mesenchymal stromal cells (MSCs) and articular cartilage progenitor cells (ACPCs), that were also tested in agarose hydrogel (see 4.1.1 Chondrogenesis of ACPCs and MSCs in agarose hydrogel, p. 64), were cultured in a hybrid hydrogel consisting of thiolated HA (HA-SH) and allyl-functionalized PG (P(AGE-co-G)) [164,169]. The components were crosslinked by an UV-induced radical thiol-ene coupling between thiol and allyl groups using the photo-initiator Irgacure2959. A polymer concentration of 10 wt% in total was used [164]. This hydrogel was developed at the Department for Functional Materials in Medicine and Dentistry, University of Würzburg within the framework of the EU research project HydroZONES (Bioactivated hierarchical hydrogels as zonal implants for articular cartilage regeneration). The work that is presented here was part of the *in vitro* chondrogenesis evaluation of ACPCs and MSCs in HA-SH/P(AGE-co-G) hydrogel in preparation for a long-term *in vivo* cartilage regeneration study in horses. The results of the *in vitro* and *in vivo* studies were published together [248].

In the following, chondrogenesis of ACPCs, MSCs and zonal constructs with ACPCs in the upper layer and MSCs in the lower layer was compared. A schematic depiction of the used constructs is shown in Figure 6 (p. 64), as they had the same shape as the previously described agarose constructs. A chronological experimental workflow is depicted in Figure 23. The ECM of the resulting tissues was analysed using biochemical assays, histology, and immunohistochemistry.
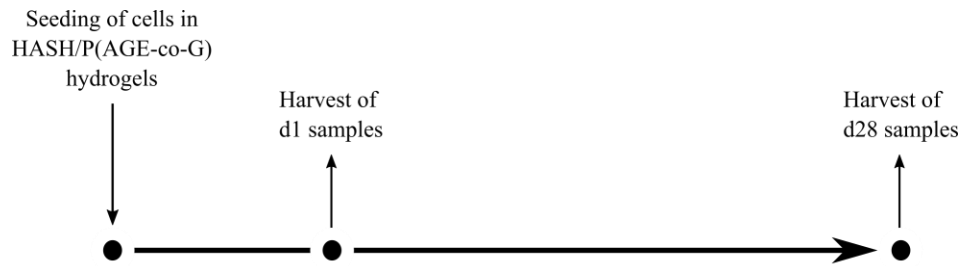
Figure 23: Experimental workflow for cartilage tissue engineering experiments in HA-SH/P(AGE-co-G) hydrogels seeded with ACPCs, MSCs or zonal constructs. Medium was exchanged every two to three days.

As a first experiment, DNA content of the different HA-SH/P(AGE-co-G) constructs was evaluated (Figure 24). In all constructs, DNA amount increased from d1 to d28. This effect was not significant but most prominent in co-cultured zonal constructs (Figure 24). Co-culture between MSCs and chondrocytes is known to promote proliferation [77,233-235], and this was also seen in agarose constructs in the present work (Figure 9, p. 67).
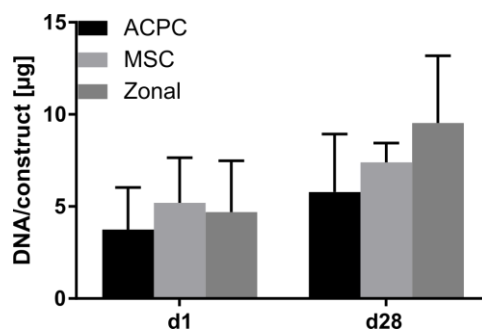

Figure 24: DNA content in ACPC, MSC, and zonal HA-SH/P(AGE-co-G). Biochemical analysis of DNA amount in HA-SH/P(AGE-co-G) hydrogel constructs, seeded with 20.0 x 10^6 cells ml^{-1}, after 1 and 28 days of chondrogenic differentiation. ACPCs and MSCs were either cultured alone or in zonally layered co-culture constructs. Three independent experiments with n=3 biological replicates were performed. Data are presented as means ± standard deviation.

Biochemical assays showed a significant production of GAG by all constructs over 28 days (Figure 25 A, B). However, MSC and zonal constructs showed significantly higher levels of GAG per construct than ACPCs (Figure 25 A). When normalized to DNA, GAG amount in zonal constructs was higher by trend than in ACPC constructs while it was significantly higher in MSC constructs (Figure 25 B). The collagen content of the different hydrogel constructs was determined with a biochemical hydroxyproline assay. It revealed that all constructs produced significant levels of collagen in the 28 days of chondrogenic

differentiation (Figure 25 C, D). MSC constructs produced significantly more collagen than ACPC or zonal constructs, both in total and when normalized to the DNA amount. Zonal constructs showed significantly higher collagen levels than ACPC constructs (Figure 25 C, D)
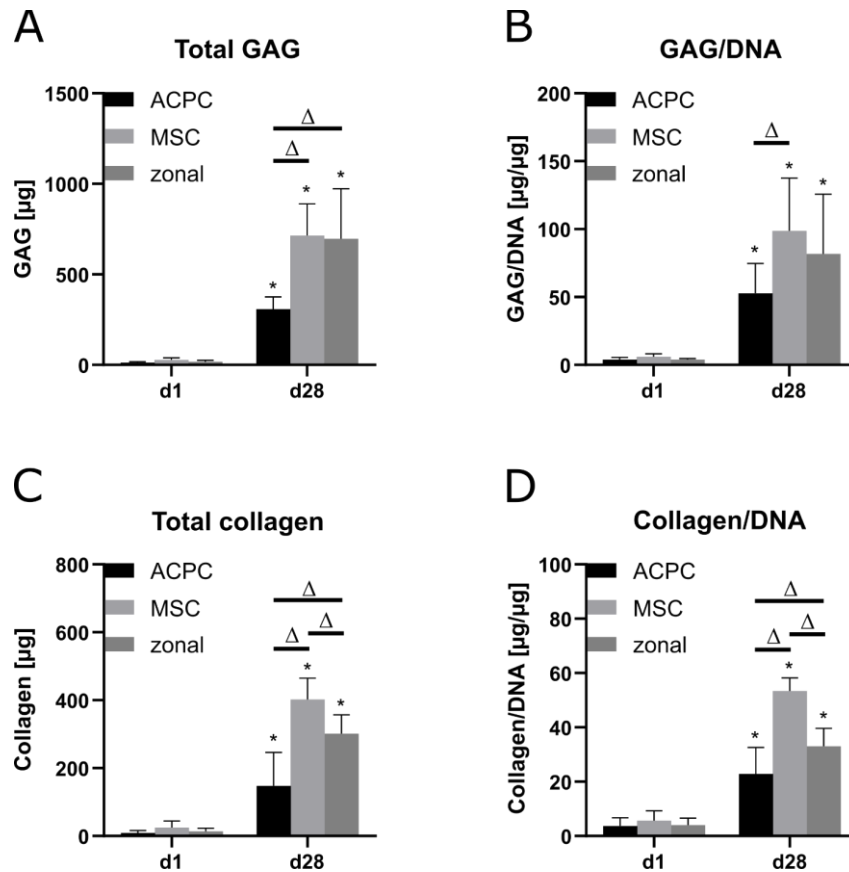

Figure 25: GAG and collagen production in ACPC, MSC, and zonal HA-SH/P(AGE-co-G) constructs. Biochemical analysis of GAG and collagen in HA-SH/P(AGE-co-G) hydrogel constructs, seeded with 20.0×10^6 cells ml^{-1}, after 1 and 28 days of chondrogenic differentiation. ACPCs and MSCs were either cultured alone or in zonally layered co-culture constructs. **(A)** Production of total GAG (GAG/construct), **(B)** GAG normalized to DNA (GAG/DNA), **(C)** total collagen (collagen/construct) and **(D)** collagen normalized to DNA (collagen/DNA). Three independent experiments with n=3 biological replicates were performed. Data are presented as means ± standard deviation. (*) indicates statistically significant differences between a d28 value and the corresponding d1 value of the same group ($p < 0.05$). (Δ) indicates statistically significant differences between groups ($p < 0.05$). This figure has been published in the journal Biofabrication and was reproduced with permission from Mancini et al. [248]. © IOP Publishing. Reproduced with permission. All rights reserved.

Next, histological and immunohistochemical staining was used to analyse distribution and differences of produced ECM. Safranin O staining revealed that at d28 GAG was distributed mostly pericellularly and was not spread through the whole hydrogels (Figure 26 A). It

should be noted that the pink background, that is also visible in d1 samples, is due to background staining of the hyaluronic acid hydrogel.
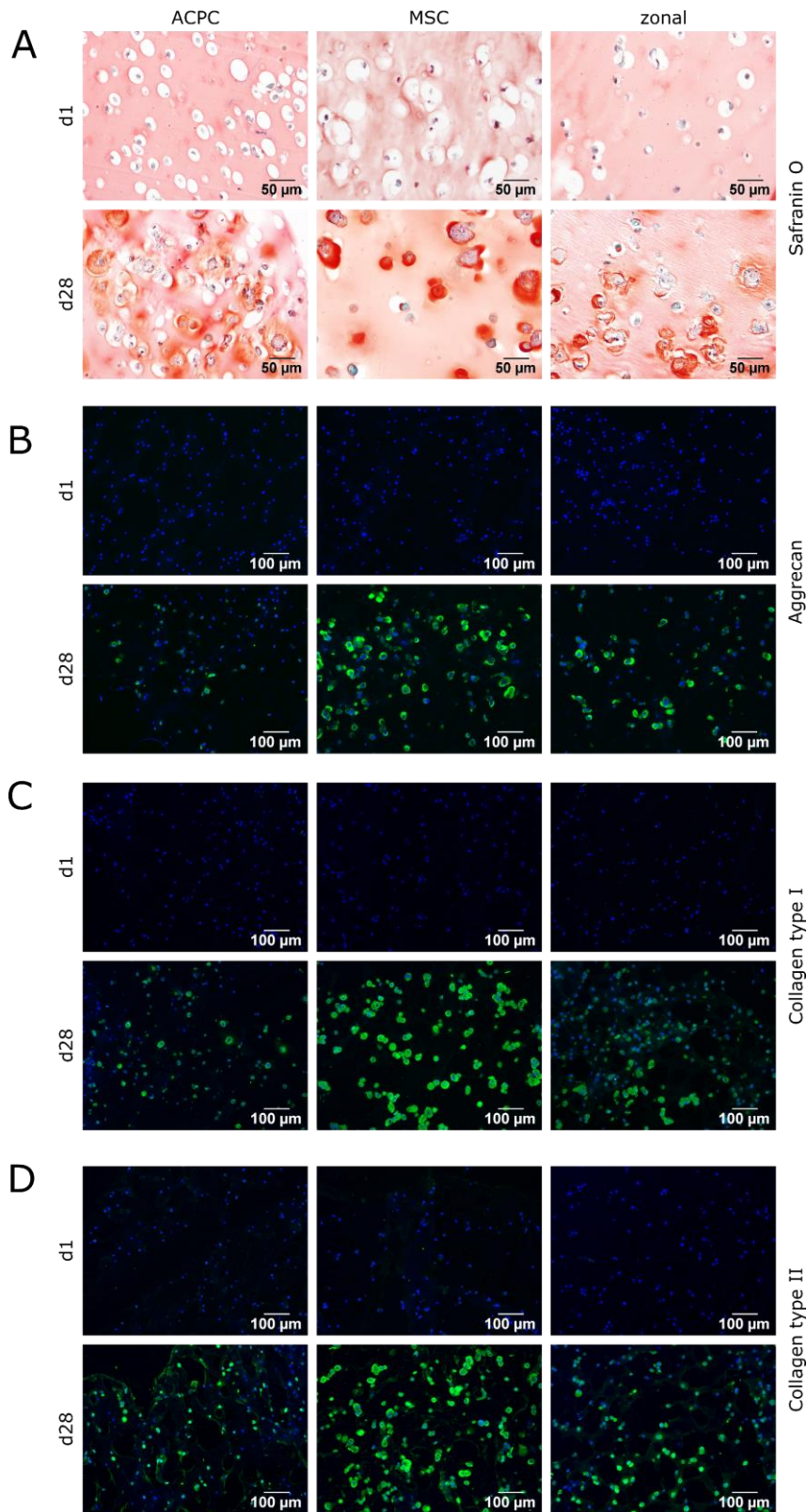

Figure 26: Staining of ACPC, MSC, and zonal HA-SH/P(AGE-co-G) constructs for GAG, aggrecan, type I and type II collagen. Histological and immunohistochemical staining of HA-SH/P(AGE-co-G) hydrogel constructs, seeded with 20.0×10^6 cells ml^{-1}, after 1 and 28 days of chondrogenic differentiation. ACPCs and MSCs were either cultured alone or in zonally layered co-culture constructs. **(A)** Histological

safranin-O staining for visualization of produced GAG. **(B)** Immunohistochemical staining for aggrecan. **(C)** Immunohistochemical staining for type I collagen. **(D)** Immunohistochemical staining for type II collagen. In zonal constructs, the upper layer contained ACPCs and the lower layer MSCs. This figure has been published in the journal Biofabrication and was reproduced with permission from Mancini et al. [248]. © IOP Publishing. Reproduced with permission. All rights reserved.

Consistent with the biochemical assays (Figure 25 A, B, p. 90), safranin O staining showed more intense GAG staining in MSC constructs than in ACPC constructs. Zonal constructs reflected these findings in their respective zones (Figure 26 A). Immunohistochemical staining of the proteoglycan aggrecan showed similar tendencies with most intense staining in MSC constructs, less staining in ACPC constructs and zonal constructs that reflected these outcomes in their respective zones (Figure 26 B). Staining of type I (Figure 26 C) and type II (Figure 26 D) collagen in the HA-SH/P(AGE-co-G) hydrogel also showed higher intensities in the MSC constructs than in the ACPC constructs. Zonal constructs showed similar trends in their respective layers (Figure 26 C, D). This was in line with biochemical assays (Figure 25 C, D, p. 90). However, all ECM that was produced in HA-SH/P(AGE-co-G) hydrogels was located only around the cells and was not spread throughout the whole hydrogel. High magnification images of ACPCs and MSCs in HA-SH/P(AGE-co-G) hydrogels (Figure 27) demonstrated the intra- and mostly pericellular distribution of the ECM components aggrecan and type II collagen. The black arrows indicate pericellular matrix and the red arrows indicate cell boundaries (Figure 27).
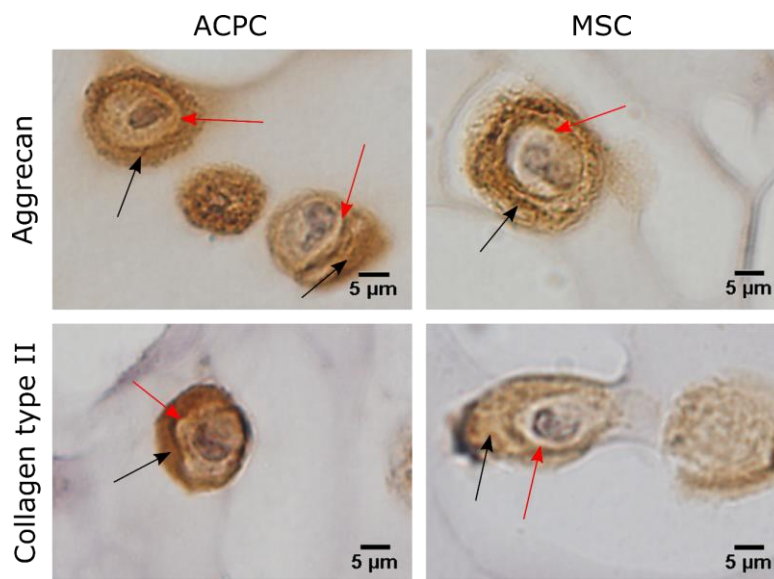

Figure 27: Immunohistochemical HRP/diaminobenzidine staining of ACPC and MSC in HA-SH/P(AGE-co-G) constructs for aggrecan and type II collagen in high magnification. Immunohistochemical staining of HA-SH/P(AGE-co-G) constructs, seeded with 20 x 10⁶ cells ml⁻¹ and stained after 28 days of chondrogenic differentiation. Black arrows indicate pericellular matrix and red arrows indicate cell

In addition to the produced ECM, the activity of ALP, marker for endochondral ossification, was analysed. MSC and zonal constructs had higher ALP activity than ACPC constructs already on d1 (Figure 28). After 28 days, ALP activity in MSC constructs was significantly increased compared to d1, while ACPC constructs showed even smaller activity levels than on d1. ALP activity in zonal constructs was slightly increased on d28 compared to d1. (Figure 28). These results were similar to ALP activity in agarose constructs (Figure 14, p. 75). However, in HA-SH/P(AGE-co-G) hydrogels, zonal constructs showed significantly less ALP activity than MSCs on d28 (Figure 28), while MSC and zonal agarose constructs showed similar ALP levels on d28 (Figure 14, p. 75). This was probably the effect of the different microenvironment provided by the different hydrogels. It is possible that the effects (e.g., secreted factors) that the co-cultured cells had on each other were changed in different microenvironment. However, the characteristics of ACPCs and MSCs regarding ALP activity were the same in both agarose and HA-SH/P(AGE-co-G) hydrogels. For prevention of endochondral ossification in cartilage constructs, ACPCs seemed to be the better choice than MSCs.
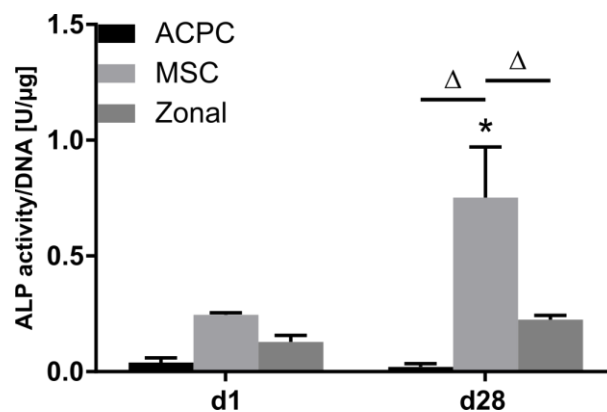
Figure 28: Alkaline phosphatase activity in ACPC, MSC, and zonal HA-SH/P(AGE-co-G) constructs. ALP activity in HA-SH/P(AGE-co-G) hydrogel constructs, seeded with 20.0×10^6 cells ml^{-1}, after 1 and 28 days of chondrogenic differentiation. ACPCs and MSCs were either cultured alone or in zonally layered co-culture constructs. Data are presented as means ± standard deviation (n=3 biological replicates). (*) indicates statistically significant differences between a d28 value and the corresponding d1 value of the same group ($p < 0.05$). (Δ) indicates statistically significant differences between groups ($p < 0.05$).

Summing up, ACPCs, MSCs and zonal constructs (consisting of an upper layer with ACPCs and a lower layer with MSCs) were able to produce distinct amounts of cartilage ECM in HA-SH/P(AGE-co-G) hydrogel. MSC constructs produced more GAG and collagen than ACPC constructs, and zonal constructs mostly showed values that lay between those of MSCs and ACPCs. While MSCs produced more ECM, ACPCs showed very small ALP activity levels compared to MSC constructs. However, the pericellular ECM distribution in all constructs was not optimal as it did not resemble natural ECM and did not lead to a continuous, tissue-like construct. This effect has been seen before when high polymer content or high network density in hydrogels restricted homogenous ECM distribution of the encapsulated cells [164,249-253]. Characteristics of crosslinked HA-SH/P(AGE-co-G) hydrogels also depend on the length of the used HA-SH and its degree of modification. In general, the shorter the HA-SH, the more polymer is needed in total to generate a stable hydrogel through crosslinking. If the polymer content is too small, no gel forms. The HA-SH that was used here was relatively small and therefore, a high polymer content was needed to form a gel with it. Additionally, the used hydrogel composition with a total polymer content of 10 wt% was originally chosen to produce a 3D-printable hydrogel. A high concentration of polymers is often used for 3D-printing materials to improve stability and shape fidelity during and after the printing process [150]. With 10 wt% polymer content and additional unmodified high MW HA (1-2 MDa) to increase viscosity, it was possible to double print the HA-SH/P(AGE-co-G) hydrogel together with polycaprolactone (PCL) in a previous study [164]. As the hydrogel was not 3D-printed for the *in vivo* horse study [248], the corresponding *in vitro* experiments in the present study were also performed without 3D bioprinting. Another study with a very similar hydrogel system proved that a reduction of polymer content resulted in improved ECM distribution [169]. Therefore, the used HA-SH/P(AGE-co-G) hydrogel should be developed further to find a way to combine the needs of the used cells and, for example, the requirements for a stable hydrogel for bioprinting with high shape fidelity.

4.1.3 Influence of different hydrogels on chondrogenesis of ACPCs and MSCs

In the present study, equine ACPCs and MSCs were investigated for their potential to form articular cartilage tissue in two different hydrogels, agarose and HA-SH/P(AGE-co-G). Both cell types were able to produce distinct amounts of cartilage ECM in both hydrogels. However, cell types did not perform the same in the different hydrogels. Interestingly, ACPCs and MSCs showed homogenous ECM distribution in agarose hydrogels, while the matrix was restricted mainly to the pericellular region in HA-SH/P(AGE-co-G) hydrogels. As mentioned before, this is probably mainly the effect of the high polymer content and high network density in the HA-SH/P(AGE-co-G) hydrogel (10 wt%) [164,249-253]. However, there was another striking difference as ACPCs clearly outperformed MSCs in agarose hydrogel but not in HA-SH/P(AGE-co-G) hydrogels. ACPCs produced significantly less GAG and collagen than MSCs in the HA-based hydrogels. The comparison between agarose and HA-SH/P(AGE-co-G) in the present study that used the same cells and the same cultivation conditions for both hydrogels, demonstrated the distinct influence that the used hydrogel can have on the different cell types. Chondrogenesis and production of cartilage ECM of ACPCs and MSCs were compared before in different hydrogel systems, namely GelMA [103], GelMA/gellan and GelMA/gellan/HAMA [107]. In these hydrogels, MSCs always outperformed ACPCs regarding ECM production similar to the results in HA-SH/P(AGE-co-G) hydrogels in the present study. Hydrogels like GelMA or HA-SH/P(AGE-co-G) that contain biopolymers like collagen and hyaluronic acid, appeared to favour MSC chondrogenesis. These more biomimetic hydrogels could have promoted MSC chondrogenesis through attachment and signalling between the material and the cells. In contrast, agarose has no biological cues that the cells could adhere to. However, agarose is a well-characterized chondro-permissive hydrogel that has been reported to support native chondrocyte phenotype and morphology [32,229]. In other previous studies that compared cartilage ECM production of chondrocytes and MSCs in agarose or other materials without biological cues, chondrocytes outperformed MSCs [131,254,255] like the ACPCs did in the present study in agarose hydrogel. Therefore, agarose hydrogel seemed to be a favourable environment for chondrocytes and ACPCs that are a subpopulation of chondrocytes. MSCs needed to undergo the whole differentiation process towards chondrocytes, and it seemed plausible that signals from the microenvironment would help in this process, as they do in normal embryonic development [4,256,257]. Chondrocytes, in contrast, are already mature cells that profit from an environment that preserves and supports their properties, like agarose. ACPCs, progenitor cells for mature chondrocytes and derived from articular cartilage,

appeared to resemble chondrocytes in this regard. These results demonstrated clearly that it is of paramount importance to choose the right microenvironment or hydrogel to achieve the best performance of the different cell types.

4.2 Contribution of hyaluronan to chondrogenic gene expression of MSCs

Hyaluronic acid is a natural polysaccharide with a multitude of functions in the human body. It is important as structural component and plays different roles in cell and organ development, cell migration and proliferation, cancer, inflammation and tissue injury [174]. HA is one of the main components of articular cartilage ECM and a popular material for the construction of scaffolds and hydrogels for cartilage tissue engineering [212,220]. It is often used in combination with MSCs as it has been shown that it can enhance MSC chondrogenesis when it is part of the 3D tissue engineering construct [164,165,258]. Some HA-containing scaffolds have been reported to induce expression of chondrogenic markers in basal medium without growth factors [165,259-261]. Induction and support of chondrogenesis in MSC pellets through HA supplementation of culture medium was demonstrated [262,263], but the use of TGFβ as common chondro-inductor still lead to better results [263]. Another recent study tested HA as medium supplementation for MSCs in fibrin-polyurethan constructs. However, the effects on chondrogenesis were small in comparison to the condition in which HA was directly mixed into the construct [264].

The effects of HA on chondrocytes have also been studied. Enhanced proliferation of chondrocytes was one effect of HA that was found [265-268]. The production of articular cartilage ECM by chondrocytes was also enhanced with the addition of HA to culture medium or 3D scaffolds [209,265,267]. Interestingly, one observation that was similar in several chondrocyte studies was that a lower concentration of HA often led to better results than a higher concentration [209,265-267].

HA has additionally been shown to reduce mouse and human MSC aging and to maintain differentiation potential at high population doublings [269,270]. It has been suggested to be an important part of the stem cell niche *in vivo* as it can influence stem cell fate and behaviour in many different ways [271].

HA acts as signalling molecule through binding to its cell surface receptors. The most important HA-receptors are CD44 and CD168. HA-receptors have been shown to influence many different signalling pathways, for example PI3K/PDK1/Akt, Ras/RAF1/MEK/ ERK1/2, PLCε-Ca^{2+} signalling and SMAD signalling for BMP7 activation as well as FAK, PKC, c-Src, and NF-κB signalling [178,192]. The binding of HA to its receptors can also influence chondrogenesis as it can affect signalling pathways that are important in chondrogenesis, like TFGβ and BMP signalling, sonic hedgehog or Wnt signalling [201-208]. However, even if many signalling pathways are known to be influenced by HA and the signalling of its receptors, the exact mechanisms and correlations are mostly not well-established so

far. As HA can affect so many different pathways and there are so many conditions that can change the function of it (cell type, concentration, MW, binding partners, receptor dimerization and clustering etc.), it is not easy to entangle these complex biological interactions. When HA is used for the construction of tissue engineering hydrogels, it is often necessary to introduce chemical modifications that are needed to crosslink the polysaccharides to a mechanically stable construct and to provide more versatile applications of the material [213]. However, changing the HA structure and chemically active groups by adding modifications could change or abolish the effects that HA has on the cells through binding to its receptors. Most important for CD44-HA binding are the carboxyl group of glucuronic acid and the N-acetyl-group of N-acetyl-glucosamine, but also the hydroxyl groups on C6 of N-acetyl-glucosamine and on C3 and C2 of glucuronic acid are involved [217]. A previous study has shown that removing the N-acetyl group of HA or adding of a sulfate group decreases CD44-HA binding [218]. Kwon et al. analysed HA that carried a norbornene modification on its carboxyl group and compared it to HA with a norbornene modification on the C6 hydroxyl group of N-acetyl-glucosamine and a HA with a smaller methacrylate modification also on C6. All modifications decreased CD44-HA binding when the degree of modification was increased (circa 40 %) and modification with hydrophobic norbornene on the carboxyl group decreased adhesion of CD44-modified beads to HA hydrogels the most. This modification also decreased chondrogenesis of MSCs at 40 % degree of modification [219].

In the present work, HA hydrogels were produced from thiol-modified HA (HA-SH). The used HA was modified on the carboxyl group of the glucuronic acid in HA. This modification has not been investigated yet for its effect on CD44-HA binding or chondrogenic induction. It is of great interest to evaluate to what extend the modified and crosslinked HA in the hydrogels contributes to the chondrogenic differentiation in these hydrogels.

3D bioprinting offers attractive new applications for materials like HA-based hydrogels. 3D bioprinting of cells with suitable materials is a promising tool for the generation of complex and customized 3D tissue engineering constructs that are clinically relevant [150]. However, cells are exposed to shear forces when they are printed, and they can die from the printing process if the shear stress is too high. Additionally, it has been shown that the 3D bioprinting process can alter the gene expression profile of MSCs [107]. Therefore, it is interesting if and how 3D bioprinting in HA-based hydrogels affects gene expression of MSCs and if the signalling effects of HA are modulated by the printing process.

Hence, in the present study, unmodified HA was added to the basic serum-free medium of human MSCs in 2D monolayer and 3D pellet culture, and the effects on MSC gene expression were evaluated. Gene expression of human MSCs encapsulated in HA-SH/PEGDA/PEG-Allyl/Irgacure2959 hydrogels was investigated in basic chondrogenic medium without TGFβ1. Gene expression changes of HA receptors (CD44, CD168), transcription factors (SOX9, SOX5, SOX6, RUNX2, PPARG), chondrogenic markers (COL2A1, ACAN) and stemness factors (SOX2, Nanog, OCT4) were analysed by qRT-PCR over seven days of hydrogel culture. Hydrogels were either cast or 3D bioprinted to analyse the effects of printing on the gene expression of MSCs in HA-SH/PEGDA/PEG-Allyl/Irgacure2959 hydrogels.

4.2.1 Influence of hyaluronan on HA-receptors CD44 and CD168

The expression of the HA receptors CD44 and CD168 in MSCs was analysed by flow cytometry, qRT-PCR and immunohistochemical stainings. First, the basal expression was determined. Then, unmodified HA was added to the culture medium of MSCs grown in 2D monolayer or 3D pellets, and the effect was analysed by qRT-PCR. Subsequently, the expression of CD44 and CD168 in a HA-SH hydrogel was examined by qRT-PCR, and the effects of 3D bioprinting on the receptor expression were analysed.

4.2.1.1 Basal expression of CD44 and CD168

Human MSCs were stained with antibodies against CD44, CD168 or the appropriate isotype control and the respective secondary antibody. For CD168, the stained cells showed the same result as the isotype control which meant that no CD168-positive cells were detected (Figure 29 A). However, when the same cells were stained with the same antibodies, but Triton X-100 was added for permeabilization of the cells, the peak shifted to the right (Figure 29 B), indicating that CD168-positive cells were detected. Only a small number of cells were still negative for CD168, as represented by the small peak that fell together with the isotype control (Figure 29 B). This result suggested that CD168 could not be detected on the cell surface of the investigated MSCs but that CD168 was present intracellularly. As CD168 is a nonintegral membrane protein and is only tethered to the cell surface by a GPI-anchor [272], it can be suggested that the treatment with trypsin for cell detachment that was performed before the staining could be the reason for the absence of CD168 on the cell

surface in the flow cytometry analysis. Figure 29 C shows that most of the cells were positive for CD44. That could mean that CD44 on the cell surface was less affected by the cell detachment process than CD168. A previous study also showed only a small CD168-positive cell fraction in flow cytometry analysis after cell detachment with trypsin. The study showed also that most of the cells were positive for CD44 [211].
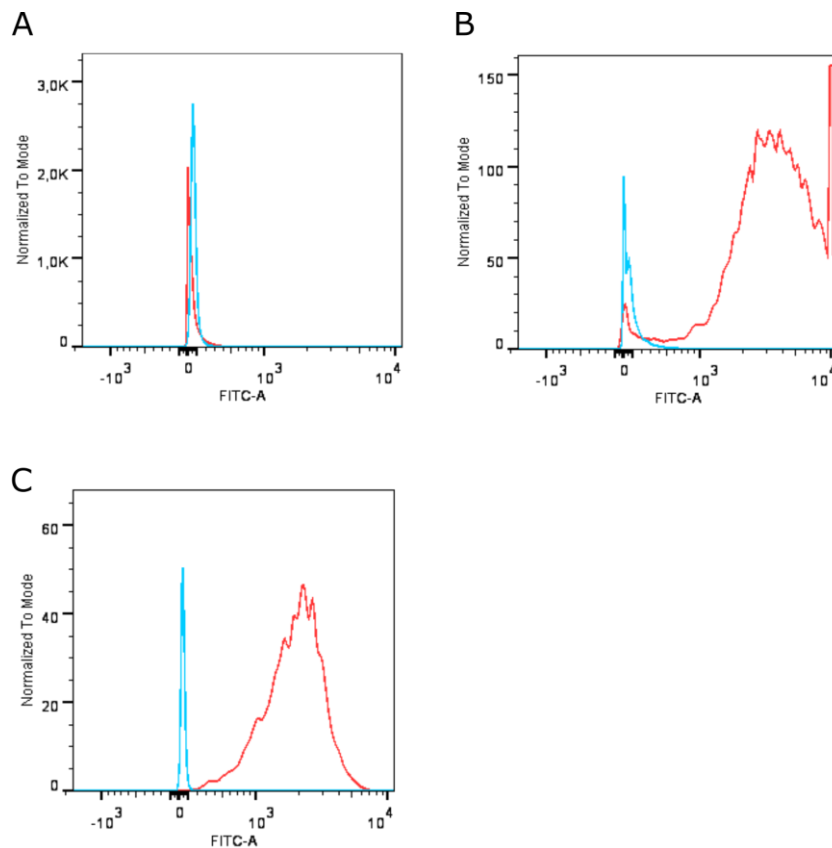

Figure 29: Flow cytometry of MSC surface expression of CD168 and CD44. The red line indicates cells treated with the specific antibody. The blue line indicates cells treated with an isotype control instead of the specific antibody. **(A)** Flow cytometry of MSC surface expression of CD168. **(B)** Flow cytometry of MSC expression of CD168. Cells were additionally treated with Triton X-100 for cell permeabilization. **(C)** Flow cytometry of MSC surface expression of CD44.

To further demonstrate the basal expression of CD44 and CD168, immunohistochemical staining of MSCs was performed. Both CD44 and CD168 could be detected (Figure 30). CD168 was localised on the cell surface as small clusters, in the cytoplasm and in the nucleus (Figure 30). The same was true for CD44 (Figure 30). CD44 is known to be expressed in many different cells and tissues [273], including bone-marrow derived MSCs [274-276]. As cell surface protein, CD44 is of course localised on the cell surface membrane but it can also be internalised [277,278], and it has been shown that CD44 fragments/full-length CD44

can be translocated to the nucleus [279,280]. CD168 can also be present in different sub-cellular locations. On the cell surface, it acts as receptor for HA together with CD44. Intra-cellularly, it is important in the control of mitotic-spindle integrity and microtubule and is also present in the nucleus [281].
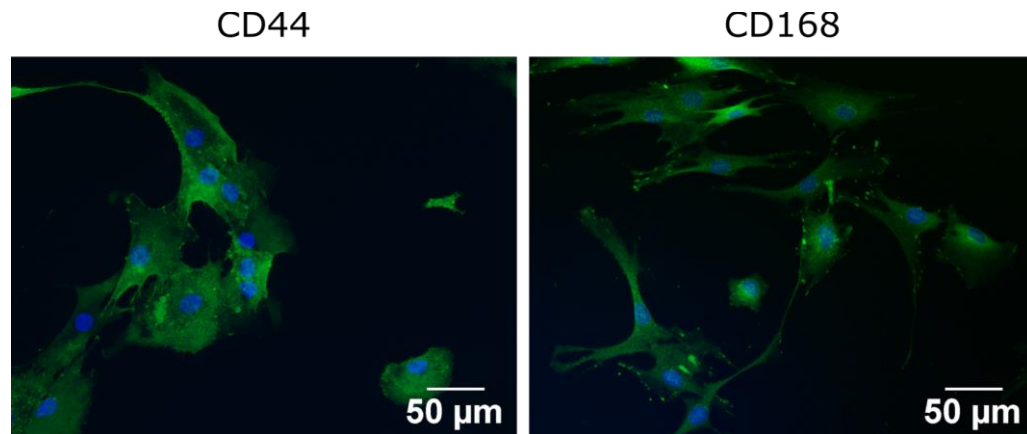

Figure 30: Immunohistochemical staining of CD44 and CD168 in human MSC. Human MSCs were cultured in 2D monolayer culture before they were fixed and stained for CD44 and CD168. CD44 and CD168 were detected on the cell surface, in the cytoplasm and in the nucleus of the stained cells.

4.2.1.2 Effects of HA on CD44 and CD168

To determine how HA can affect MSCs in different environments, HA was added to basic serum-free medium of human MSCs in 2D culture and in 3D pellet culture. HA supplementation had no significant effect on CD44 gene expression levels in 2D culture (Figure 31 A) or in 3D pellet culture (Figure 31 C). The relative gene expression of CD168 was slightly upregulated in 2D (Figure 31 B) and significantly upregulated in 3D pellets (Figure 31 D). It has been shown previously that medium supplementation with HA has no significant influence on the relative gene expression of CD44 in 2D monolayer cultures [264,282]. The effect of HA in medium on CD168 gene expression has not been studied extensively so far. However, it appears that CD168 gene expression is differently affected by the addition of HA than CD44. Further studies would be needed to investigate the mechanisms behind these results.
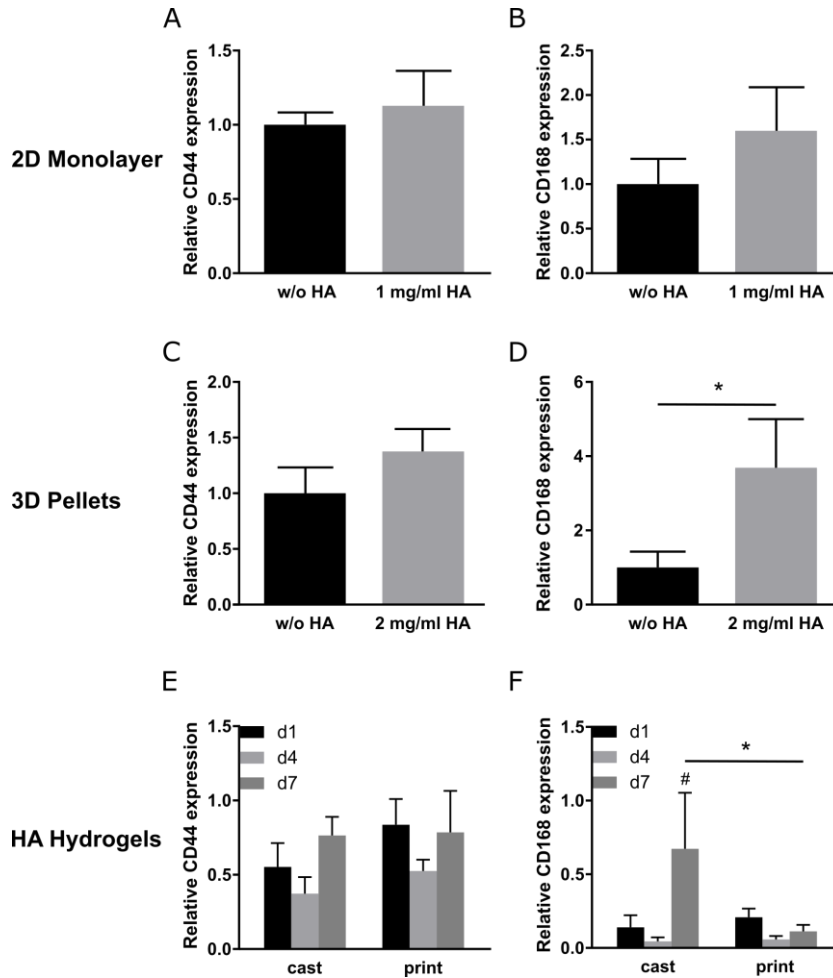
Figure 31: Relative gene expression of CD44 and CD168 in human MSCs in 2D monolayer and 3D pellets, or HA-based hydrogels. MSCs in 2D monolayer and 3D pellets were cultured with or without HA (0.6-1.0 MDa). Relative gene expression in 2D monolayer culture after two days in basic serum-free medium with or without 1 mg/ml HA, **(A)** CD44 and **(B)** CD168. Relative gene expression in 3D pellet culture after one day in basic serum-free medium with or without 2 mg/ml HA, **(C)** CD44 and **(D)** CD168. Relative gene expression of **(E)** CD44 and **(F)** CD168 in HA-SH hydrogels (HA-SH/PEGDA/PEG-allyl/Irgacure2959 hydrogel) after one, four and seven days in basic chondrogenic medium without TGFβ1. Hydrogels were either cast or 3D bioprinted before crosslinking. Data are presented as means ± standard deviation (n=3 biological replicates). (*) indicates statistically significant differences between two values ($p < 0.05$). (#) indicates statistically significant differences between this time point and the other two time points in the same condition (cast or print) ($p < 0.05$). Gene expression levels of 2D cultured MSCs (**A, B**) and 3D pellet cultured MSCs (**C, D**) were normalized to the gene expression of the housekeeping gene GAPDH and to the gene expression of the respective value without HA. Gene expression levels of MSCs encapsulated in HA-SH hydrogel (**E, F**) were normalized to the gene expression of the housekeeping gene GAPDH and to the gene expression of MSCs before they were encapsulated in the hydrogel.

When MSCs were encapsulated in a HA-SH hydrogel, CD44 gene expression was not significantly influenced, and no significant differences were detected between hydrogels that were cast or 3D bioprinted. CD44 was downregulated by trend from d1 to d4 and upregulated again by trend on d7 (Figure 31 E, F). CD168 was strongly downregulated on d1 and d4 of hydrogel culture in comparison to MSCs before encapsulation in the hydrogel (the value that the gene expression was normalized to; equates to 1). It even decreased further

from d1 to d4. On d7, CD168 gene expression was upregulated significantly in cast constructs but not in 3D bioprinted constructs.

CD44 and CD168 are both receptors for HA that can act together, but they have both additional individual functions and can therefore probably be regulated independently. The results suggested that CD44 gene expression appears not to be influenced by addition of HA or culture in the 3D environment of a HA-SH hydrogel. It has been shown that CD44 reacts with different clustering to HA of different MW [283]. Further studies concerning clustering behaviour, protein expression and maybe posttranslational modifications would reveal if and how HA can influence its receptor CD44. In contrast to CD44, CD168 was upregulated by HA in 3D pellet culture but strongly downregulated in HA-SH hydrogels on d1 and d4 in comparison to MSCs before they were encapsulated in the hydrogel (the value that the gene expression was normalized to; equates to 1). As HA had shown no negative effects on CD168 gene expression in MSCs in other cultures (2D, 3D pellets), it could be assumed that this downregulation was maybe a reaction to the encapsulation in the 3D environment. CD168 gene expression is cell-cycle dependent [284]. It has been shown that cell cycle regulation in adipose derived stem cells is changed in 3D HA hydrogels in comparison to 2D culture [285]. Maybe this could explain the downregulation of gene expression of CD168 in the HA-SH hydrogels in the present study. On d7 CD168 gene expression was upregulated again but not higher than in MSCs before encapsulation. Maybe the expression would increase further after a longer cultivation time.

In 3D bioprinted constructs, however, the CD168 gene expression did not increase on d7. This significant difference between cast and printed hydrogels showed that the printing process might have influenced and damaged the cells so that their gene expression and ability to react to external stimuli (HA, 3D environment) was changed. When the printing process is too harsh and cells experience strong shear forces, they can even die from the procedure. Smaller changes in the cells can also occur that might not be visible at first but affect the performance of the cells in later experiments, which has been demonstrated before [107]. Therefore, it is important to monitor if the printing process changed the cells or their abilities and characteristics.

4.2.2 Influence of hyaluronan on stemness markers

In 2D monolayer culture of human MSCs, the addition of HA to the basic serum-free medium significantly upregulated the gene expression of the stemness markers SOX2 (Figure

32 A), Nanog (Figure 32 B) and OCT4 (Figure 32 C) after two days. In 3D pellet culture with the same basic medium, HA significantly upregulated SOX2 (Figure 32 D) and Nanog (Figure 32 E) after one day, OCT4 was upregulated by trend (Figure 32 F).

When the cells were seeded in a HA-SH hydrogel, gene expression was significantly up-regulated on d7 for SOX2, Nanog and OCT4 in cast constructs. SOX2 gene expression was not increased on d7 in 3D bioprinted hydrogels, and the difference between cast and printed constructs was significant. Nanog and OCT4 showed similar levels of upregulation for both conditions on d7.
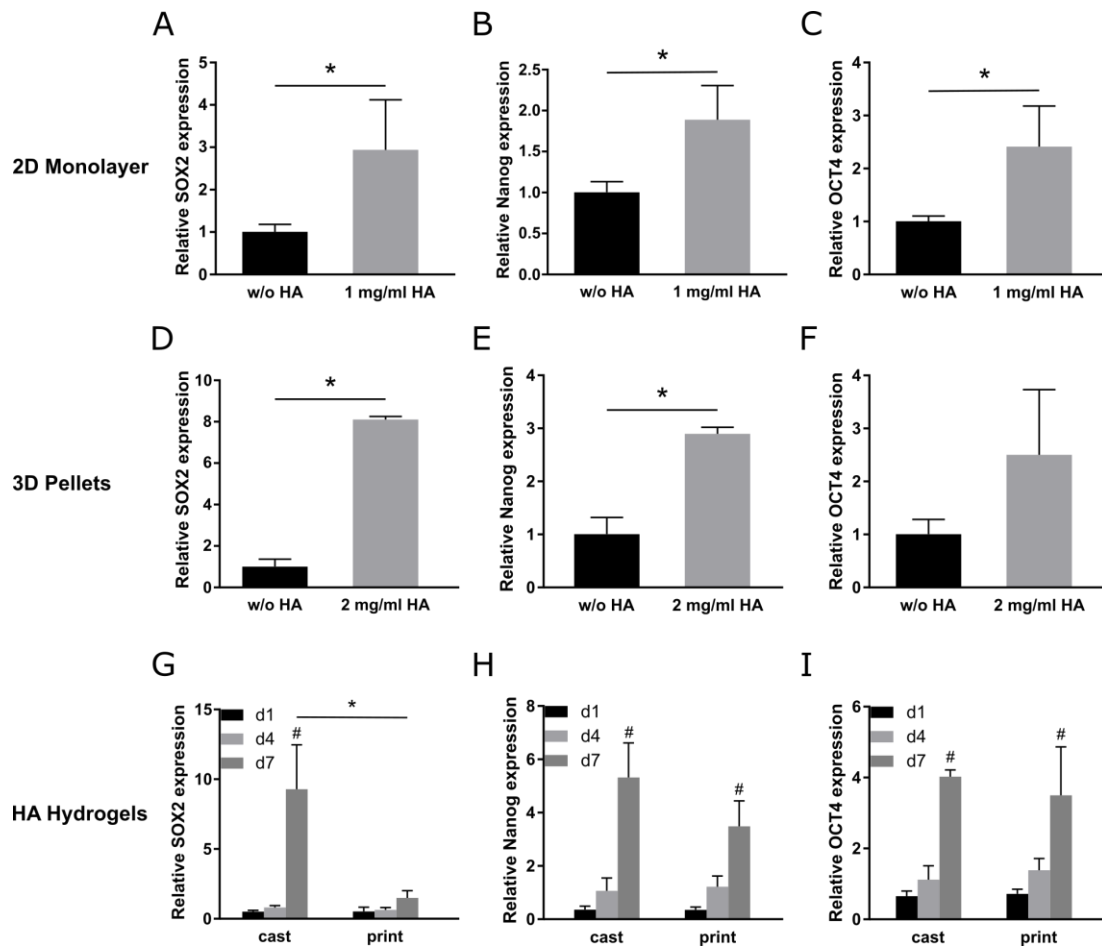

Figure 32: Relative gene expression of SOX2, Nanog and OCT4 in human MSCs in 2D monolayer and 3D pellets, or HA-based hydrogels. MSCs in 2D monolayer and 3D pellets were cultured with or without HA (0.6-1.0 MDa). Relative gene expression in 2D monolayer culture after two days in basic serum-free medium with or without 1 mg/ml HA, **(A)** SOX2, **(B)** Nanog and **(C)** OCT4. Relative gene expression in 3D pellet culture after one day in basic serum-free medium with or without 2 mg/ml HA, **(D)** SOX2, **(E)** Nanog and **(F)** OCT4. Relative gene expression of **(G)** SOX2, **(H)** Nanog and **(I)** OCT4 in HA-SH hydrogels (HA-SH/PEGDA/PEG-allyl/Irgacure2959 hydrogel) after one, four and seven days in basic chondrogenic medium without TGFβ1. Hydrogels were either cast or 3D bioprinted before crosslinking. Data are presented as means ± standard deviation (n=3 biological replicates). (*) indicates statistically significant differences between two values ($p < 0.05$). (#) indicates statistically significant differences between this time point and the other two time points in the same condition (cast or print) ($p < 0.05$). Gene expression levels of 2D cultured MSCs (**A, B, C**) and 3D pellet cultured MSCs (**D, E, F**) were normalized to the gene expression of the housekeeping gene GAPDH and to the gene expression of the respective value without HA. Gene expression levels of MSCs

encapsulated in HA-SH hydrogel (**G, H, I**) were normalized to the gene expression of the housekeeping gene GAPDH and to the gene expression of MSCs before they were encapsulated in the hydrogel.

Maintenance of MSC stemness is an important topic for regenerative medicine because the necessary step of *in vitro* expansion in 2D monolayer can reduce proliferation and differentiation capacity in these cells, probably through aging processes [286-288]. MSCs are defined by their ability to self-renew and to differentiate into chondrogenic, osteogenic and adipogenic direction. Stemness is a prerequisite for these abilities [289]. If stemness is reduced in MSCs, so is the ability of the cells to differentiate.

SOX2, Nanog and OCT4 are stemness markers of embryonic stem cells (ESCs), and they are also expressed in MSCs [290-292]. SOX2, OCT4 and Nanog have been shown to act together as a core transcriptional network to maintain stemness [292]. When OCT4, SOX2 or Nanog were overexpressed in MSCs of different origin, proliferation and differentiation capacity were enhanced [293-295]. In previous studies, HA has been found to maintain stemness in MSCs [269,270] and to increase the expression of SOX2, Nanog and OCT4 [296,297]. The same was observed in the present study when HA was added to the basic serum-free culture medium of 2D monolayer and 3D pellet cultures. MSCs in the HA-SH hydrogel showed significant upregulation of the stemness markers on d7 which suggested that maybe HA had similar biological functions when it was modified and crosslinked in comparison to when it was added unmodified to the culture medium. The 3D microenvironment in a hydrogel could also contribute to the maintenance or upregulation over time of stemness in MSCs. The relation between stemness, HA signalling and 3D microenvironment would be an intriguing topic for further research.

On d7, cast hydrogels showed increased gene expression of MSCs for stemness markers but 3D bioprinted constructs had lower SOX2 gene expression levels in comparison. This suggested that the 3D bioprinting process affected the MSCs in a way that gene regulation of SOX2 was changed.

4.2.3 Influence of hyaluronan on different transcription factors

The impact of HA on differentiation of MSCs was investigated. Therefore, gene expression of transcription factors of major differentiation directions of MSCs were analysed with HA supplementation in basic serum-free medium and in HA-based hydrogels. The chondrogenic transcription factors SOX9, SOX5 and SOX6, the osteogenic transcription factor

RUNX2 and the adipogenic transcription factor PPARG were examined in the present study.

4.2.3.1 Influence on SOX9, SOX5 and SOX6

In 2D monolayer culture, the gene expression of SOX9 was significantly upregulated when HA was added to the serum-free basic medium (Figure 33 A). SOX5 and SOX6 gene expression were not affected by HA in 2D monolayer (Figure 33 B, C). SOX9 gene expression was also significantly upregulated in 3D pellet culture with HA (Figure 33 D), and SOX5 showed an increase by trend (Figure 33 E). SOX6 gene expression was not influenced by HA in 3D pellet culture. (Figure 33 F). When MSCs were encapsulated in the HA-SH hydrogel, the gene expression of SOX9, SOX5 and SOX6 was significantly upregulated from d1 to d7. SOX5 gene expression on d7 was slightly higher in printed constructs than in cast constructs (Figure 33 H). SOX9, SOX5 and SOX6 are known to be transcription factors that are essential for chondrogenesis [296-300]. They act cooperatively to activate transcription of several chondrogenic genes like COL2A1 and ACAN through binding and activation of enhancer sequences [301]. It has been shown previously that when SOX9 was lacking in early chondrogenesis, no proper ECM could be produced because cells could not express the respective genes [302]. When both SOX5 and SOX6 were lacking, expression of cartilage specific genes was severely hampered even though SOX9 was expressed normally [303]. As the expression and cooperation of these three transcription factors is very important for early chondrogenesis, it was tested if HA can influence them. HA signalling has been shown before to positively regulate chondrogenesis and, among other chondrogenesis-associated factors, SOX9 gene expression [164,165,259,260,262,263,304,305]. Less is known about the influence of HA on gene expression of SOX5 and SOX6. Here, HA did not induce significant changes in SOX5 or SOX6 gene expression in 2D or 3D pellet culture even if SOX5 was upregulated by trend in 3D pellet culture. HA might influence the different SOX gene expressions differently. They act cooperatively, but they also have individual functions in the formation of cartilage and in other tissues. SOX9 but not SOX5 and SOX6 were, for example, needed in pre-cartilaginous condensations [303]. On the other hand, SOX5 and SOX6 did not need SOX9 for activation at the beginning of chondrogenesis [306]. The results of the present study showed that HA influenced the gene expression of SOX9 more than that of SOX5 and SOX6.
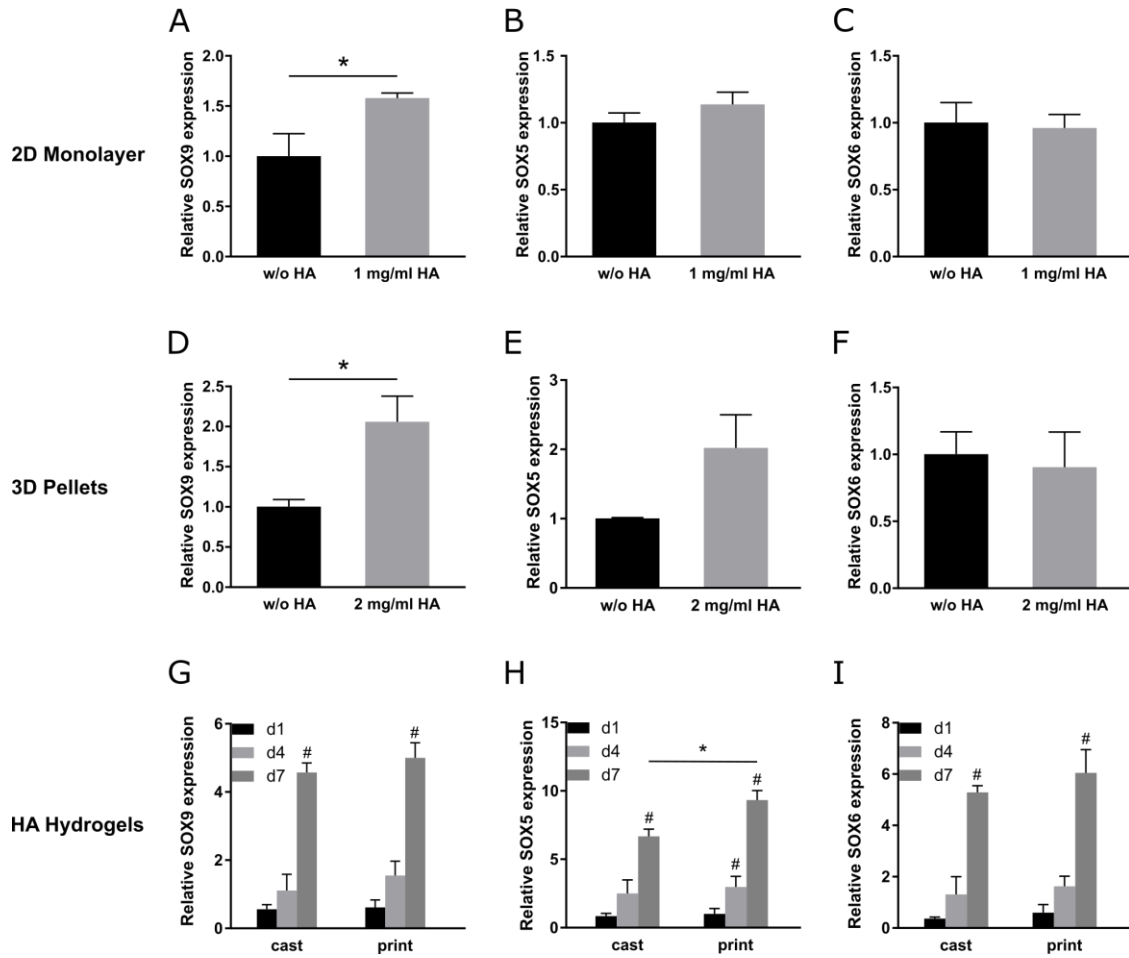
Figure 33: Relative gene expression of SOX9, SOX5 and SOX6 in human MSCs in 2D monolayer and 3D pellets, or HA-based hydrogels. MSCs in 2D monolayer and 3D pellets were cultured with or without HA (0.6-1.0 MDa). Relative gene expression in 2D monolayer culture after two days in basic serum-free medium with or without 1 mg/ml HA, **(A)** SOX9, **(B)** SOX5 and **(C)** SOX6. Relative gene expression in 3D pellet culture after one day in basic serum-free medium with or without 2 mg/ml HA, **(D)** SOX9, **(E)** SOX5 and **(F)** SOX6. Relative gene expression of **(G)** SOX9, **(H)** SOX5 and **(I)** SOX6 in HA-SH hydrogels (HA-SH/PEGDA/PEG-allyl/Irgacure2959 hydrogel) after one, four and seven days in basic chondrogenic medium without TGFβ1. Hydrogels were either cast or 3D bioprinted before crosslinking. Data are presented as means ± standard deviation (n=3 biological replicates). (*) indicates statistically significant differences between two values ($p < 0.05$). (#) indicates statistically significant differences between this time point and the other two time points in the same condition (cast or print) ($p < 0.05$). Gene expression levels of 2D cultured MSCs (**A, B, C**) and 3D pellet cultured MSCs (**D, E, F**) were normalized to the gene expression of the housekeeping gene GAPDH and to the gene expression of the respective value without HA. Gene expression levels of MSCs encapsulated in HA-SH hydrogel (**G, H, I**) were normalized to the gene expression of the housekeeping gene GAPDH and to the gene expression of MSCs before they were encapsulated in the hydrogel.

In HA-SH hydrogels, without TGFβ1 supplementation, the expression of all three SOX genes was significantly upregulated from d1 to d7. This suggested that the microenvironment of these HA-based hydrogels allowed MSCs to upregulate chondrogenic transcription factors even without the addition of growth factors like TGFβ1. This indicated that the HA hydrogels provided a beneficial environment for possible chondrogenesis.

107

4.2.3.2 Influence on RUNX2 and PPARG

To assess the influence of HA on osteogenic and adipogenic gene expression in addition to chondrogenic gene expression of MSCs, gene expression levels of RUNX2, a transcription factor of osteogenic genes, and of PPARG, a transcription factor of adipogenic genes, were investigated. HA in basic serum-free medium did not change gene expression of RUNX2 and PPARG in 2D monolayer culture or in 3D pellet culture (Figure 34 A, B, C, D). When cells were cultured in HA-SH hydrogels, no significant upregulation was observed from d1 to d4. However, at d7 of hydrogel culture, both transcription factors were significantly up-regulated in cast and 3D-bioprinted constructs (Figure 34 E, F).
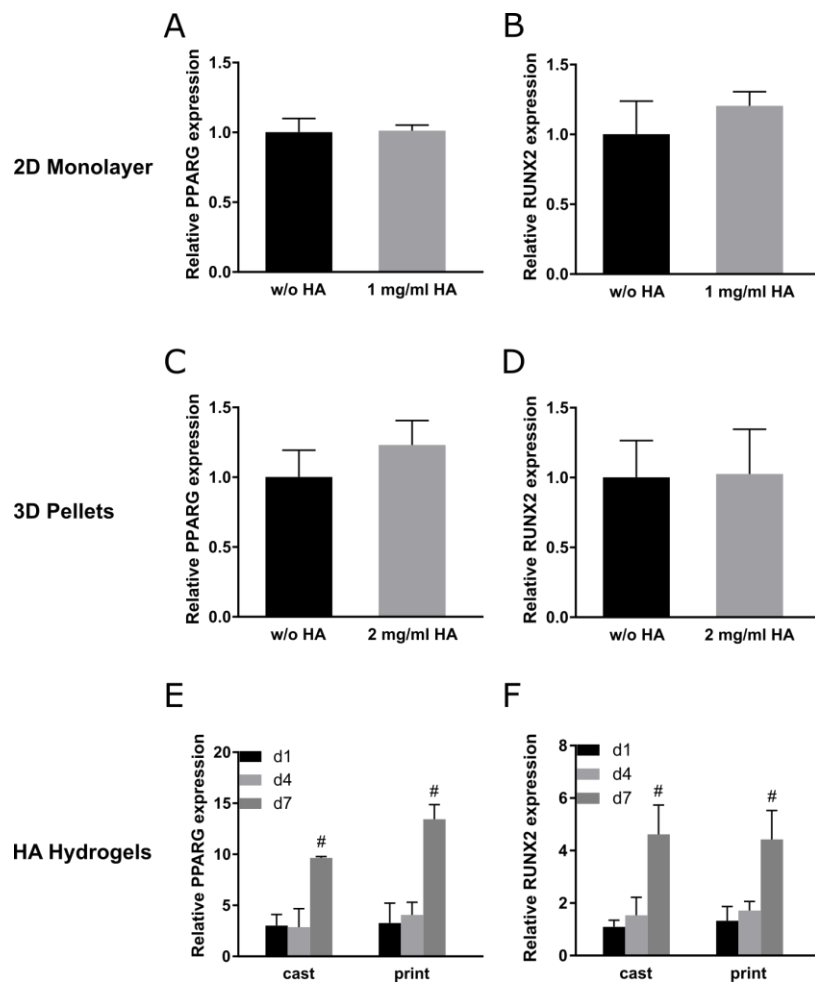

Figure 34: Relative gene expression of PPARG and RUNX2 in human MSCs in 2D monolayer and 3D pellets, or HA-based hydrogels. MSCs in 2D monolayer and 3D pellets were cultured with or without HA (0.6-1.0 MDa). Relative gene expression in 2D monolayer culture after two days in basic serum-free medium with or without 1 mg/ml HA, **(A)** PPARG and **(B)** RUNX2. Relative gene expression in 3D pellet culture after one day in basic serum-free medium with or without 2 mg/ml HA, **(C)** PPARG and **(D)** RUNX2. Relative gene expression of **(E)** PPARG and **(F)** RUNX2 in HA-SH hydrogels (HA-SH/PEGDA/PEG-al-lyl/Irgacure2959 hydrogel) after one, four and seven days in basic chondrogenic medium without TGFβ1. Hydrogels were either cast or 3D bioprinted before crosslinking. Data are presented as means ± standard

deviation (n=3 biological replicates). (*) indicates statistically significant differences between two values (p < 0.05). (#) indicates statistically significant differences between this time point and the other two time points in the same condition (cast or print) (p < 0.05). Gene expression levels of 2D cultured MSCs (**A, B**) and 3D pellet cultured MSCs (**C, D**) were normalized to the gene expression of the housekeeping gene GAPDH and to the gene expression of the respective value without HA. Gene expression levels of MSCs encapsulated in HA-SH hydrogel (**E, F**) were normalized to the gene expression of the housekeeping gene GAPDH and to the gene expression of MSCs before they were encapsulated in the hydrogel.

Unmodified HA did not influence the gene expression of the osteogenic transcription factor RUNX2 or the adipogenic transcription factor PPARG, while it significantly upregulated the chondrogenic transcription factor SOX9 in 2D and 3D pellet culture (Figure 33 A, D, p. 107). The reports about effects of HA on osteogenic or adipogenic differentiation are controversial. Some studies found that HA increased osteogenesis marker or bone formation [307-310], others did not see any effects or even downregulation [296,311]. These studies also showed that MW and concentration of HA can have different effects on the different factors of osteogenesis [308,310]. Some of the conflicting results are probably due to these or other differences in the culture conditions, cell types or HA delivery methods. Zou et al. demonstrated that 2D cultured MSCs in basic medium with addition of HA upregulated SOX9 gene expression after seven days but downregulated the gene expression of the osteogenic markers RUNX2, SP7 (osterix), ALP, COL1A1 and COL10A1 (type X collagen) [312]. In the present study, gene expression was only examined after two days but the upregulation of SOX9 was already visible. RUNX2 gene expression was not changed by HA after two days of 2D culture with HA. These results suggested that HA in basic medium without serum supported the chondrogenic lineage of MSC differentiation rather than the osteogenic lineage. The gene expression of RUNX2 in HA-SH hydrogels showed significant upregulation in both cast and 3D bioprinted constructs from d1 to d7 and from d4 to d7. This was not in line with the results from 2D and 3D pellet experiments. However, the hydrogel experiment was longer than the others and RUNX2 expression only increased significantly after 7 days. A longer experiment for 2D and 3D pellets could show how RUNX2 expression develops after a longer cultivation time under these conditions. However, even if the exact effects of HA on osteogenesis are not completely clear yet, the application of HA materials as cell and growth factor carriers in bone regeneration has generated promising results [313,314]. The upregulation of RUNX2 gene expression in the HA-SH hydrogel in the present study might be the result of the specific 3D environment that the hydrogel provided for the cells and/or of a biological effect of HA on the cells that has yet to be elucidated.

The effect of HA on PPARG gene expression was very similar to the effect on RUNX2. Studies about the effect of HA on adipogenesis had conflicting results, probably also due to the inconsistencies in study design like different MW, concentrations, culture conditions or cell types. Some works reported inhibitory effects of HA on adipogenesis [315-317], while others showed that HA could promote adipogenesis [318,319]. However, a previous work could demonstrate that CD44 and CD168 influenced adipogenesis very differently: While CD44 was required for adipogenesis, CD168 was found to suppress adipogenesis [320]. These opposing functions of receptors that can both be influenced by HA could also be the reason behind previous conflicting results. In the present study, PPARG gene expression was not changed by HA in 2D monolayer or 3D pellet culture. Gene expression was only analysed for one or two days in these experiments, and it is possible that PPARG expression could change after a longer cultivation time. However, SOX9 was already significantly up-regulated at these early time points and that suggested that HA promoted chondrogenic differentiation stronger or earlier than it did adipogenic differentiation, similar to osteogenic differentiation. PPARG gene expression was significantly upregulated in cells that were cultivated for seven days in HA-SH hydrogels. HA-based gels and materials have been used successfully for adipose tissue regeneration, even though the direct effects of HA on these processes are not fully known. As the HA-SH hydrogel in the present study permitted up-regulation of the adipogenic transcription factor PPARG, it may also be a suitable material for adipogenic differentiation of MSCs.

4.2.4 Influence of hyaluronan on chondrogenic markers ACAN and COL2A1

After the result that HA influenced the chondrogenic transcription factor SOX9 more than the osteogenic transcription factor RUNX2 and the adipogenic transcription factor PPARG, the effect of HA on the chondrogenic markers type II collagen and aggrecan was evaluated. The addition of HA to basic serum-free medium in 2D monolayer culture of MSCs significantly upregulated the gene expression of COL2A1 (type II collagen) (Figure 35 A) and ACAN (aggrecan) (Figure 35 B) after two days. In 3D pellet culture, gene expression of COL2A1 (Figure 35 C) but not ACAN (Figure 35 D) was significantly upregulated after one day of culture in basic serum-free medium with HA. When MSCs were encapsulated in HA-SH hydrogels, COL2A1 gene expression was not changed significantly from d1 to d4 or between cast and 3D bioprinted constructs. However, after seven days COL2A1 was significantly upregulated in cast, but not in 3D bioprinted hydrogels (Figure 35 E). ACAN

gene expression of MSCs in HA-SH hydrogels decreased significantly from d1 to d4 but increased again on d7 for both cast and bioprinted hydrogels (Figure 35 F).
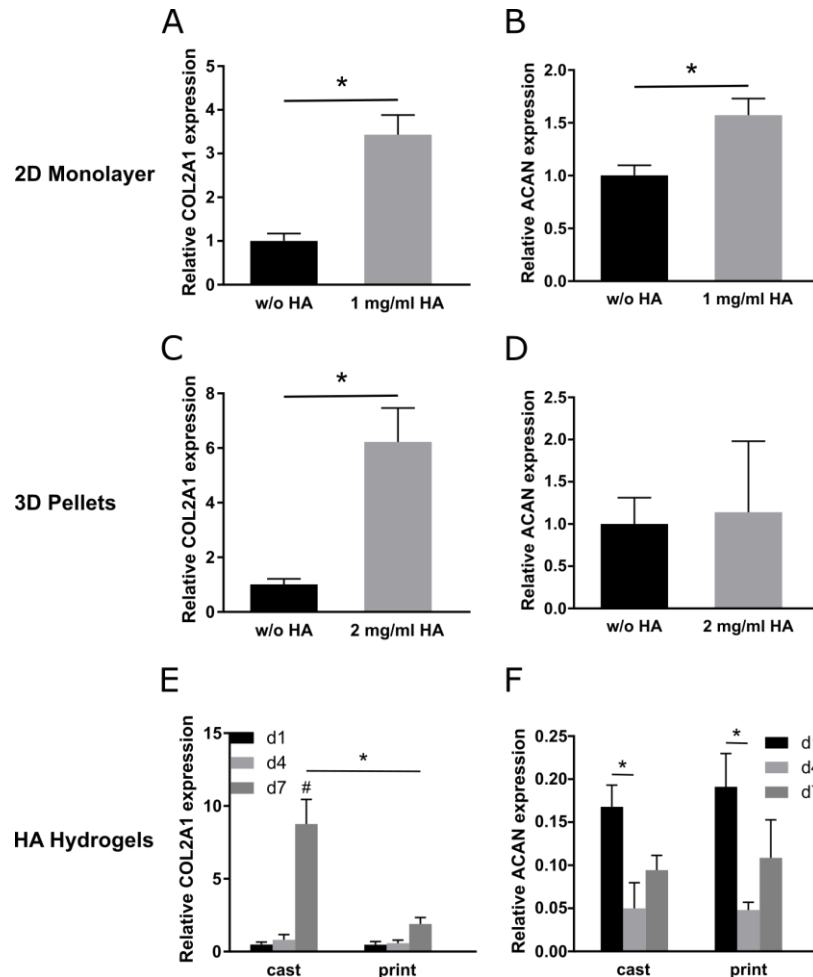

Figure 35: Relative gene expression of COL2A1 and ACAN in human MSCs in 2D monolayer and 3D pellets, or HA-based hydrogels. MSCs in 2D monolayer and 3D pellets were cultured with or without HA (0.6-1.0 MDa). Relative gene expression in 2D monolayer culture after two days in basic serum-free medium with or without 1 mg/ml HA, **(A)** COL2A1 and **(B)** ACAN. Relative gene expression in 3D pellet culture after one day in basic serum-free medium with or without 2 mg/ml HA, **(C)** COL2A1 and **(D)** ACAN. Relative gene expression of **(E)** COL2A1 and **(F)** ACAN in HA-SH hydrogels (HA-SH/PEGDA/PEG-al-lyl/Irgacure2959 hydrogel) after one, four and seven days in basic chondrogenic medium without TGFβ1. Hydrogels were either cast or 3D bioprinted before crosslinking. Data are presented as means ± standard deviation (n=3 biological replicates). (*) indicates statistically significant differences between two values (p < 0.05). (#) indicates statistically significant differences between this time point and the other two time points in the same condition (cast or print) (p < 0.05). Gene expression levels of 2D cultured MSCs (**A, B**) and 3D pellet cultured MSCs (**C, D**) were normalized to the gene expression of the housekeeping gene GAPDH and to the gene expression of the respective value without HA. Gene expression levels of MSCs encapsulated in HA-SH hydrogel (**E, F**) were normalized to the gene expression of the housekeeping gene GAPDH and to the gene expression of MSCs before they were encapsulated in the hydrogel.

The upregulation of COL2A1 and ACAN gene expression in 2D culture showed that HA was able to induce chondrogenic markers in serum-free medium without other

chondrogenic inducers, probably via influencing SOX9 gene expression. The same was true for COL2A1 in 3D pellet cultures. Cells in HA-SH hydrogels showed an upregulation of COL2A1 gene expression on d7 but only in cast and not in printed constructs. The low levels of COL2A1 gene expression on d7 in printed hydrogels in comparison to cast hydrogels indicated a negative effect of the printing procedure on the cells. A similar effect of 3D bioprinting on MSC gene expression has also been shown in a previous study [107]. This effect illustrates again that it is important to monitor the effects of 3D bioprinting procedures on the cells.

ACAN gene expression was not influenced by the 3D printing process. However, it was strongly downregulated on all time points in the HA-SH hydrogel in comparison to the MSCs before they were encapsulated in the hydrogel (the value that the gene expression was normalized to; equates to 1). Gene expression of ACAN even dropped from d1 to d4. On d7 it was upregulated in comparison to d4 but still not as high as on d1. It is interesting that gene expression of COL2A1 and ACAN that are both targets of SOX9 transcription factor were so differently affected by the culture in HA-SH hydrogels. A previous study showed that after 28 days of chondrogenic differentiation with TGFβ3 the gene expression of ACAN was significantly reduced in HA hydrogels with increasing polymer content (1 %, 3 %, 5 %), while COL2A1 gene expression was not affected [253]. This shows one factor, namely polymer content, that can affect the gene expression of COL2A1 and ACAN differently. The HA-SH/PEGDA/PEG-Allyl/Irgacure2959 hydrogel in the present study had a polymer content of 2 %, and it has been shown before that MSCs can produce abundant aggrecan when they are chondrogenically differentiated with TGFβ1 for 21 days in this hydrogel (Hauptstein et al., manuscript in preparation). However, in the present study, MSCs were cultured without TGFβ1 and only for seven days. It appeared that the presence of the cells in the 3D HA-based microenvironment and the upregulated SOX9 were not enough to promote ACAN gene expression as they did for COL2A1. Maybe ACAN gene expression is only upregulated when a stronger chondrogenic induction takes place, and maybe the amount of polymer in the HA-SH/PEGDA/PEG-Allyl/Irgacure2959 hydrogel affected ACAN gene expression negatively in this setting.

4.2.5 Summary of the effects of hyaluronan on MSCs

The effects of unmodified HA on the gene expression of 2D monolayer and 3D pellet cultivated MSCs was investigated as well as the gene expression of MSCs encapsulated in cast or 3D bioprinted HA-SH hydrogels. It was demonstrated that unmodified HA in the basic serum-free culture medium of 2D cultured human MSCs upregulated the chondrogenic transcription factor SOX9 (but not SOX5 and SOX6) rather than the osteogenic transcription factor RUNX2 or the adipogenic transcription factor PPARG. Probably as a result from SOX9 upregulation the chondrogenic markers COL2A1 and ACAN were also upregulated, while the gene expression of the HA receptors CD44 and CD168 was not changed significantly. In addition to the chondrogenic markers, the stemness markers SOX2, Nanog and OCT4 were upregulated by HA supplementation as has been described in the literature [165,262,263,296,297]. Unmodified HA alone cannot induce a complete chondrogenesis with abundant ECM production and differentiation of MSCs to chondrocyte-like cells like TGFβ1. In comparison to the upregulation of chondrogenic genes that happens under the influence of TGFβ1 in HA-SH hydrogels until d7 (ACAN: up to 200-fold; COL2A1: up to 10000-fold [169], the upregulation under HA alone was much smaller for COL2A1 after seven days (8-fold) and ACAN was even downregulated. HA supplementation rather caused a tendency towards chondrogenic differentiation than a strong induction of chondrogenesis. HA might be involved in the signalling pathways that direct chondrogenesis, but it is also involved in the maintenance of stemness. Differentiation and maintenance of stemness are two processes that are inevitably connected with one another. The maintenance of stemness is in the end also the maintenance of the ability to differentiate [289]. HA has been suggested to regulate the balance between differentiation and quiescence of stem cells especially in the stem cell niche [271]. The MSCs under the influence of HA were most likely still stem cells but with a tendency towards chondrogenic differentiation. Therefore, it was possible that both stemness markers and chondrogenic markers were upregulated. The exact mechanism of HA function in this context should be further analysed, for example with investigation of the involved proteins and signalling pathways in addition to gene expression.

The effects of HA on relative gene expression in MSCs that were cultured in 3D pellets were mostly similar to the HA effects on gene expression of MSCs in 2D monolayer culture. The small differences between 2D monolayer and 3D pellet culture that were seen in the gene expression levels were most likely the results of the different cell microenvironments. 3D cell cultures like pellets usually represent the natural environment of cells better than

2D cultures. Several factors are different in 3D culture, for example cell shape, exposure to medium, cell junctions, gene expression levels and response to stimuli [321].

The regulation of the relative gene expression of MSCs in cast HA-SH hydrogels (HA-SH/PEGDA/PEG-allyl/Irgacure2959 hydrogel) was similar for most of the investigated markers. The genes showed significant upregulation of expression from d1 to d7. This effect of cultivation in HA-based hydrogels did not correspond entirely to the effects of HA that were seen in 2D and 3D pellet cultures. For example, RUNX2 and PPARG were not affected by HA in 2D or 3D pellet culture but were strongly upregulated in HA hydrogels. It is possible that the upregulations in the hydrogel did not (only) originate from biological effects of HA but also from the 3D environment as such that the hydrogel provided for the cells. HA-based hydrogels are often used successfully for regeneration of adipose or bone tissue [313,314,319,322,323]. Here, it was demonstrated that our HA-SH/PEGDA/PEG-allyl/Irgacure2959 hydrogel that is usually used in chondrogenic differentiation experiments of MSCs, might also be suitable for osteogenesis or adipogenesis as it did not inhibit the upregulation of RUNX2 and PPARG. The HA-SH hydrogel also appeared to be suitable for the maintenance of stemness in MSCs. As all of these genes were upregulated at the same time in the same cells, it can be suggested that no exclusive differentiation direction was induced in the HA-SH hydrogel without growth factors like TGFβ1 for chondrogenesis. This could mean that either the biological activity of HA was reduced when it was modified and crosslinked into a hydrogel or that the influence of the microenvironment that was provided by the hydrogel was so strong that other effects, like that of HA, were overruled. A combination of both is also possible. Previous studies have shown that modification of HA can reduce its binding to and effects on cells [218,219].

CD168, CD44 and ACAN gene expression levels were regulated differently from the rest of the investigated genes in HA-SH hydrogels. These genes might probably be influenced by additional other factors like cell cycle regulation for CD168, clustering for CD44 or polymer content for ACAN. Further research would be needed to investigate the different factors that are influencing gene expression in this context in more detail.

3D bioprinting of MSCs in HA-SH precursor solution mostly did not change relative gene expression levels in comparison to MSCs in cast hydrogels. Interestingly, COL2A1, SOX2, and CD168 showed significantly lower gene expression levels on d7 in printed than in cast hydrogel constructs. This suggested that the printing process itself influenced the cells in a way that gene expression of several factors was still affected after seven days of culture in HA-SH hydrogels. A downregulation of COL2A1 in MSCs in printed hydrogel constructs

was also demonstrated in a previous work [107]. Further studies with different applied printing pressure and viscosity of the hydrogel solution would be needed to elucidate how and why gene expression is changed by the mechanical forces that act on the cells during printing. Analysis of involved proteins and signalling pathways could add valuable information to such investigations. If the involved mechanisms could be elucidated, it would not only expand our knowledge about the effects of mechanical stress on MSCs and the role of the 3D environment of HA-SH hydrogels in MSC gene expression regulation, but it could also enable us to make 3D bioprinting more cell-friendly.

The gene expression studies that were performed in this work can act as preliminary results for a continued project on the signalling effects of HA in general and on the effects of HA in 3D hydrogels in particular. For example, the effects of HA of different MW or concentration could be further analysed. The experiments that were presented here were also mostly of short duration, and HA effects could also be evaluated in the long-term. Additionally, the three culture conditions that were analysed in this study cannot completely be compared to each other as several factors are different between them that could modulate the effects of HA on the cells. For example, 2D and 3D pellet experiments could be performed with modified HA to directly compare it to unmodified HA in the same culture conditions. To evaluate the contribution of HA signalling to the different effects in HA hydrogels, HA receptors like CD44 or CD168 could be blocked, or hydrogels with similar characteristics but without HA could be used for comparison. Binding of unmodified HA and modified HA to CD44 could also be directly analysed, for example with FACS studies. Also, the underlying signalling pathways and regulations could be further studied. As only gene expression was analysed so far, protein expression and activity would be very interesting additional results. All this and more will probably be done in future studies. This work on the effect of HA on cells can be seen as a preliminary study for a future project.

Conclusion

5 Conclusion

Articular cartilage is a tissue without blood supply and therefore limited capacity for self-regeneration upon injury. As a result, cartilage injury can lead to degeneration of the tissue and the development of osteoarthritis. Osteoarthritis is one of the leading causes of disability in the elderly population due to chronic pain and reduced mobility. Current clinical treatments cannot regenerate the damaged tissue to its previous native form and function. Tissue engineering and 3D bioprinting are promising to improve the results of cartilage repair tissue in the future. Even if the regeneration of the native form of articular cartilage has not been achieved so far, the potential of tissue engineering is still tremendous. New cell sources, new materials and signals for the cells are constantly discovered, developed, improved and tested with the aim to enhance the quality of the resulting tissue.

A relatively new, promising cell source, articular cartilage progenitor cells (ACPCs), was investigated in this work in comparison to mesenchymal stromal cells (MSCs). In agarose, a gold-standard hydrogel for cartilage tissue engineering, ACPCs produced a more articular cartilage-like tissue with more GAG, less type I collagen and low ALP activity in comparison to the neo-cartilage tissue assembled by MSCs. Hypoxic conditions improved the quality of the neo-cartilage tissue produced by MSCs by making it less hypertrophic and less fibrocartilaginous. An increase in ECM production was not achieved by hypoxic conditions or by zonal co-culturing of ACPCs and MSCs. However, interactions between the two cell types in zonal agarose constructs were detected as, for example, the staining intensities of type II and type I collagen were modulated in zonal constructs in comparison to non-zonal monoculture constructs under normoxic and hypoxic conditions. In the HA-based hydrogel HA-SH/P(AGE-co-G), MSCs produced more cartilage ECM than ACPCs and achieved thereby a zonal ECM distribution that was similar to native articular cartilage with more ECM in the deep zone. However, for both cell types, the formed ECM was located only pericellularly and was not spread throughout the whole hydrogel like in agarose. These results clearly emphasised that the chondrogenic potential of ACPCs and MSCs is strongly dependent on the cell microenvironment. ACPCs can be a promising cell source for articular cartilage engineering if they are cultivated in a suitable hydrogel environment like agarose. When the present thesis and previous studies [103,107,131,254,255] were taken into consideration, it appeared that chondrogenesis of ACPCs was supported by hydrogels without biological attachment sites, such as agarose, and that hydrogels containing biological cues like HA were beneficial for chondrogenic differentiation of MSCs. Additionally, a microenvironment with a high polymer content like in HA-SH/

P(AGE-co-G) hydrogels can prevent homogenous ECM distribution by restricting the ECM to the pericellular region. Therefore, it is of paramount importance to thoroughly evaluate compatibility between cells and their hydrogel microenvironment to achieve the best possible results in the engineering of articular cartilage tissue.

As HA appeared to have beneficial effects on the chondrogenesis of MSCs in the present work and in previous studies [164,165,258], the contribution of HA to chondrogenic gene expression was investigated in more detail. It was shown that HA supplementation supported chondrogenic but not adipogenic or osteogenic gene expression in 2D and 3D pellet cultures. The investigated HA-based hydrogel did not support a specific differentiation lineage in encapsulated MSCs but appeared to be a suitable environment for several different applications like maintenance of stemness and chondrogenic, osteogenic or adipogenic differentiation. The investigation of MSCs´ gene expression under the influence of HA in this work showed promising results for the use of HA in MSC-based tissue engineering. The effects of modified and crosslinked HA in hydrogels on the cells is of special interest and should be elucidated further in future studies. This might enable tissue engineering approaches that can use the full potential that the versatile, bioactive molecule HA has to offer.

The investigation of the 3D bioprinting process of MSCs in HA-based hydrogels showed that 3D printing did not influence most of the examined gene expression levels in MSCs, but nevertheless, three genes were downregulated in printed versus cast constructs. These results highlighted that 3D printing can change the behaviour of cells in the long-term, and that printed cells should be monitored for these changes before other experiments are performed with them. However, these results also offer the opportunity for more extensive research that could expand our knowledge about the influence of mechanical stress and 3D microenvironment on MSCs and lead to the development of more cell-friendly printing processes.

In total, it was shown that the chondrogenic potential of ACPCs and MSCs is strongly dependent on the cell microenvironment, especially the used hydrogels. ACPCs can be a promising cell source for articular cartilage engineering if they are cultivated in a suitable hydrogel like agarose. The results of this thesis expand the knowledge in the area of articular cartilage engineering with regard to the rational combination of cell types and hydrogel materials and open up new possible approaches to the regeneration of articular cartilage tissue.

Bibliography

6 Bibliography

1. Naumann, A.; Dennis, J.E.; Awadallah, A.; Carrino, D.A.; Mansour, J.M.; Kastenbauer, E.; Caplan, A.I. Immunochemical and mechanical characterization of cartilage subtypes in rabbit. *J Histochem Cytochem* **2002**, *50*, 1049-1058, doi:10.1177/002215540205000807.
2. Fithian, D.C.; Kelly, M.A.; Mow, V.C. Material properties and structure-function relationships in the menisci. *Clin Orthop Relat Res* **1990**, 19-31.
3. Carballo, C.B.; Nakagawa, Y.; Sekiya, I.; Rodeo, S.A. Basic Science of Articular Cartilage. *Clin Sports Med* **2017**, *36*, 413-425, doi:10.1016/j.csm.2017.02.001.
4. Camarero-Espinosa, S.; Rothen-Rutishauser, B.; Foster, E.J.; Weder, C. Articular cartilage: from formation to tissue engineering. *Biomater Sci* **2016**, *4*, 734-767, doi:10.1039/c6bm00068a.
5. Fox, S.A.J.; Bedi, A.; Rodeo, S.A. The basic science of articular cartilage: structure, composition, and function. *Sports Health* **2009**, *1*, 461-468, doi:10.1177/1941738109350438.
6. Monaghan, N.G.; Wyss, J.F. Joint Pain. In *Pain Management and Palliative Care: A Comprehensive Guide*, Sackheim, K.A., Ed. Springer New York: New York, NY, **2015**; doi:10.1007/978-1-4939-2462-2_19pp. 131-140.
7. Decker, R.S.; Koyama, E.; Pacifici, M. Articular Cartilage: Structural and Developmental Intricacies and Questions. *Curr Osteoporos Rep* **2015**, *13*, 407-414, doi:10.1007/s11914-015-0290-z.
8. Ondrésik, M.; Oliveira, J.M.; Reis, R.L. Knee Articular Cartilage. In *Regenerative Strategies for the Treatment of Knee Joint Disabilities*, Oliveira, J.M., Reis, R.L., Eds. Springer International Publishing: Cham, **2017**; doi:10.1007/978-3-319-44785-8_1pp. 3-20.
9. Sanchez-Adams, J.; Leddy, H.A.; McNulty, A.L.; O'Conor, C.J.; Guilak, F. The mechanobiology of articular cartilage: bearing the burden of osteoarthritis. *Curr Rheumatol Rep* **2014**, *16*, 451, doi:10.1007/s11926-014-0451-6.
10. Houck, D.A.; Kraeutler, M.J.; Belk, J.W.; Frank, R.M.; McCarty, E.C.; Bravman, J.T. Do Focal Chondral Defects of the Knee Increase the Risk for Progression to Osteoarthritis? A Review of the Literature. *Orthop J Sports Med* **2018**, *6*, 2325967118801931, doi:10.1177/2325967118801931.
11. Sacitharan, P.K. Ageing and Osteoarthritis. *Subcell Biochem* **2019**, *91*, 123-159, doi:10.1007/978-981-13-3681-2_6.
12. Glyn-Jones, S.; Palmer, A.J.; Agricola, R.; Price, A.J.; Vincent, T.L.; Weinans, H.; Carr, A.J. Osteoarthritis. *Lancet* **2015**, *386*, 376-387, doi:10.1016/s0140-6736(14)60802-3.
13. Cross, M.; Smith, E.; Hoy, D.; Nolte, S.; Ackerman, I.; Fransen, M.; Bridgett, L.; Williams, S.; Guillemin, F.; Hill, C.L.; Laslett, L.L.; Jones, G.; Cicuttini, F.; Osborne, R.; Vos, T.; Buchbinder, R.; Woolf, A.; March, L. The global burden of hip and knee osteoarthritis: estimates from the global burden of disease 2010 study. *Ann Rheum Dis* **2014**, *73*, 1323-1330, doi:10.1136/annrheumdis-2013-204763.
14. Schizas, N.; Savvidou, O.; Triantafyllopoulos, I.; Papadakis, S.; Dontas, I.; Papagelopoulos, P. Adjuvant therapies for the enhancement of microfracture technique in cartilage repair. *Orthop Rev (Pavia)* **2019**, *11*, 7950-7950, doi:10.4081/or.2019.7950.
15. Richter, D.L.; Schenck, R.C., Jr.; Wascher, D.C.; Treme, G. Knee Articular Cartilage Repair and Restoration Techniques: A Review of the Literature. *Sports Health* **2016**, *8*, 153-160, doi:10.1177/1941738115611350.

16. Makris, E.A.; Gomoll, A.H.; Malizos, K.N.; Hu, J.C.; Athanasiou, K.A. Repair and tissue engineering techniques for articular cartilage. *Nat Rev Rheumatol* **2015**, *11*, 21-34, doi:10.1038/nrrheum.2014.157.

17. Hangody, L.; Füles, P. Autologous osteochondral mosaicplasty for the treatment of full-thickness defects of weight-bearing joints: ten years of experimental and clinical experience. *J Bone Joint Surg Am* **2003**, *85-A Suppl 2*, 25-32, doi:10.2106/00004623-200300002-00004.

18. Levy, Y.D.; Görtz, S.; Pulido, P.A.; McCauley, J.C.; Bugbee, W.D. Do fresh osteochondral allografts successfully treat femoral condyle lesions? *Clin Orthop Relat Res* **2013**, *471*, 231-237, doi:10.1007/s11999-012-2556-4.

19. Jiang, S.; Guo, W.; Tian, G.; Luo, X.; Peng, L.; Liu, S.; Sui, X.; Guo, Q.; Li, X. Clinical Application Status of Articular Cartilage Regeneration Techniques: Tissue-Engineered Cartilage Brings New Hope. *Stem Cells Int* **2020**, *2020*, 5690252, doi:10.1155/2020/5690252.

20. Minas, T.; Von Keudell, A.; Bryant, T.; Gomoll, A.H. The John Insall Award: A minimum 10-year outcome study of autologous chondrocyte implantation. *Clin Orthop Relat Res* **2014**, *472*, 41-51, doi:10.1007/s11999-013-3146-9.

21. Peterson, L.; Vasiliadis, H.S.; Brittberg, M.; Lindahl, A. Autologous chondrocyte implantation: a long-term follow-up. *Am J Sports Med* **2010**, *38*, 1117-1124, doi:10.1177/0363546509357915.

22. O'Brien, F.J. Biomaterials & scaffolds for tissue engineering. *Mater Today* **2011**, *14*, 88-95, doi:10.1016/S1369-7021(11)70058-X.

23. Huang, B.J.; Hu, J.C.; Athanasiou, K.A. Cell-based tissue engineering strategies used in the clinical repair of articular cartilage. *Biomaterials* **2016**, *98*, 1-22, doi:10.1016/j.biomaterials.2016.04.018.

24. Kwon, H.; Brown, W.E.; Lee, C.A.; Wang, D.; Paschos, N.; Hu, J.C.; Athanasiou, K.A. Surgical and tissue engineering strategies for articular cartilage and meniscus repair. *Nat Rev Rheumatol* **2019**, *15*, 550-570, doi:10.1038/s41584-019-0255-1.

25. Kon, E.; Filardo, G.; Di Martino, A.; Marcacci, M. ACI and MACI. *J Knee Surg* **2012**, *25*, 17-22, doi:10.1055/s-0031-1299651.

26. Schuette, H.B.; Kraeutler, M.J.; McCarty, E.C. Matrix-Assisted Autologous Chondrocyte Transplantation in the Knee: A Systematic Review of Mid- to Long-Term Clinical Outcomes. *Orthop J Sports Med* **2017**, *5*, 2325967117709250, doi:10.1177/2325967117709250.

27. Marlovits, S.; Aldrian, S.; Wondrasch, B.; Zak, L.; Albrecht, C.; Welsch, G.; Trattnig, S. Clinical and radiological outcomes 5 years after matrix-induced autologous chondrocyte implantation in patients with symptomatic, traumatic chondral defects. *Am J Sports Med* **2012**, *40*, 2273-2280, doi:10.1177/0363546512457008.

28. Kreuz, P.C.; Müller, S.; Freymann, U.; Erggelet, C.; Niemeyer, P.; Kaps, C.; Hirschmüller, A. Repair of focal cartilage defects with scaffold-assisted autologous chondrocyte grafts: clinical and biomechanical results 48 months after transplantation. *Am J Sports Med* **2011**, *39*, 1697-1705, doi:10.1177/0363546511403279.

29. Schneider, U.; Rackwitz, L.; Andereya, S.; Siebenlist, S.; Fensky, F.; Reichert, J.; Löer, I.; Barthel, T.; Rudert, M.; Nöth, U. A prospective multicenter study on the outcome of type I collagen hydrogel-based autologous chondrocyte implantation (CaReS) for the repair of articular cartilage defects in the knee. *Am J Sports Med* **2011**, *39*, 2558-2565, doi:10.1177/0363546511423369.

30. Müller, P.E.; Gallik, D.; Hammerschmid, F.; Baur-Melnyk, A.; Pietschmann, M.F.; Zhang, A.; Niethammer, T.R. Third-generation autologous chondrocyte implantation after failed bone marrow stimulation leads to inferior clinical results. *Knee Surg Sports Traumatol Arthrosc* **2020**, *28*, 470-477, doi:10.1007/s00167-019-05661-6.

31.   Matricali, G.A.; Dereymaeker, G.P.; Luyten, F.P. Donor site morbidity after articular cartilage repair procedures: a review. *Acta Orthop Belg* **2010**, *76*, 669-674.

32.   Benya, P.D.; Shaffer, J.D. Dedifferentiated chondrocytes reexpress the differentiated collagen phenotype when cultured in agarose gels. *Cell* **1982**, *30*, 215-224, doi:10.1016/0092-8674(82)90027-7.

33.   Schnabel, M.; Marlovits, S.; Eckhoff, G.; Fichtel, I.; Gotzen, L.; Vécsei, V.; Schlegel, J. Dedifferentiation-associated changes in morphology and gene expression in primary human articular chondrocytes in cell culture. *Osteoarthr Cartil* **2002**, *10*, 62-70, doi:10.1053/joca.2001.0482.

34.   Caron, M.M.; Emans, P.J.; Coolsen, M.M.; Voss, L.; Surtel, D.A.; Cremers, A.; van Rhijn, L.W.; Welting, T.J. Redifferentiation of dedifferentiated human articular chondrocytes: comparison of 2D and 3D cultures. *Osteoarthr Cartil* **2012**, *20*, 1170-1178, doi:10.1016/j.joca.2012.06.016.

35.   Johnstone, B.; Hering, T.M.; Caplan, A.I.; Goldberg, V.M.; Yoo, J.U. In vitro chondrogenesis of bone marrow-derived mesenchymal progenitor cells. *Exp Cell Res* **1998**, *238*, 265-272, doi:10.1006/excr.1997.3858.

36.   Johnstone, B.; Yoo, J.U. Autologous mesenchymal progenitor cells in articular cartilage repair. *Clin Orthop Relat Res* **1999**, *367 Suppl*, S156-162, doi:10.1097/00003086-199910001-00017.

37.   Pittenger, M.F.; Mackay, A.M.; Beck, S.C.; Jaiswal, R.K.; Douglas, R.; Mosca, J.D.; Moorman, M.A.; Simonetti, D.W.; Craig, S.; Marshak, D.R. Multilineage potential of adult human mesenchymal stem cells. *Science* **1999**, *284*, 143-147, doi:10.1126/science.284.5411.143.

38.   Confalonieri, D.; Schwab, A.; Walles, H.; Ehlicke, F. Advanced Therapy Medicinal Products: A Guide for Bone Marrow-derived MSC Application in Bone and Cartilage Tissue Engineering. *Tissue Eng Part B Rev* **2018**, *24*, 155-169, doi:10.1089/ten.TEB.2017.0305.

39.   Marquez-Curtis, L.A.; Janowska-Wieczorek, A.; McGann, L.E.; Elliott, J.A. Mesenchymal stromal cells derived from various tissues: Biological, clinical and cryopreservation aspects. *Cryobiology* **2015**, *71*, 181-197, doi:10.1016/j.cryobiol.2015.07.003.

40.   Dominici, M.; Le Blanc, K.; Mueller, I.; Slaper-Cortenbach, I.; Marini, F.; Krause, D.; Deans, R.; Keating, A.; Prockop, D.; Horwitz, E. Minimal criteria for defining multipotent mesenchymal stromal cells. The International Society for Cellular Therapy position statement. *Cytotherapy* **2006**, *8*, 315-317, doi:10.1080/14653240600855905.

41.   Shetty, A.A.; Kim, S.J.; Ahmed, S.; Trattnig, S.; Kim, S.A.; Jang, H.J. A cost-effective cell- and matrix-based minimally invasive single-stage chondroregenerative technique developed with validated vertical translation methodology. *Ann R Coll Surg Engl* **2018**, *100*, 240-246, doi:10.1308/rcsann.2017.0223.

42.   Gupta, P.K.; Chullikana, A.; Rengasamy, M.; Shetty, N.; Pandey, V.; Agarwal, V.; Wagh, S.Y.; Vellotare, P.K.; Damodaran, D.; Viswanathan, P.; Thej, C.; Balasubramanian, S.; Majumdar, A.S. Efficacy and safety of adult human bone marrow-derived, cultured, pooled, allogeneic mesenchymal stromal cells (Stempeucel®): preclinical and clinical trial in osteoarthritis of the knee joint. *Arthritis Res Ther* **2016**, *18*, 301, doi:10.1186/s13075-016-1195-7.

43.   Shapiro, S.A.; Kazmerchak, S.E.; Heckman, M.G.; Zubair, A.C.; O'Connor, M.I. A Prospective, Single-Blind, Placebo-Controlled Trial of Bone Marrow Aspirate Concentrate for Knee Osteoarthritis. *Am J Sports Med* **2017**, *45*, 82-90, doi:10.1177/0363546516662455.

44.   Lamo-Espinosa, J.M.; Mora, G.; Blanco, J.F.; Granero-Moltó, F.; Nuñez-Córdoba, J.M.; Sánchez-Echenique, C.; Bondía, J.M.; Aquerreta, J.D.; Andreu, E.J.; Ornilla, E.;

Villarón, E.M.; Valentí-Azcárate, A.; Sánchez-Guijo, F.; Del Cañizo, M.C.; Valentí-Nin, J.R.; Prósper, F. Intra-articular injection of two different doses of autologous bone marrow mesenchymal stem cells versus hyaluronic acid in the treatment of knee osteoarthritis: multicenter randomized controlled clinical trial (phase I/II). *J Transl Med* **2016**, *14*, 246, doi:10.1186/s12967-016-0998-2.

45. Soler, R.; Orozco, L.; Munar, A.; Huguet, M.; López, R.; Vives, J.; Coll, R.; Codinach, M.; Garcia-Lopez, J. Final results of a phase I-II trial using ex vivo expanded autologous Mesenchymal Stromal Cells for the treatment of osteoarthritis of the knee confirming safety and suggesting cartilage regeneration. *Knee* **2016**, *23*, 647-654, doi:10.1016/j.knee.2015.08.013.

46. Davatchi, F.; Sadeghi Abdollahi, B.; Mohyeddin, M.; Nikbin, B. Mesenchymal stem cell therapy for knee osteoarthritis: 5 years follow-up of three patients. *Int J Rheum Dis* **2016**, *19*, 219-225, doi:10.1111/1756-185x.12670.

47. Vega, A.; Martín-Ferrero, M.A.; Del Canto, F.; Alberca, M.; García, V.; Munar, A.; Orozco, L.; Soler, R.; Fuertes, J.J.; Huguet, M.; Sánchez, A.; García-Sancho, J. Treatment of Knee Osteoarthritis With Allogeneic Bone Marrow Mesenchymal Stem Cells: A Randomized Controlled Trial. *Transplantation* **2015**, *99*, 1681-1690, doi:10.1097/tp.0000000000000678.

48. Orozco, L.; Munar, A.; Soler, R.; Alberca, M.; Soler, F.; Huguet, M.; Sentís, J.; Sánchez, A.; García-Sancho, J. Treatment of knee osteoarthritis with autologous mesenchymal stem cells: a pilot study. *Transplantation* **2013**, *95*, 1535-1541, doi:10.1097/TP.0b013e318291a2da.

49. Pers, Y.M.; Rackwitz, L.; Ferreira, R.; Pullig, O.; Delfour, C.; Barry, F.; Sensebe, L.; Casteilla, L.; Fleury, S.; Bourin, P.; Noël, D.; Canovas, F.; Cyteval, C.; Lisignoli, G.; Schrauth, J.; Haddad, D.; Domergue, S.; Noeth, U.; Jorgensen, C. Adipose Mesenchymal Stromal Cell-Based Therapy for Severe Osteoarthritis of the Knee: A Phase I Dose-Escalation Trial. *Stem Cells Transl Med* **2016**, *5*, 847-856, doi:10.5966/sctm.2015-0245.

50. Fodor, P.B.; Paulseth, S.G. Adipose Derived Stromal Cell (ADSC) Injections for Pain Management of Osteoarthritis in the Human Knee Joint. *Aesthet Surg J* **2016**, *36*, 229-236, doi:10.1093/asj/sjv135.

51. Jo, C.H.; Lee, Y.G.; Shin, W.H.; Kim, H.; Chai, J.W.; Jeong, E.C.; Kim, J.E.; Shim, H.; Shin, J.S.; Shin, I.S.; Ra, J.C.; Oh, S.; Yoon, K.S. Intra-articular injection of mesenchymal stem cells for the treatment of osteoarthritis of the knee: a proof-of-concept clinical trial. *Stem Cells* **2014**, *32*, 1254-1266, doi:10.1002/stem.1634.

52. Emadedin, M.; Aghdami, N.; Taghiyar, L.; Fazeli, R.; Moghadasali, R.; Jahangir, S.; Farjad, R.; Baghaban Eslaminejad, M. Intra-articular injection of autologous mesenchymal stem cells in six patients with knee osteoarthritis. *Arch Iran Med* **2012**, *15*, 422-428.

53. Colombini, A.; Perucca Orfei, C.; Kouroupis, D.; Ragni, E.; De Luca, P.; ViganÒ, M.; Correa, D.; de Girolamo, L. Mesenchymal stem cells in the treatment of articular cartilage degeneration: New biological insights for an old-timer cell. *Cytotherapy* **2019**, *21*, 1179-1197, doi:10.1016/j.jcyt.2019.10.004.

54. Ha, C.W.; Park, Y.B.; Kim, S.H.; Lee, H.J. Intra-articular Mesenchymal Stem Cells in Osteoarthritis of the Knee: A Systematic Review of Clinical Outcomes and Evidence of Cartilage Repair. *Arthroscopy* **2019**, *35*, 277-288.e272, doi:10.1016/j.arthro.2018.07.028.

55. Im, G.I. Tissue Engineering in Osteoarthritis: Current Status and Prospect of Mesenchymal Stem Cell Therapy. *Biodrugs* **2018**, *32*, 183-192, doi:10.1007/s40259-018-0276-3.

56.   Zhang, R.; Ma, J.; Han, J.; Zhang, W.; Ma, J. Mesenchymal stem cell related therapies for cartilage lesions and osteoarthritis. *Am J Transl Res* **2019**, *11*, 6275-6289.

57.   Arshi, A.; Petrigliano, F.A.; Williams, R.J.; Jones, K.J. Stem Cell Treatment for Knee Articular Cartilage Defects and Osteoarthritis. *Curr Rev Musculoskelet Med* **2020**, *13*, 20-27, doi:10.1007/s12178-020-09598-z.

58.   Zhang, S.; Chu, W.C.; Lai, R.C.; Lim, S.K.; Hui, J.H.; Toh, W.S. Exosomes derived from human embryonic mesenchymal stem cells promote osteochondral regeneration. *Osteoarthr Cartil* **2016**, *24*, 2135-2140, doi:10.1016/j.joca.2016.06.022.

59.   Toh, W.S.; Lai, R.C.; Hui, J.H.P.; Lim, S.K. MSC exosome as a cell-free MSC therapy for cartilage regeneration: Implications for osteoarthritis treatment. *Semin Cell Dev Biol* **2017**, *67*, 56-64, doi:10.1016/j.semcdb.2016.11.008.

60.   Vonk, L.A.; van Dooremalen, S.F.J.; Liv, N.; Klumperman, J.; Coffer, P.J.; Saris, D.B.F.; Lorenowicz, M.J. Mesenchymal Stromal/stem Cell-derived Extracellular Vesicles Promote Human Cartilage Regeneration In Vitro. *Theranostics* **2018**, *8*, 906-920, doi:10.7150/thno.20746.

61.   Nejadnik, H.; Hui, J.H.; Feng Choong, E.P.; Tai, B.C.; Lee, E.H. Autologous bone marrow-derived mesenchymal stem cells versus autologous chondrocyte implantation: an observational cohort study. *Am J Sports Med* **2010**, *38*, 1110-1116, doi:10.1177/0363546509359067.

62.   Akgun, I.; Unlu, M.C.; Erdal, O.A.; Ogut, T.; Erturk, M.; Ovali, E.; Kantarci, F.; Caliskan, G.; Akgun, Y. Matrix-induced autologous mesenchymal stem cell implantation versus matrix-induced autologous chondrocyte implantation in the treatment of chondral defects of the knee: a 2-year randomized study. *Arch Orthop Trauma Surg* **2015**, *135*, 251-263, doi:10.1007/s00402-014-2136-z.

63.   Park, Y.-B.; Ha, C.-W.; Lee, C.-H.; Yoon, Y.C.; Park, Y.-G. Cartilage Regeneration in Osteoarthritic Patients by a Composite of Allogeneic Umbilical Cord Blood-Derived Mesenchymal Stem Cells and Hyaluronate Hydrogel: Results from a Clinical Trial for Safety and Proof-of-Concept with 7 Years of Extended Follow-Up. *Stem Cells Transl Med* **2017**, *6*, 613-621, doi:10.5966/sctm.2016-0157.

64.   Kuroda, R.; Ishida, K.; Matsumoto, T.; Akisue, T.; Fujioka, H.; Mizuno, K.; Ohgushi, H.; Wakitani, S.; Kurosaka, M. Treatment of a full-thickness articular cartilage defect in the femoral condyle of an athlete with autologous bone-marrow stromal cells. *Osteoarthr Cartil* **2007**, *15*, 226-231, doi:10.1016/j.joca.2006.08.008.

65.   Wakitani, S.; Nawata, M.; Tensho, K.; Okabe, T.; Machida, H.; Ohgushi, H. Repair of articular cartilage defects in the patello-femoral joint with autologous bone marrow mesenchymal cell transplantation: three case reports involving nine defects in five knees. *J Tissue Eng Regen Med* **2007**, *1*, 74-79, doi:10.1002/term.8.

66.   Haleem, A.M.; Singergy, A.A.; Sabry, D.; Atta, H.M.; Rashed, L.A.; Chu, C.R.; El Shewy, M.T.; Azzam, A.; Abdel Aziz, M.T. The Clinical Use of Human Culture-Expanded Autologous Bone Marrow Mesenchymal Stem Cells Transplanted on Platelet-Rich Fibrin Glue in the Treatment of Articular Cartilage Defects: A Pilot Study and Preliminary Results. *Cartilage* **2010**, *1*, 253-261, doi:10.1177/1947603510366027.

67.   Wakitani, S.; Mitsuoka, T.; Nakamura, N.; Toritsuka, Y.; Nakamura, Y.; Horibe, S. Autologous bone marrow stromal cell transplantation for repair of full-thickness articular cartilage defects in human patellae: two case reports. *Cell Transplant* **2004**, *13*, 595-600, doi:10.3727/000000004783983747.

68.   Wakitani, S.; Okabe, T.; Horibe, S.; Mitsuoka, T.; Saito, M.; Koyama, T.; Nawata, M.; Tensho, K.; Kato, H.; Uematsu, K.; Kuroda, R.; Kurosaka, M.; Yoshiya, S.; Hattori, K.; Ohgushi, H. Safety of autologous bone marrow-derived mesenchymal stem cell transplantation for cartilage repair in 41 patients with 45 joints followed for up to 11 years and 5 months. *J Tissue Eng Regen Med* **2011**, *5*, 146-150, doi:10.1002/term.299.

69. Koh, Y.G.; Choi, Y.J.; Kwon, O.R.; Kim, Y.S. Second-Look Arthroscopic Evaluation of Cartilage Lesions After Mesenchymal Stem Cell Implantation in Osteoarthritic Knees. *Am J Sports Med* **2014**, *42*, 1628-1637, doi:10.1177/0363546514529641.

70. Armiento, A.R.; Alini, M.; Stoddart, M.J. Articular fibrocartilage - Why does hyaline cartilage fail to repair? *Adv Drug Deliv Rev* **2019**, *146*, 289-305, doi:10.1016/j.addr.2018.12.015.

71. Pelttari, K.; Winter, A.; Steck, E.; Goetzke, K.; Hennig, T.; Ochs, B.G.; Aigner, T.; Richter, W. Premature induction of hypertrophy during in vitro chondrogenesis of human mesenchymal stem cells correlates with calcification and vascular invasion after ectopic transplantation in SCID mice. *Arthritis Rheum* **2006**, *54*, 3254-3266, doi:10.1002/art.22136.

72. Somoza, R.A.; Welter, J.F.; Correa, D.; Caplan, A.I. Chondrogenic differentiation of mesenchymal stem cells: challenges and unfulfilled expectations. *Tissue Eng Part B Rev* **2014**, *20*, 596-608, doi:10.1089/ten.TEB.2013.0771.

73. Studer, D.; Millan, C.; Öztürk, E.; Maniura-Weber, K.; Zenobi-Wong, M. Molecular and biophysical mechanisms regulating hypertrophic differentiation in chondrocytes and mesenchymal stem cells. *Eur Cell Mater* **2012**, *24*, 118-135; discussion 135, doi:10.22203/ecm.v024a09.

74. Mueller, M.B.; Tuan, R.S. Functional characterization of hypertrophy in chondrogenesis of human mesenchymal stem cells. *Arthritis Rheum* **2008**, *58*, 1377-1388, doi:10.1002/art.23370.

75. Fischer, J.; Dickhut, A.; Rickert, M.; Richter, W. Human articular chondrocytes secrete parathyroid hormone-related protein and inhibit hypertrophy of mesenchymal stem cells in coculture during chondrogenesis. *Arthritis Rheum* **2010**, *62*, 2696-2706, doi:10.1002/art.27565.

76. Cooke, M.E.; Allon, A.A.; Cheng, T.; Kuo, A.C.; Kim, H.T.; Vail, T.P.; Marcucio, R.S.; Schneider, R.A.; Lotz, J.C.; Alliston, T. Structured three-dimensional co-culture of mesenchymal stem cells with chondrocytes promotes chondrogenic differentiation without hypertrophy. *Osteoarthr Cartil* **2011**, *19*, 1210-1218, doi:10.1016/j.joca.2011.07.005.

77. Acharya, C.; Adesida, A.; Zajac, P.; Mumme, M.; Riesle, J.; Martin, I.; Barbero, A. Enhanced chondrocyte proliferation and mesenchymal stromal cells chondrogenesis in coculture pellets mediate improved cartilage formation. *J Cell Physiol* **2012**, *227*, 88-97, doi:10.1002/jcp.22706.

78. Bian, L.; Zhai, D.Y.; Mauck, R.L.; Burdick, J.A. Coculture of human mesenchymal stem cells and articular chondrocytes reduces hypertrophy and enhances functional properties of engineered cartilage. *Tissue Eng Part A* **2011**, *17*, 1137-1145, doi:10.1089/ten.TEA.2010.0531.

79. Sheehy, E.J.; Buckley, C.T.; Kelly, D.J. Oxygen tension regulates the osteogenic, chondrogenic and endochondral phenotype of bone marrow derived mesenchymal stem cells. *Biochem Biophys Res Commun* **2012**, *417*, 305-310, doi:10.1016/j.bbrc.2011.11.105.

80. Zhu, M.; Feng, Q.; Bian, L. Differential effect of hypoxia on human mesenchymal stem cell chondrogenesis and hypertrophy in hyaluronic acid hydrogels. *Acta Biomater* **2014**, *10*, 1333-1340, doi:10.1016/j.actbio.2013.12.015.

81. Leijten, J.; Georgi, N.; Moreira Teixeira, L.; van Blitterswijk, C.A.; Post, J.N.; Karperien, M. Metabolic programming of mesenchymal stromal cells by oxygen tension directs chondrogenic cell fate. *Proc Natl Acad Sci U S A* **2014**, *111*, 13954-13959, doi:10.1073/pnas.1410977111.

82. Gawlitta, D.; van Rijen, M.H.; Schrijver, E.J.; Alblas, J.; Dhert, W.J. Hypoxia impedes hypertrophic chondrogenesis of human multipotent stromal cells. *Tissue Eng Part A* **2012**, *18*, 1957-1966, doi:10.1089/ten.TEA.2011.0657.

83. Choi, K.H.; Choi, B.H.; Park, S.R.; Kim, B.J.; Min, B.H. The chondrogenic differentiation of mesenchymal stem cells on an extracellular matrix scaffold derived from porcine chondrocytes. *Biomaterials* **2010**, *31*, 5355-5365, doi:10.1016/j.biomaterials.2010.03.053.

84. Varghese, S.; Hwang, N.S.; Canver, A.C.; Theprungsirikul, P.; Lin, D.W.; Elisseeff, J. Chondroitin sulfate based niches for chondrogenic differentiation of mesenchymal stem cells. *Matrix Biol* **2008**, *27*, 12-21, doi:10.1016/j.matbio.2007.07.002.

85. Feng, Q.; Lin, S.; Zhang, K.; Dong, C.; Wu, T.; Huang, H.; Yan, X.; Zhang, L.; Li, G.; Bian, L. Sulfated hyaluronic acid hydrogels with retarded degradation and enhanced growth factor retention promote hMSC chondrogenesis and articular cartilage integrity with reduced hypertrophy. *Acta Biomater* **2017**, *53*, 329-342, doi:10.1016/j.actbio.2017.02.015.

86. Kim, Y.J.; Kim, H.J.; Im, G.I. PTHrP promotes chondrogenesis and suppresses hypertrophy from both bone marrow-derived and adipose tissue-derived MSCs. *Biochem Biophys Res Commun* **2008**, *373*, 104-108, doi:10.1016/j.bbrc.2008.05.183.

87. Kafienah, W.; Mistry, S.; Dickinson, S.C.; Sims, T.J.; Learmonth, I.; Hollander, A.P. Three-dimensional cartilage tissue engineering using adult stem cells from osteoarthritis patients. *Arthritis Rheum* **2007**, *56*, 177-187, doi:10.1002/art.22285.

88. Narcisi, R.; Cleary, M.A.; Brama, P.A.; Hoogduijn, M.J.; Tüysüz, N.; ten Berge, D.; van Osch, G.J. Long-term expansion, enhanced chondrogenic potential, and suppression of endochondral ossification of adult human MSCs via WNT signaling modulation. *Stem Cell Rep* **2015**, *4*, 459-472, doi:10.1016/j.stemcr.2015.01.017.

89. Deng, Y.; Lei, G.; Lin, Z.; Yang, Y.; Lin, H.; Tuan, R.S. Engineering hyaline cartilage from mesenchymal stem cells with low hypertrophy potential via modulation of culture conditions and Wnt/β-catenin pathway. *Biomaterials* **2019**, *192*, 569-578, doi:10.1016/j.biomaterials.2018.11.036.

90. Yang, Y.; Liu, Y.; Lin, Z.; Shen, H.; Lucas, C.; Kuang, B.; Tuan, R.S.; Lin, H. Condensation-Driven Chondrogenesis of Human Mesenchymal Stem Cells within Their Own Extracellular Matrix: Formation of Cartilage with Low Hypertrophy and Physiologically Relevant Mechanical Properties. *Adv Biosyst* **2019**, *3*, e1900229, doi:10.1002/adbi.201900229.

91. Castro-Viñuelas, R.; Sanjurjo-Rodríguez, C.; Piñeiro-Ramil, M.; Hermida-Gómez, T.; Fuentes-Boquete, I.M.; de Toro-Santos, F.J.; Blanco-García, F.J.; Díaz-Prado, S.M. Induced pluripotent stem cells for cartilage repair: current status and future perspectives. *Eur Cell Mater* **2018**, *36*, 96-109, doi:10.22203/eCM.v036a08.

92. Alsalameh, S.; Amin, R.; Gemba, T.; Lotz, M. Identification of mesenchymal progenitor cells in normal and osteoarthritic human articular cartilage. *Arthritis Rheum* **2004**, *50*, 1522-1532, doi:10.1002/art.20269.

93. Dowthwaite, G.P.; Bishop, J.C.; Redman, S.N.; Khan, I.M.; Rooney, P.; Evans, D.J.; Haughton, L.; Bayram, Z.; Boyer, S.; Thomson, B.; Wolfe, M.S.; Archer, C.W. The surface of articular cartilage contains a progenitor cell population. *J Cell Sci* **2004**, *117*, 889-897, doi:10.1242/jcs.00912.

94. Williams, R.; Khan, I.M.; Richardson, K.; Nelson, L.; McCarthy, H.E.; Analbelsi, T.; Singhrao, S.K.; Dowthwaite, G.P.; Jones, R.E.; Baird, D.M.; Lewis, H.; Roberts, S.; Shaw, H.M.; Dudhia, J.; Fairclough, J.; Briggs, T.; Archer, C.W. Identification and clonal characterisation of a progenitor cell sub-population in normal human articular cartilage. *PLoS One* **2010**, *5*, e13246, doi:10.1371/journal.pone.0013246.

95.   Majumdar, M.K.; Thiede, M.A.; Mosca, J.D.; Moorman, M.; Gerson, S.L. Phenotypic and functional comparison of cultures of marrow-derived mesenchymal stem cells (MSCs) and stromal cells. *J Cell Physiol* **1998**, *176*, 57-66, doi:10.1002/(sici)1097-4652(199807)176:1<57::Aid-jcp7>3.0.Co;2-7.

96.   Koelling, S.; Kruegel, J.; Irmer, M.; Path, J.R.; Sadowski, B.; Miro, X.; Miosge, N. Migratory chondrogenic progenitor cells from repair tissue during the later stages of human osteoarthritis. *Cell Stem Cell* **2009**, *4*, 324-335, doi:10.1016/j.stem.2009.01.015.

97.   Fickert, S.; Fiedler, J.; Brenner, R.E. Identification of subpopulations with characteristics of mesenchymal progenitor cells from human osteoarthritic cartilage using triple staining for cell surface markers. *Arthritis Res Ther* **2004**, *6*, R422-432, doi:10.1186/ar1210.

98.   Jiang, Y.; Cai, Y.; Zhang, W.; Yin, Z.; Hu, C.; Tong, T.; Lu, P.; Zhang, S.; Neculai, D.; Tuan, R.S.; Ouyang, H.W. Human Cartilage-Derived Progenitor Cells From Committed Chondrocytes for Efficient Cartilage Repair and Regeneration. *Stem Cells Transl Med* **2016**, *5*, 733-744, doi:10.5966/sctm.2015-0192.

99.   Yu, Y.; Zheng, H.; Buckwalter, J.A.; Martin, J.A. Single cell sorting identifies progenitor cell population from full thickness bovine articular cartilage. *Osteoarthr Cartil* **2014**, *22*, 1318-1326, doi:10.1016/j.joca.2014.07.002.

100.   Nelson, L.; McCarthy, H.E.; Fairclough, J.; Williams, R.; Archer, C.W. Evidence of a Viable Pool of Stem Cells within Human Osteoarthritic Cartilage. *Cartilage* **2014**, *5*, 203-214, doi:10.1177/1947603514544953.

101.   Khan, I.M.; Bishop, J.C.; Gilbert, S.; Archer, C.W. Clonal chondroprogenitors maintain telomerase activity and Sox9 expression during extended monolayer culture and retain chondrogenic potential. *Osteoarthr Cartil* **2009**, *17*, 518-528, doi:10.1016/j.joca.2008.08.002.

102.   McCarthy, H.E.; Bara, J.J.; Brakspear, K.; Singhrao, S.K.; Archer, C.W. The comparison of equine articular cartilage progenitor cells and bone marrow-derived stromal cells as potential cell sources for cartilage repair in the horse. *Vet J* **2012**, *192*, 345-351, doi:10.1016/j.tvjl.2011.08.036.

103.   Levato, R.; Webb, W.R.; Otto, I.A.; Mensinga, A.; Zhang, Y.; van Rijen, M.; van Weeren, R.; Khan, I.M.; Malda, J. The bio in the ink: cartilage regeneration with bioprintable hydrogels and articular cartilage-derived progenitor cells. *Acta Biomater* **2017**, *61*, 41-53, doi:10.1016/j.actbio.2017.08.005.

104.   Frisbie, D.D.; McCarthy, H.E.; Archer, C.W.; Barrett, M.F.; McIlwraith, C.W. Evaluation of articular cartilage progenitor cells for the repair of articular defects in an equine model. *J Bone Joint Surg Am* **2015**, *97*, 484-493, doi:10.2106/jbjs.N.00404.

105.   Xue, K.; Zhang, X.; Gao, Z.; Xia, W.; Qi, L.; Liu, K. Cartilage progenitor cells combined with PHBV in cartilage tissue engineering. *J Transl Med* **2019**, *17*, 104, doi:10.1186/s12967-019-1855-x.

106.   Vinod, E.; James, J.V.; Sabareeswaran, A.; Amirtham, S.M.; Thomas, G.; Sathishkumar, S.; Ozbey, O.; Boopalan, P. Intraarticular injection of allogenic chondroprogenitors for treatment of osteoarthritis in rabbit knee model. *J Clin Orthop Trauma* **2019**, *10*, 16-23, doi:10.1016/j.jcot.2018.07.003.

107.   Mouser, V.H.M.; Levato, R.; Mensinga, A.; Dhert, W.J.A.; Gawlitta, D.; Malda, J. Bio-ink development for three-dimensional bioprinting of hetero-cellular cartilage constructs. *Connect Tissue Res* **2020**, *61*, 137-151, doi:10.1080/03008207.2018.1553960.

108.   Ortiz-Prado, E.; Dunn, J.F.; Vasconez, J.; Castillo, D.; Viscor, G. Partial pressure of oxygen in the human body: a general review. *Am J Blood Res* **2019**, *9*, 1-14.

109. Carreau, A.; El Hafny-Rahbi, B.; Matejuk, A.; Grillon, C.; Kieda, C. Why is the partial oxygen pressure of human tissues a crucial parameter? Small molecules and hypoxia. *J Cell Mol Med* **2011**, *15*, 1239-1253, doi:10.1111/j.1582-4934.2011.01258.x.

110. Lund-Olesen, K. Oxygen tension in synovial fluids. *Arthritis Rheum* **1970**, *13*, 769-776, doi:10.1002/art.1780130606.

111. Milner, P.I.; Fairfax, T.P.; Browning, J.A.; Wilkins, R.J.; Gibson, J.S. The effect of O2 tension on pH homeostasis in equine articular chondrocytes. *Arthritis Rheum* **2006**, *54*, 3523-3532, doi:10.1002/art.22209.

112. Zhou, S.; Cui, Z.; Urban, J.P. Factors influencing the oxygen concentration gradient from the synovial surface of articular cartilage to the cartilage-bone interface: a modeling study. *Arthritis Rheum* **2004**, *50*, 3915-3924, doi:10.1002/art.20675.

113. Lafont, J.E. Lack of oxygen in articular cartilage: consequences for chondrocyte biology. *Int J Exp Pathol* **2010**, *91*, 99-106, doi:10.1111/j.1365-2613.2010.00707.x.

114. Sun, X.; Wei, Y. The role of hypoxia-inducible factor in osteogenesis and chondrogenesis. *Cytotherapy* **2009**, *11*, 261-267, doi:10.1080/14653240902824765.

115. Thoms, B.L.; Dudek, K.A.; Lafont, J.E.; Murphy, C.L. Hypoxia promotes the production and inhibits the destruction of human articular cartilage. *Arthritis Rheum* **2013**, *65*, 1302-1312, doi:10.1002/art.37867.

116. Provot, S.; Schipani, E. Fetal growth plate: a developmental model of cellular adaptation to hypoxia. *Ann N Y Acad Sci* **2007**, *1117*, 26-39, doi:10.1196/annals.1402.076.

117. Lafont, J.E.; Talma, S.; Hopfgarten, C.; Murphy, C.L. Hypoxia promotes the differentiated human articular chondrocyte phenotype through SOX9-dependent and -independent pathways. *J Biol Chem* **2008**, *283*, 4778-4786, doi:10.1074/jbc.M707729200.

118. Lafont, J.E.; Talma, S.; Murphy, C.L. Hypoxia-inducible factor 2alpha is essential for hypoxic induction of the human articular chondrocyte phenotype. *Arthritis Rheum* **2007**, *56*, 3297-3306, doi:10.1002/art.22878.

119. Murphy, C.L.; Sambanis, A. Effect of oxygen tension and alginate encapsulation on restoration of the differentiated phenotype of passaged chondrocytes. *Tissue Eng* **2001**, *7*, 791-803, doi:10.1089/107632701753337735.

120. Ströbel, S.; Loparic, M.; Wendt, D.; Schenk, A.D.; Candrian, C.; Lindberg, R.L.; Moldovan, F.; Barbero, A.; Martin, I. Anabolic and catabolic responses of human articular chondrocytes to varying oxygen percentages. *Arthritis Res Ther* **2010**, *12*, R34, doi:10.1186/ar2942.

121. Markway, B.D.; Cho, H.; Johnstone, B. Hypoxia promotes redifferentiation and suppresses markers of hypertrophy and degeneration in both healthy and osteoarthritic chondrocytes. *Arthritis Res Ther* **2013**, *15*, R92, doi:10.1186/ar4272.

122. Pattappa, G.; Johnstone, B.; Zellner, J.; Docheva, D.; Angele, P. The Importance of Physioxia in Mesenchymal Stem Cell Chondrogenesis and the Mechanisms Controlling Its Response. *Int J Mol Sci* **2019**, *20*, 484, doi:10.3390/ijms20030484.

123. Pattappa, G.; Schewior, R.; Hofmeister, I.; Seja, J.; Zellner, J.; Johnstone, B.; Docheva, D.; Angele, P. Physioxia Has a Beneficial Effect on Cartilage Matrix Production in Interleukin-1 Beta-Inhibited Mesenchymal Stem Cell Chondrogenesis. *Cells* **2019**, *8*, 936, doi:10.3390/cells8080936.

124. Bae, H.C.; Park, H.J.; Wang, S.Y.; Yang, H.R.; Lee, M.C.; Han, H.S. Hypoxic condition enhances chondrogenesis in synovium-derived mesenchymal stem cells. *Biomater Res* **2018**, *22*, 28, doi:10.1186/s40824-018-0134-x.

125. Portron, S.; Merceron, C.; Gauthier, O.; Lesoeur, J.; Sourice, S.; Masson, M.; Fellah, B.H.; Geffroy, O.; Lallemand, E.; Weiss, P.; Guicheux, J.; Vinatier, C. Effects of in vitro low oxygen tension preconditioning of adipose stromal cells on their in vivo

chondrogenic potential: application in cartilage tissue repair. *PLoS One* **2013**, *8*, e62368, doi:10.1371/journal.pone.0062368.

126. Khan, W.S.; Adesida, A.B.; Tew, S.R.; Lowe, E.T.; Hardingham, T.E. Bone marrow-derived mesenchymal stem cells express the pericyte marker 3G5 in culture and show enhanced chondrogenesis in hypoxic conditions. *J Orthop Res* **2010**, *28*, 834-840, doi:10.1002/jor.21043.

127. Adesida, A.B.; Mulet-Sierra, A.; Jomha, N.M. Hypoxia mediated isolation and expansion enhances the chondrogenic capacity of bone marrow mesenchymal stromal cells. *Stem Cell Res Ther* **2012**, *3*, 9, doi:10.1186/scrt100.

128. Rodenas-Rochina, J.; Kelly, D.J.; Gómez Ribelles, J.L.; Lebourg, M. Influence of oxygen levels on chondrogenesis of porcine mesenchymal stem cells cultured in polycaprolactone scaffolds. *J Biomed Mater Res A* **2017**, *105*, 1684-1691, doi:10.1002/jbm.a.36043.

129. Desancé, M.; Contentin, R.; Bertoni, L.; Gomez-Leduc, T.; Branly, T.; Jacquet, S.; Betsch, J.M.; Batho, A.; Legendre, F.; Audigié, F.; Galéra, P.; Demoor, M. Chondrogenic Differentiation of Defined Equine Mesenchymal Stem Cells Derived from Umbilical Cord Blood for Use in Cartilage Repair Therapy. *Int J Mol Sci* **2018**, *19*, 537, doi:10.3390/ijms19020537.

130. Portron, S.; Hivernaud, V.; Merceron, C.; Lesoeur, J.; Masson, M.; Gauthier, O.; Vinatier, C.; Beck, L.; Guicheux, J. Inverse regulation of early and late chondrogenic differentiation by oxygen tension provides cues for stem cell-based cartilage tissue engineering. *Cell Physiol Biochem* **2015**, *35*, 841-857, doi:10.1159/000369742.

131. Meretoja, V.V.; Dahlin, R.L.; Wright, S.; Kasper, F.K.; Mikos, A.G. The effect of hypoxia on the chondrogenic differentiation of co-cultured articular chondrocytes and mesenchymal stem cells in scaffolds. *Biomaterials* **2013**, *34*, 4266-4273, doi:10.1016/j.biomaterials.2013.02.064.

132. Merceron, C.; Vinatier, C.; Portron, S.; Masson, M.; Amiaud, J.; Guigand, L.; Chérel, Y.; Weiss, P.; Guicheux, J. Differential effects of hypoxia on osteochondrogenic potential of human adipose-derived stem cells. *Am J Physiol Cell Physiol* **2010**, *298*, C355-364, doi:10.1152/ajpcell.00398.2009.

133. Anderson, D.E.; Markway, B.D.; Bond, D.; McCarthy, H.E.; Johnstone, B. Responses to altered oxygen tension are distinct between human stem cells of high and low chondrogenic capacity. *Stem Cell Res Ther* **2016**, *7*, 154, doi:10.1186/s13287-016-0419-8.

134. Munir, S.; Foldager, C.B.; Lind, M.; Zachar, V.; Søballe, K.; Koch, T.G. Hypoxia enhances chondrogenic differentiation of human adipose tissue-derived stromal cells in scaffold-free and scaffold systems. *Cell Tissue Res* **2014**, *355*, 89-102, doi:10.1007/s00441-013-1732-5.

135. Quinn, T.M.; Häuselmann, H.J.; Shintani, N.; Hunziker, E.B. Cell and matrix morphology in articular cartilage from adult human knee and ankle joints suggests depth-associated adaptations to biomechanical and anatomical roles. *Osteoarthr Cartil* **2013**, *21*, 1904-1912, doi:10.1016/j.joca.2013.09.011.

136. Schuurman, W.; Klein, T.J.; Dhert, W.J.; van Weeren, P.R.; Hutmacher, D.W.; Malda, J. Cartilage regeneration using zonal chondrocyte subpopulations: a promising approach or an overcomplicated strategy? *J Tissue Eng Regen Med* **2015**, *9*, 669-678, doi:10.1002/term.1638.

137. Klein, T.J.; Malda, J.; Sah, R.L.; Hutmacher, D.W. Tissue engineering of articular cartilage with biomimetic zones. *Tissue Eng Part B Rev* **2009**, *15*, 143-157, doi:10.1089/ten.TEB.2008.0563.

138. Bothe, F.; Deubel, A.K.; Hesse, E.; Lotz, B.; Groll, J.; Werner, C.; Richter, W.; Hagmann, S. Treatment of Focal Cartilage Defects in Minipigs with Zonal

Chondrocyte/Mesenchymal Progenitor Cell Constructs. *Int J Mol Sci* **2019**, *20*, 653, doi:10.3390/ijms20030653.

139. Klein, T.J.; Schumacher, B.L.; Schmidt, T.A.; Li, K.W.; Voegtline, M.S.; Masuda, K.; Thonar, E.J.; Sah, R.L. Tissue engineering of stratified articular cartilage from chondrocyte subpopulations. *Osteoarthr Cartil* **2003**, *11*, 595-602, doi:10.1016/s1063-4584(03)00090-6.

140. Kim, T.K.; Sharma, B.; Williams, C.G.; Ruffner, M.A.; Malik, A.; McFarland, E.G.; Elisseeff, J.H. Experimental model for cartilage tissue engineering to regenerate the zonal organization of articular cartilage. *Osteoarthr Cartil* **2003**, *11*, 653-664, doi:10.1016/s1063-4584(03)00120-1.

141. Sharma, B.; Williams, C.G.; Kim, T.K.; Sun, D.; Malik, A.; Khan, M.; Leong, K.; Elisseeff, J.H. Designing zonal organization into tissue-engineered cartilage. *Tissue Eng* **2007**, *13*, 405-414, doi:10.1089/ten.2006.0068.

142. Ng, K.W.; Ateshian, G.A.; Hung, C.T. Zonal chondrocytes seeded in a layered agarose hydrogel create engineered cartilage with depth-dependent cellular and mechanical inhomogeneity. *Tissue Eng Part A* **2009**, *15*, 2315-2324, doi:10.1089/ten.tea.2008.0391.

143. Singh, M.; Berkland, C.; Detamore, M.S. Strategies and applications for incorporating physical and chemical signal gradients in tissue engineering. *Tissue Eng Part B Rev* **2008**, *14*, 341-366, doi:10.1089/ten.teb.2008.0304.

144. Singh, M.; Morris, C.P.; Ellis, R.J.; Detamore, M.S.; Berkland, C. Microsphere-based seamless scaffolds containing macroscopic gradients of encapsulated factors for tissue engineering. *Tissue Eng Part C Methods* **2008**, *14*, 299-309, doi:10.1089/ten.tec.2008.0167.

145. Woodfield, T.B.; Van Blitterswijk, C.A.; De Wijn, J.; Sims, T.J.; Hollander, A.P.; Riesle, J. Polymer scaffolds fabricated with pore-size gradients as a model for studying the zonal organization within tissue-engineered cartilage constructs. *Tissue Eng* **2005**, *11*, 1297-1311, doi:10.1089/ten.2005.11.1297.

146. Owida, H.A.; Yang, R.; Cen, L.; Kuiper, N.J.; Yang, Y. Induction of zonal-specific cellular morphology and matrix synthesis for biomimetic cartilage regeneration using hybrid scaffolds. *J R Soc Interface* **2018**, *15*, 20180310, doi:10.1098/rsif.2018.0310.

147. Cohen, D.L.; Lipton, J.I.; Bonassar, L.J.; Lipson, H. Additive manufacturing for in situ repair of osteochondral defects. *Biofabrication* **2010**, *2*, 035004, doi:10.1088/1758-5082/2/3/035004.

148. Fedorovich, N.E.; Schuurman, W.; Wijnberg, H.M.; Prins, H.J.; van Weeren, P.R.; Malda, J.; Alblas, J.; Dhert, W.J. Biofabrication of osteochondral tissue equivalents by printing topologically defined, cell-laden hydrogel scaffolds. *Tissue Eng Part C Methods* **2012**, *18*, 33-44, doi:10.1089/ten.TEC.2011.0060.

149. Schuurman, W.; Khristov, V.; Pot, M.W.; van Weeren, P.R.; Dhert, W.J.; Malda, J. Bioprinting of hybrid tissue constructs with tailorable mechanical properties. *Biofabrication* **2011**, *3*, 021001, doi:10.1088/1758-5082/3/2/021001.

150. Malda, J.; Visser, J.; Melchels, F.P.; Jüngst, T.; Hennink, W.E.; Dhert, W.J.; Groll, J.; Hutmacher, D.W. 25th anniversary article: Engineering hydrogels for biofabrication. *Adv Mater* **2013**, *25*, 5011-5028, doi:10.1002/adma.201302042.

151. Armiento, A.R.; Stoddart, M.J.; Alini, M.; Eglin, D. Biomaterials for articular cartilage tissue engineering: Learning from biology. *Acta Biomater* **2018**, *65*, 1-20, doi:10.1016/j.actbio.2017.11.021.

152. Zhang, L.; Hu, J.; Athanasiou, K.A. The role of tissue engineering in articular cartilage repair and regeneration. *Crit Rev Biomed Eng* **2009**, *37*, 1-57, doi:10.1615/critrevbiomedeng.v37.i1-2.10.

153. Wasyłeczko, M.; Sikorska, W.; Chwojnowski, A. Review of Synthetic and Hybrid Scaffolds in Cartilage Tissue Engineering. *Membranes (Basel)* **2020**, *10*, 348, doi:10.3390/membranes10110348.

154. Spiller, K.L.; Maher, S.A.; Lowman, A.M. Hydrogels for the repair of articular cartilage defects. *Tissue Eng Part B Rev* **2011**, *17*, 281-299, doi:10.1089/ten.TEB.2011.0077.

155. Benwood, C.; Chrenek, J.; Kirsch, R.L.; Masri, N.Z.; Richards, H.; Teetzen, K.; Willerth, S.M. Natural Biomaterials and Their Use as Bioinks for Printing Tissues. *Bioengineering (Basel)* **2021**, *8*, 27, doi:10.3390/bioengineering8020027.

156. Lee, K.Y.; Mooney, D.J. Alginate: properties and biomedical applications. *Prog Polym Sci* **2012**, *37*, 106-126, doi:10.1016/j.progpolymsci.2011.06.003.

157. Daly, A.C.; Critchley, S.E.; Rencsok, E.M.; Kelly, D.J. A comparison of different bioinks for 3D bioprinting of fibrocartilage and hyaline cartilage. *Biofabrication* **2016**, *8*, 045002, doi:10.1088/1758-5090/8/4/045002.

158. Rowley, J.A.; Madlambayan, G.; Mooney, D.J. Alginate hydrogels as synthetic extracellular matrix materials. *Biomaterials* **1999**, *20*, 45-53, doi:10.1016/s0142-9612(98)00107-0.

159. Nettles, D.L.; Elder, S.H.; Gilbert, J.A. Potential use of chitosan as a cell scaffold material for cartilage tissue engineering. *Tissue Eng* **2002**, *8*, 1009-1016, doi:10.1089/107632702320934100.

160. Sorushanova, A.; Delgado, L.M.; Wu, Z.; Shologu, N.; Kshirsagar, A.; Raghunath, R.; Mullen, A.M.; Bayon, Y.; Pandit, A.; Raghunath, M.; Zeugolis, D.I. The Collagen Suprafamily: From Biosynthesis to Advanced Biomaterial Development. *Adv Mater* **2019**, *31*, e1801651, doi:10.1002/adma.201801651.

161. Hospodiuk, M.; Dey, M.; Sosnoski, D.; Ozbolat, I.T. The bioink: A comprehensive review on bioprintable materials. *Biotechnol Adv* **2017**, *35*, 217-239, doi:10.1016/j.biotechadv.2016.12.006.

162. Kleinman, H.K.; Klebe, R.J.; Martin, G.R. Role of collagenous matrices in the adhesion and growth of cells. *J Cell Biol* **1981**, *88*, 473-485, doi:10.1083/jcb.88.3.473.

163. Zhou, F.; Zhang, X.; Cai, D.; Li, J.; Mu, Q.; Zhang, W.; Zhu, S.; Jiang, Y.; Shen, W.; Zhang, S.; Ouyang, H.W. Silk fibroin-chondroitin sulfate scaffold with immuno-inhibition property for articular cartilage repair. *Acta Biomater* **2017**, *63*, 64-75, doi:10.1016/j.actbio.2017.09.005.

164. Stichler, S.; Böck, T.; Paxton, N.; Bertlein, S.; Levato, R.; Schill, V.; Smolan, W.; Malda, J.; Teßmar, J.; Blunk, T.; Groll, J. Double printing of hyaluronic acid/poly(glycidol) hybrid hydrogels with poly(ε-caprolactone) for MSC chondrogenesis. *Biofabrication* **2017**, *9*, 044108, doi:10.1088/1758-5090/aa8cb7.

165. Chung, C.; Burdick, J.A. Influence of three-dimensional hyaluronic acid microenvironments on mesenchymal stem cell chondrogenesis. *Tissue Eng Part A* **2009**, *15*, 243-254, doi:10.1089/ten.tea.2008.0067.

166. Böck, T.; Schill, V.; Krähnke, M.; Steinert, A.F.; Tessmar, J.; Blunk, T.; Groll, J. TGF-β1-Modified Hyaluronic Acid/Poly(glycidol) Hydrogels for Chondrogenic Differentiation of Human Mesenchymal Stromal Cells. *Macromol Biosci* **2018**, *18*, e1700390, doi:10.1002/mabi.201700390.

167. Pina, S.; Ribeiro, V.P.; Marques, C.F.; Maia, F.R.; Silva, T.H.; Reis, R.L.; Oliveira, J.M. Scaffolding Strategies for Tissue Engineering and Regenerative Medicine Applications. *Materials (Basel)* **2019**, *12*, 1824, doi:10.3390/ma12111824.

168. McCall, J.D.; Luoma, J.E.; Anseth, K.S. Covalently tethered transforming growth factor beta in PEG hydrogels promotes chondrogenic differentiation of encapsulated human mesenchymal stem cells. *Drug Deliv Transl Res* **2012**, *2*, 305-312, doi:10.1007/s13346-012-0090-2.

169. Hauptstein, J.; Böck, T.; Bartolf-Kopp, M.; Forster, L.; Stahlhut, P.; Nadernezhad, A.; Blahetek, G.; Zernecke-Madsen, A.; Detsch, R.; Jüngst, T.; Groll, J.; Teßmar, J.; Blunk, T. Hyaluronic Acid-Based Bioink Composition Enabling 3D Bioprinting and Improving Quality of Deposited Cartilaginous Extracellular Matrix. *Adv Healthc Mater* **2020**, *9*, e2000737, doi:10.1002/adhm.202000737.

170. Abatangelo, G.; Vindigni, V.; Avruscio, G.; Pandis, L.; Brun, P. Hyaluronic Acid: Redefining Its Role. *Cells* **2020**, *9*, 1743, doi:10.3390/cells9071743.

171. Fraser, J.R.; Laurent, T.C.; Laurent, U.B. Hyaluronan: its nature, distribution, functions and turnover. *J Intern Med* **1997**, *242*, 27-33, doi:10.1046/j.1365-2796.1997.00170.x.

172. Kogan, G.; Soltés, L.; Stern, R.; Gemeiner, P. Hyaluronic acid: a natural biopolymer with a broad range of biomedical and industrial applications. *Biotechnol Lett* **2007**, *29*, 17-25, doi:10.1007/s10529-006-9219-z.

173. Allison, D.D.; Grande-Allen, K.J. Review. Hyaluronan: a powerful tissue engineering tool. *Tissue Eng* **2006**, *12*, 2131-2140, doi:10.1089/ten.2006.12.2131.

174. Garantziotis, S.; Savani, R.C. Hyaluronan biology: A complex balancing act of structure, function, location and context. *Matrix Biol* **2019**, *78-79*, 1-10, doi:10.1016/j.matbio.2019.02.002.

175. Heldin, P.; Lin, C.Y.; Kolliopoulos, C.; Chen, Y.H.; Skandalis, S.S. Regulation of hyaluronan biosynthesis and clinical impact of excessive hyaluronan production. *Matrix Biol* **2019**, *78-79*, 100-117, doi:10.1016/j.matbio.2018.01.017.

176. Lokeshwar, V.B.; Selzer, M.G. Hyalurondiase: both a tumor promoter and suppressor. *Semin Cancer Biol* **2008**, *18*, 281-287, doi:10.1016/j.semcancer.2008.03.008.

177. Itano, N.; Sawai, T.; Yoshida, M.; Lenas, P.; Yamada, Y.; Imagawa, M.; Shinomura, T.; Hamaguchi, M.; Yoshida, Y.; Ohnuki, Y.; Miyauchi, S.; Spicer, A.P.; McDonald, J.A.; Kimata, K. Three isoforms of mammalian hyaluronan synthases have distinct enzymatic properties. *J Biol Chem* **1999**, *274*, 25085-25092, doi:10.1074/jbc.274.35.25085.

178. Vigetti, D.; Karousou, E.; Viola, M.; Deleonibus, S.; De Luca, G.; Passi, A. Hyaluronan: biosynthesis and signaling. *Biochim Biophys Acta* **2014**, *1840*, 2452-2459, doi:10.1016/j.bbagen.2014.02.001.

179. McCourt, P.A.; Hansen, B.; Svistuonov, D.; Johansson, S.; Longati, P.; Schledzewski, K.; Kzhyshkowska, J.; Goerdt, S.; Johansson, S.; Smedsrød, B. The liver sinusoidal endothelial cell hyaluronan receptor and its homolog, stabilin-1 - Their roles (known and unknown) in endocytosis. *Comp Hepatol* **2004**, *3 Suppl 1*, S24, doi:10.1186/1476-5926-2-s1-s24.

180. Litwiniuk, M.; Krejner, A.; Speyrer, M.S.; Gauto, A.R.; Grzela, T. Hyaluronic Acid in Inflammation and Tissue Regeneration. *Wounds* **2016**, *28*, 78-88.

181. McKee, C.M.; Penno, M.B.; Cowman, M.; Burdick, M.D.; Strieter, R.M.; Bao, C.; Noble, P.W. Hyaluronan (HA) fragments induce chemokine gene expression in alveolar macrophages. The role of HA size and CD44. *J Clin Invest* **1996**, *98*, 2403-2413, doi:10.1172/jci119054.

182. Tian, X.; Azpurua, J.; Hine, C.; Vaidya, A.; Myakishev-Rempel, M.; Ablaeva, J.; Mao, Z.; Nevo, E.; Gorbunova, V.; Seluanov, A. High-molecular-mass hyaluronan mediates the cancer resistance of the naked mole rat. *Nature* **2013**, *499*, 346-349, doi:10.1038/nature12234.

183. Cyphert, J.M.; Trempus, C.S.; Garantziotis, S. Size Matters: Molecular Weight Specificity of Hyaluronan Effects in Cell Biology. *Int J Cell Biol* **2015**, *2015*, 563818, doi:10.1155/2015/563818.

184. Auvinen, P.; Tammi, R.; Kosma, V.M.; Sironen, R.; Soini, Y.; Mannermaa, A.; Tumelius, R.; Uljas, E.; Tammi, M. Increased hyaluronan content and stromal cell

CD44 associate with HER2 positivity and poor prognosis in human breast cancer. *Int J Cancer* **2013**, *132*, 531-539, doi:10.1002/ijc.27707.

185. Pirinen, R.; Tammi, R.; Tammi, M.; Hirvikoski, P.; Parkkinen, J.J.; Johansson, R.; Böhm, J.; Hollmén, S.; Kosma, V.M. Prognostic value of hyaluronan expression in non-small-cell lung cancer: Increased stromal expression indicates unfavorable outcome in patients with adenocarcinoma. *Int J Cancer* **2001**, *95*, 12-17, doi:10.1002/1097-0215(20010120)95:1<12::aid-ijc1002>3.0.co;2-e.

186. Liu, M.; Tolg, C.; Turley, E. Dissecting the Dual Nature of Hyaluronan in the Tumor Microenvironment. *Front Immunol* **2019**, *10*, 947, doi:10.3389/fimmu.2019.00947.

187. Knudson, C.B. Hyaluronan and CD44: strategic players for cell-matrix interactions during chondrogenesis and matrix assembly. *Birth Defects Res C Embryo Today* **2003**, *69*, 174-196, doi:10.1002/bdrc.10013.

188. Sherman, L.; Sleeman, J.; Herrlich, P.; Ponta, H. Hyaluronate receptors: key players in growth, differentiation, migration and tumor progression. *Curr Opin Cell Biol* **1994**, *6*, 726-733, doi:10.1016/0955-0674(94)90100-7.

189. Chen, C.; Zhao, S.; Karnad, A.; Freeman, J.W. The biology and role of CD44 in cancer progression: therapeutic implications. *J Hematol Oncol* **2018**, *11*, 64, doi:10.1186/s13045-018-0605-5.

190. Prochazka, L.; Tesarik, R.; Turanek, J. Regulation of alternative splicing of CD44 in cancer. *Cell Signal* **2014**, *26*, 2234-2239, doi:10.1016/j.cellsig.2014.07.011.

191. Knudson, C.B.; Knudson, W. Hyaluronan and CD44: modulators of chondrocyte metabolism. *Clin Orthop Relat Res* **2004**, S152-162.

192. Peterson, R.S.; Andhare, R.A.; Rousche, K.T.; Knudson, W.; Wang, W.; Grossfield, J.B.; Thomas, R.O.; Hollingsworth, R.E.; Knudson, C.B. CD44 modulates Smad1 activation in the BMP-7 signaling pathway. *J Cell Biol* **2004**, *166*, 1081-1091, doi:10.1083/jcb.200402138.

193. Toole, B.P. Hyaluronan: from extracellular glue to pericellular cue. *Nat Rev Cancer* **2004**, *4*, 528-539, doi:10.1038/nrc1391.

194. Turley, E.A.; Noble, P.W.; Bourguignon, L.Y. Signaling properties of hyaluronan receptors. *J Biol Chem* **2002**, *277*, 4589-4592, doi:10.1074/jbc.R100038200.

195. Telmer, P.G.; Tolg, C.; McCarthy, J.B.; Turley, E.A. How does a protein with dual mitotic spindle and extracellular matrix receptor functions affect tumor susceptibility and progression? *Commun Integr Biol* **2011**, *4*, 182-185, doi:10.4161/cib.4.2.14270.

196. Zhang, S.; Chang, M.C.; Zylka, D.; Turley, S.; Harrison, R.; Turley, E.A. The hyaluronan receptor RHAMM regulates extracellular-regulated kinase. *J Biol Chem* **1998**, *273*, 11342-11348, doi:10.1074/jbc.273.18.11342.

197. Hamilton, S.R.; Fard, S.F.; Paiwand, F.F.; Tolg, C.; Veiseh, M.; Wang, C.; McCarthy, J.B.; Bissell, M.J.; Koropatnick, J.; Turley, E.A. The hyaluronan receptors CD44 and Rhamm (CD168) form complexes with ERK1,2 that sustain high basal motility in breast cancer cells. *J Biol Chem* **2007**, *282*, 16667-16680, doi:10.1074/jbc.M702078200.

198. Burdick, J.A.; Prestwich, G.D. Hyaluronic acid hydrogels for biomedical applications. *Adv Mater* **2011**, *23*, H41-56, doi:10.1002/adma.201003963.

199. Halbleib, M.; Skurk, T.; de Luca, C.; von Heimburg, D.; Hauner, H. Tissue engineering of white adipose tissue using hyaluronic acid-based scaffolds. I: in vitro differentiation of human adipocyte precursor cells on scaffolds. *Biomaterials* **2003**, *24*, 3125-3132, doi:10.1016/s0142-9612(03)00156-x.

200. Prein, C.; Beier, F. ECM signaling in cartilage development and endochondral ossification. *Curr Top Dev Biol* **2019**, *133*, 25-47, doi:10.1016/bs.ctdb.2018.11.003.

201. Andhare, R.A.; Takahashi, N.; Knudson, W.; Knudson, C.B. Hyaluronan promotes the chondrocyte response to BMP-7. *Osteoarthr Cartil* **2009**, *17*, 906-916, doi:10.1016/j.joca.2008.12.007.

202. Luo, N.; Knudson, W.; Askew, E.B.; Veluci, R.; Knudson, C.B. CD44 and hyaluronan promote the bone morphogenetic protein 7 signaling response in murine chondrocytes. *Arthritis Rheumatol* **2014**, *66*, 1547-1558, doi:10.1002/art.38388.

203. Li, J.; Gorski, D.J.; Anemaet, W.; Velasco, J.; Takeuchi, J.; Sandy, J.D.; Plaas, A. Hyaluronan injection in murine osteoarthritis prevents TGFbeta 1-induced synovial neovascularization and fibrosis and maintains articular cartilage integrity by a CD44-dependent mechanism. *Arthritis Res Ther* **2012**, *14*, R151, doi:10.1186/ar3887.

204. Mariani, E.; Pulsatelli, L.; Facchini, A. Signaling pathways in cartilage repair. *Int J Mol Sci* **2014**, *15*, 8667-8698, doi:10.3390/ijms15058667.

205. Liu, J.; Li, Q.; Kuehn, M.R.; Litingtung, Y.; Vokes, S.A.; Chiang, C. Sonic hedgehog signaling directly targets Hyaluronic Acid Synthase 2, an essential regulator of phalangeal joint patterning. *Dev Biol* **2013**, *375*, 160-171, doi:10.1016/j.ydbio.2012.12.018.

206. Ongchai, S.; Somnoo, O.; Kongdang, P.; Peansukmanee, S.; Tangyuenyong, S. TGF-β1 upregulates the expression of hyaluronan synthase 2 and hyaluronan synthesis in culture models of equine articular chondrocytes. *J Vet Sci* **2018**, *19*, 735-743, doi:10.4142/jvs.2018.19.6.735.

207. Liu, R.-M.; Sun, R.-G.; Zhang, L.-T.; Zhang, Q.-F.; Chen, D.-X.; Zhong, J.-J.; Xiao, J.-H. Hyaluronic acid enhances proliferation of human amniotic mesenchymal stem cells through activation of Wnt/β-catenin signaling pathway. *Exp Cell Res* **2016**, *345*, 218-229, doi:10.1016/j.yexcr.2016.05.019.

208. Schmitt, M.; Metzger, M.; Gradl, D.; Davidson, G.; Orian-Rousseau, V. CD44 functions in Wnt signaling by regulating LRP6 localization and activation. *Cell Death Differ* **2015**, *22*, 677-689, doi:10.1038/cdd.2014.156.

209. Amann, E.; Wolff, P.; Breel, E.; van Griensven, M.; Balmayor, E.R. Hyaluronic acid facilitates chondrogenesis and matrix deposition of human adipose derived mesenchymal stem cells and human chondrocytes co-cultures. *Acta Biomater* **2017**, *52*, 130-144, doi:10.1016/j.actbio.2017.01.064.

210. Levett, P.A.; Hutmacher, D.W.; Malda, J.; Klein, T.J. Hyaluronic acid enhances the mechanical properties of tissue-engineered cartilage constructs. *PLoS One* **2014**, *9*, e113216, doi:10.1371/journal.pone.0113216.

211. Bian, L.; Guvendiren, M.; Mauck, R.L.; Burdick, J.A. Hydrogels that mimic developmentally relevant matrix and N-cadherin interactions enhance MSC chondrogenesis. *Proc Natl Acad Sci U S A* **2013**, *110*, 10117-10122, doi:10.1073/pnas.1214100110.

212. Chircov, C.; Grumezescu, A.M.; Bejenaru, L.E. Hyaluronic acid-based scaffolds for tissue engineering. *Rom J Morphol Embryol* **2018**, *59*, 71-76.

213. Highley, C.B.; Prestwich, G.D.; Burdick, J.A. Recent advances in hyaluronic acid hydrogels for biomedical applications. *Curr Opin Biotechnol* **2016**, *40*, 35-40, doi:10.1016/j.copbio.2016.02.008.

214. Noh, I.; Kim, N.; Tran, H.N.; Lee, J.; Lee, C. 3D printable hyaluronic acid-based hydrogel for its potential application as a bioink in tissue engineering. *Biomater Res* **2019**, *23*, 3, doi:10.1186/s40824-018-0152-8.

215. Antich, C.; de Vicente, J.; Jiménez, G.; Chocarro, C.; Carrillo, E.; Montañez, E.; Gálvez-Martín, P.; Marchal, J.A. Bio-inspired hydrogel composed of hyaluronic acid and alginate as a potential bioink for 3D bioprinting of articular cartilage engineering constructs. *Acta Biomater* **2020**, *106*, 114-123, doi:10.1016/j.actbio.2020.01.046.

216. Petta, D.; D'Amora, U.; Ambrosio, L.; Grijpma, D.W.; Eglin, D.; D'Este, M. Hyaluronic acid as a bioink for extrusion-based 3D printing. *Biofabrication* **2020**, *12*, 032001, doi:10.1088/1758-5090/ab8752.

217. Banerji, S.; Wright, A.J.; Noble, M.; Mahoney, D.J.; Campbell, I.D.; Day, A.J.; Jackson, D.G. Structures of the Cd44-hyaluronan complex provide insight into a fundamental carbohydrate-protein interaction. *Nat Struct Mol Biol* **2007**, *14*, 234-239, doi:10.1038/nsmb1201.

218. Bhattacharya, D.; Svechkarev, D.; Souchek, J.J.; Hill, T.K.; Taylor, M.A.; Natarajan, A.; Mohs, A.M. Impact of structurally modifying hyaluronic acid on CD44 interaction. *J Mater Chem B* **2017**, *5*, 8183-8192, doi:10.1039/c7tb01895a.

219. Kwon, M.Y.; Wang, C.; Galarraga, J.H.; Puré, E.; Han, L.; Burdick, J.A. Influence of hyaluronic acid modification on CD44 binding towards the design of hydrogel biomaterials. *Biomaterials* **2019**, *222*, 119451, doi:10.1016/j.biomaterials.2019.119451.

220. Laurent, T.C.; Laurent, U.B.; Fraser, J.R. The structure and function of hyaluronan: An overview. *Immunol Cell Biol* **1996**, *74*, A1-7, doi:10.1038/icb.1996.32.

221. Visser, J.; Gawlitta, D.; Benders, K.E.; Toma, S.M.; Pouran, B.; van Weeren, P.R.; Dhert, W.J.; Malda, J. Endochondral bone formation in gelatin methacrylamide hydrogel with embedded cartilage-derived matrix particles. *Biomaterials* **2015**, *37*, 174-182, doi:10.1016/j.biomaterials.2014.10.020.

222. Kim, Y.J.; Sah, R.L.; Doong, J.Y.; Grodzinsky, A.J. Fluorometric assay of DNA in cartilage explants using Hoechst 33258. *Anal Biochem* **1988**, *174*, 168-176, doi:10.1016/0003-2697(88)90532-5.

223. Farndale, R.W.; Buttle, D.J.; Barrett, A.J. Improved quantitation and discrimination of sulphated glycosaminoglycans by use of dimethylmethylene blue. *Biochim Biophys Acta* **1986**, *883*, 173-177, doi:10.1016/0304-4165(86)90306-5.

224. Woessner, J.F., Jr. The determination of hydroxyproline in tissue and protein samples containing small proportions of this imino acid. *Arch Biochem Biophys* **1961**, *93*, 440-447, doi:10.1016/0003-9861(61)90291-0.

225. Hollander, A.P.; Heathfield, T.F.; Webber, C.; Iwata, Y.; Bourne, R.; Rorabeck, C.; Poole, A.R. Increased damage to type II collagen in osteoarthritic articular cartilage detected by a new immunoassay. *J Clin Invest* **1994**, *93*, 1722-1732, doi:10.1172/jci117156.

226. Bessey, O.A.; Lowry, O.H.; Brock, M.J. A method for the rapid determination of alkaline phosphates with five cubic millimeters of serum. *J Biol Chem* **1946**, *164*, 321-329.

227. Hubka, K.M.; Dahlin, R.L.; Meretoja, V.V.; Kasper, F.K.; Mikos, A.G. Enhancing chondrogenic phenotype for cartilage tissue engineering: monoculture and coculture of articular chondrocytes and mesenchymal stem cells. *Tissue Eng Part B Rev* **2014**, *20*, 641-654, doi:10.1089/ten.TEB.2014.0034.

228. Schmidt, S.; Abinzano, F.; Mensinga, A.; Teßmar, J.; Groll, J.; Malda, J.; Levato, R.; Blunk, T. Differential Production of Cartilage ECM in 3D Agarose Constructs by Equine Articular Cartilage Progenitor Cells and Mesenchymal Stromal Cells. *Int J Mol Sci* **2020**, *21*, 7071, doi:10.3390/ijms21197071.

229. Lee, D.A.; Bader, D.L. The development and characterization of an in vitro system to study strain-induced cell deformation in isolated chondrocytes. *In Vitro Cell Dev Biol Anim* **1995**, *31*, 828-835, doi:10.1007/bf02634565.

230. Salati, M.A.; Khazai, J.; Tahmuri, A.M.; Samadi, A.; Taghizadeh, A.; Taghizadeh, M.; Zarrintaj, P.; Ramsey, J.D.; Habibzadeh, S.; Seidi, F.; Saeb, M.R.; Mozafari, M. Agarose-Based Biomaterials: Opportunities and Challenges in Cartilage Tissue Engineering. *Polymers (Basel)* **2020**, *12*, 1150, doi:10.3390/polym12051150.

231. Cigan, A.D.; Roach, B.L.; Nims, R.J.; Tan, A.R.; Albro, M.B.; Stoker, A.M.; Cook, J.L.; Vunjak-Novakovic, G.; Hung, C.T.; Ateshian, G.A. High seeding density of human chondrocytes in agarose produces tissue-engineered cartilage approaching native

mechanical and biochemical properties. *J Biomech* **2016**, *49*, 1909-1917, doi:10.1016/j.jbiomech.2016.04.039.

232. Anderson, D.E.; Markway, B.D.; Weekes, K.J.; McCarthy, H.E.; Johnstone, B. Physioxia Promotes the Articular Chondrocyte-Like Phenotype in Human Chondroprogenitor-Derived Self-Organized Tissue. *Tissue Eng Part A* **2018**, *24*, 264-274, doi:10.1089/ten.TEA.2016.0510.

233. Wu, L.; Leijten, J.C.; Georgi, N.; Post, J.N.; van Blitterswijk, C.A.; Karperien, M. Trophic effects of mesenchymal stem cells increase chondrocyte proliferation and matrix formation. *Tissue Eng Part A* **2011**, *17*, 1425-1436, doi:10.1089/ten.TEA.2010.0517.

234. Wu, L.; Leijten, J.; van Blitterswijk, C.A.; Karperien, M. Fibroblast growth factor-1 is a mesenchymal stromal cell-secreted factor stimulating proliferation of osteoarthritic chondrocytes in co-culture. *Stem Cells Dev* **2013**, *22*, 2356-2367, doi:10.1089/scd.2013.0118.

235. Liu, Y.; Lin, L.; Zou, R.; Wen, C.; Wang, Z.; Lin, F. MSC-derived exosomes promote proliferation and inhibit apoptosis of chondrocytes via lncRNA-KLF3-AS1/miR-206/GIT1 axis in osteoarthritis. *Cell Cycle* **2018**, *17*, 2411-2422, doi:10.1080/15384101.2018.1526603.

236. Luo, Y.; Sinkeviciute, D.; He, Y.; Karsdal, M.; Henrotin, Y.; Mobasheri, A.; Önnerfjord, P.; Bay-Jensen, A. The minor collagens in articular cartilage. *Protein Cell* **2017**, *8*, 560-572, doi:10.1007/s13238-017-0377-7.

237. Poole, C.A.; Ayad, S.; Schofield, J.R. Chondrons from articular cartilage: I. Immunolocalization of type VI collagen in the pericellular capsule of isolated canine tibial chondrons. *J Cell Sci* **1988**, *90 (Pt 4)*, 635-643.

238. Guilak, F.; Butler, D.L.; Goldstein, S.A. Functional tissue engineering: the role of biomechanics in articular cartilage repair. *Clin Orthop Relat Res* **2001**, *391 Suppl*, S295-305.

239. Roberts, S.; Menage, J.; Sandell, L.J.; Evans, E.H.; Richardson, J.B. Immunohistochemical study of collagen types I and II and procollagen IIA in human cartilage repair tissue following autologous chondrocyte implantation. *Knee* **2009**, *16*, 398-404, doi:10.1016/j.knee.2009.02.004.

240. Hale, J.E.; James Rudert, M.; Brown, T.D. Indentation assessment of biphasic mechanical property deficits in size-dependent osteochondral defect repair. *J Biomech* **1993**, *26*, 1319-1325, doi:10.1016/0021-9290(93)90355-i.

241. Nehrer, S.; Spector, M.; Minas, T. Histologic analysis of tissue after failed cartilage repair procedures. *Clin Orthop Relat Res* **1999**, *365*, 149-162, doi:10.1097/00003086-199908000-00020.

242. Kim, M.; Steinberg, D.R.; Burdick, J.A.; Mauck, R.L. Extracellular vesicles mediate improved functional outcomes in engineered cartilage produced from MSC/chondrocyte cocultures. *Proc Natl Acad Sci U S A* **2019**, *116*, 1569-1578, doi:10.1073/pnas.1815447116.

243. Zuo, Q.; Cui, W.; Liu, F.; Wang, Q.; Chen, Z.; Fan, W. Co-cultivated mesenchymal stem cells support chondrocytic differentiation of articular chondrocytes. *Int Orthop* **2013**, *37*, 747-752, doi:10.1007/s00264-013-1782-z.

244. Dengler, V.L.; Galbraith, M.; Espinosa, J.M. Transcriptional regulation by hypoxia inducible factors. *Crit Rev Biochem Mol Biol* **2014**, *49*, 1-15, doi:10.3109/10409238.2013.838205.

245. Yeung, H.Y.; Lai, K.P.; Chan, H.Y.; Mak, N.K.; Wagner, G.F.; Wong, C.K. Hypoxia-inducible factor-1-mediated activation of stanniocalcin-1 in human cancer cells. *Endocrinology* **2005**, *146*, 4951-4960, doi:10.1210/en.2005-0365.

246. Yuan, N.; Ge, Z.; Ji, W.; Li, J. Exosomes Secreted from Hypoxia-Preconditioned Mesenchymal Stem Cells Prevent Steroid-Induced Osteonecrosis of the Femoral Head by Promoting Angiogenesis in Rats. *Biomed Res Int* **2021**, *2021*, 6655225, doi:10.1155/2021/6655225.

247. Liu, W.; Li, L.; Rong, Y.; Qian, D.; Chen, J.; Zhou, Z.; Luo, Y.; Jiang, D.; Cheng, L.; Zhao, S.; Kong, F.; Wang, J.; Zhou, Z.; Xu, T.; Gong, F.; Huang, Y.; Gu, C.; Zhao, X.; Bai, J.; Wang, F.; Zhao, W.; Zhang, L.; Li, X.; Yin, G.; Fan, J.; Cai, W. Hypoxic mesenchymal stem cell-derived exosomes promote bone fracture healing by the transfer of miR-126. *Acta Biomater* **2020**, *103*, 196-212, doi:10.1016/j.actbio.2019.12.020.

248. Mancini, I.A.D.; Schmidt, S.; Brommer, H.; Pouran, B.; Schäfer, S.; Tessmar, J.; Mensinga, A.; van Rijen, M.H.P.; Groll, J.; Blunk, T.; Levato, R.; Malda, J.; van Weeren, P.R. A composite hydrogel-3D printed thermoplast osteochondral anchor as example for a zonal approach to cartilage repair: in vivo performance in a long-term equine model. *Biofabrication* **2020**, *12*, 035028, doi:10.1088/1758-5090/ab94ce.

249. Vainieri, M.L.; Lolli, A.; Kops, N.; D'Atri, D.; Eglin, D.; Yayon, A.; Alini, M.; Grad, S.; Sivasubramaniyan, K.; van Osch, G. Evaluation of biomimetic hyaluronic-based hydrogels with enhanced endogenous cell recruitment and cartilage matrix formation. *Acta Biomater* **2020**, *101*, 293-303, doi:10.1016/j.actbio.2019.11.015.

250. Richardson, B.M.; Wilcox, D.G.; Randolph, M.A.; Anseth, K.S. Hydrazone covalent adaptable networks modulate extracellular matrix deposition for cartilage tissue engineering. *Acta Biomater* **2019**, *83*, 71-82, doi:10.1016/j.actbio.2018.11.014.

251. Bryant, S.J.; Chowdhury, T.T.; Lee, D.A.; Bader, D.L.; Anseth, K.S. Crosslinking density influences chondrocyte metabolism in dynamically loaded photocrosslinked poly(ethylene glycol) hydrogels. *Ann Biomed Eng* **2004**, *32*, 407-417, doi:10.1023/b:abme.0000017535.00602.ca.

252. Erickson, I.E.; Huang, A.H.; Sengupta, S.; Kestle, S.; Burdick, J.A.; Mauck, R.L. Macromer density influences mesenchymal stem cell chondrogenesis and maturation in photocrosslinked hyaluronic acid hydrogels. *Osteoarthr Cartil* **2009**, *17*, 1639-1648, doi:10.1016/j.joca.2009.07.003.

253. Bian, L.; Hou, C.; Tous, E.; Rai, R.; Mauck, R.L.; Burdick, J.A. The influence of hyaluronic acid hydrogel crosslinking density and macromolecular diffusivity on human MSC chondrogenesis and hypertrophy. *Biomaterials* **2013**, *34*, 413-421, doi:10.1016/j.biomaterials.2012.09.052.

254. Mauck, R.L.; Yuan, X.; Tuan, R.S. Chondrogenic differentiation and functional maturation of bovine mesenchymal stem cells in long-term agarose culture. *Osteoarthr Cartil* **2006**, *14*, 179-189, doi:10.1016/j.joca.2005.09.002.

255. Huang, X.; Hou, Y.; Zhong, L.; Huang, D.; Qian, H.; Karperien, M.; Chen, W. Promoted Chondrogenesis of Cocultured Chondrocytes and Mesenchymal Stem Cells under Hypoxia Using In-situ Forming Degradable Hydrogel Scaffolds. *Biomacromolecules* **2018**, *19*, 94-102, doi:10.1021/acs.biomac.7b01271.

256. Richardson, S.M.; Kalamegam, G.; Pushparaj, P.N.; Matta, C.; Memic, A.; Khademhosseini, A.; Mobasheri, R.; Poletti, F.L.; Hoyland, J.A.; Mobasheri, A. Mesenchymal stem cells in regenerative medicine: Focus on articular cartilage and intervertebral disc regeneration. *Methods* **2016**, *99*, 69-80, doi:10.1016/j.ymeth.2015.09.015.

257. Decker, R.S. Articular cartilage and joint development from embryogenesis to adulthood. *Semin Cell Dev Biol* **2017**, *62*, 50-56, doi:10.1016/j.semcdb.2016.10.005.

258. Pfeifer, C.G.; Berner, A.; Koch, M.; Krutsch, W.; Kujat, R.; Angele, P.; Nerlich, M.; Zellner, J. Higher Ratios of Hyaluronic Acid Enhance Chondrogenic Differentiation of Human MSCs in a Hyaluronic Acid-Gelatin Composite Scaffold. *Materials (Basel)* **2016**, *9*, 381, doi:10.3390/ma9050381.

259. Meng, F.; He, A.; Zhang, Z.; Zhang, Z.; Lin, Z.; Yang, Z.; Long, Y.; Wu, G.; Kang, Y.; Liao, W. Chondrogenic differentiation of ATDC5 and hMSCs could be induced by a novel scaffold-tricalcium phosphate-collagen-hyaluronan without any exogenous growth factors in vitro. *J Biomed Mater Res A* **2014**, *102*, 2725-2735, doi:10.1002/jbm.a.34948.

260. Reppel, L.; Schiavi, J.; Charif, N.; Leger, L.; Yu, H.; Pinzano, A.; Henrionnet, C.; Stoltz, J.-F.; Bensoussan, D.; Huselstein, C. Chondrogenic induction of mesenchymal stromal/stem cells from Wharton's jelly embedded in alginate hydrogel and without added growth factor: an alternative stem cell source for cartilage tissue engineering. *Stem Cell Res Ther* **2015**, *6*, 260-260, doi:10.1186/s13287-015-0263-2.

261. Prè, E.D.; Conti, G.; Sbarbati, A. Hyaluronic Acid (HA) Scaffolds and Multipotent Stromal Cells (MSCs) in Regenerative Medicine. *Stem Cell Rev Rep* **2016**, *12*, 664-681, doi:10.1007/s12015-016-9684-2.

262. Erggelet, C.; Neumann, K.; Endres, M.; Haberstroh, K.; Sittinger, M.; Kaps, C. Regeneration of ovine articular cartilage defects by cell-free polymer-based implants. *Biomaterials* **2007**, *28*, 5570-5580, doi:10.1016/j.biomaterials.2007.09.005.

263. Hegewald, A.A.; Ringe, J.; Bartel, J.; Krüger, I.; Notter, M.; Barnewitz, D.; Kaps, C.; Sittinger, M. Hyaluronic acid and autologous synovial fluid induce chondrogenic differentiation of equine mesenchymal stem cells: a preliminary study. *Tissue Cell* **2004**, *36*, 431-438, doi:10.1016/j.tice.2004.07.003.

264. Monaco, G.; El Haj, A.J.; Alini, M.; Stoddart, M.J. Sodium Hyaluronate Supplemented Culture Media as a New hMSC Chondrogenic Differentiation Media-Model for in vitro/ex vivo Screening of Potential Cartilage Repair Therapies. *Front Bioeng Biotechnol* **2020**, *8*, 243, doi:10.3389/fbioe.2020.00243.

265. Akmal, M.; Singh, A.; Anand, A.; Kesani, A.; Aslam, N.; Goodship, A.; Bentley, G. The effects of hyaluronic acid on articular chondrocytes. *J Bone Joint Surg Br* **2005**, *87*, 1143-1149, doi:10.1302/0301-620x.87b8.15083.

266. Ehlers, E.M.; Behrens, P.; Wünsch, L.; Kühnel, W.; Russlies, M. Effects of hyaluronic acid on the morphology and proliferation of human chondrocytes in primary cell culture. *Ann Anat* **2001**, *183*, 13-17, doi:10.1016/s0940-9602(01)80007-8.

267. Kawasaki, K.; Ochi, M.; Uchio, Y.; Adachi, N.; Matsusaki, M. Hyaluronic acid enhances proliferation and chondroitin sulfate synthesis in cultured chondrocytes embedded in collagen gels. *J Cell Physiol* **1999**, *179*, 142-148, doi:10.1002/(sici)1097-4652(199905)179:2<142::Aid-jcp4>3.0.Co;2-q.

268. Patti, A.M.; Gabriele, A.; Vulcano, A.; Ramieri, M.T.; Della Rocca, C. Effect of hyaluronic acid on human chondrocyte cell lines from articular cartilage. *Tissue Cell* **2001**, *33*, 294-300, doi:10.1054/tice.2001.0178.

269. Chen, P.Y.; Huang, L.L.; Hsieh, H.J. Hyaluronan preserves the proliferation and differentiation potentials of long-term cultured murine adipose-derived stromal cells. *Biochem Biophys Res Commun* **2007**, *360*, 1-6, doi:10.1016/j.bbrc.2007.04.211.

270. Wong, T.Y.; Chang, C.H.; Yu, C.H.; Huang, L.L.H. Hyaluronan keeps mesenchymal stem cells quiescent and maintains the differentiation potential over time. *Aging Cell* **2017**, *16*, 451-460, doi:10.1111/acel.12567.

271. Solis, M.A.; Chen, Y.H.; Wong, T.Y.; Bittencourt, V.Z.; Lin, Y.C.; Huang, L.L. Hyaluronan regulates cell behavior: a potential niche matrix for stem cells. *Biochem Res Int* **2012**, *2012*, 346972, doi:10.1155/2012/346972.

272. Hall, C.L.; Turley, E.A. Hyaluronan: RHAMM mediated cell locomotion and signaling in tumorigenesis. *J Neurooncol* **1995**, *26*, 221-229, doi:10.1007/bf01052625.

273. Sneath, R.J.; Mangham, D.C. The normal structure and function of CD44 and its role in neoplasia. *Mol Pathol* **1998**, *51*, 191-200, doi:10.1136/mp.51.4.191.

274. Amati, E.; Perbellini, O.; Rotta, G.; Bernardi, M.; Chieregato, K.; Sella, S.; Rodeghiero, F.; Ruggeri, M.; Astori, G. High-throughput immunophenotypic characterization of bone marrow- and cord blood-derived mesenchymal stromal cells reveals common and differentially expressed markers: identification of angiotensin-converting enzyme (CD143) as a marker differentially expressed between adult and perinatal tissue sources. *Stem Cell Res Ther* **2018**, *9*, 10, doi:10.1186/s13287-017-0755-3.

275. Guest, D.J.; Ousey, J.C.; Smith, M.R. Defining the expression of marker genes in equine mesenchymal stromal cells. *Stem Cells Cloning: Adv Appl* **2008**, *1*, 1-9, doi:10.2147/sccaa.s3824.

276. Veréb, Z.; Mázló, A.; Szabó, A.; Póliska, S.; Kiss, A.; Litauszky, K.; Koncz, G.; Boda, Z.; Rajnavölgyi, É.; Bácsi, A. Vessel Wall-Derived Mesenchymal Stromal Cells Share Similar Differentiation Potential and Immunomodulatory Properties with Bone Marrow-Derived Stromal Cells. *Stem Cells Int* **2020**, *2020*, 8847038, doi:10.1155/2020/8847038.

277. Pályi-Krekk, Z.; Barok, M.; Kovács, T.; Saya, H.; Nagano, O.; Szöllosi, J.; Nagy, P. EGFR and ErbB2 are functionally coupled to CD44 and regulate shedding, internalization and motogenic effect of CD44. *Cancer Lett* **2008**, *263*, 231-242, doi:10.1016/j.canlet.2008.01.014.

278. Tammi, R.; Rilla, K.; Pienimaki, J.P.; MacCallum, D.K.; Hogg, M.; Luukkonen, M.; Hascall, V.C.; Tammi, M. Hyaluronan enters keratinocytes by a novel endocytic route for catabolism. *J Biol Chem* **2001**, *276*, 35111-35122, doi:10.1074/jbc.M103481200.

279. Janiszewska, M.; De Vito, C.; Le Bitoux, M.A.; Fusco, C.; Stamenkovic, I. Transportin regulates nuclear import of CD44. *J Biol Chem* **2010**, *285*, 30548-30557, doi:10.1074/jbc.M109.075838.

280. Okamoto, I.; Kawano, Y.; Murakami, D.; Sasayama, T.; Araki, N.; Miki, T.; Wong, A.J.; Saya, H. Proteolytic release of CD44 intracellular domain and its role in the CD44 signaling pathway. *J Cell Biol* **2001**, *155*, 755-762, doi:10.1083/jcb.200108159.

281. Maxwell, C.A.; McCarthy, J.; Turley, E. Cell-surface and mitotic-spindle RHAMM: moonlighting or dual oncogenic functions? *J Cell Sci* **2008**, *121*, 925-932, doi:10.1242/jcs.022038.

282. Gómez-Aristizábal, A.; Kim, K.P.; Viswanathan, S. A Systematic Study of the Effect of Different Molecular Weights of Hyaluronic Acid on Mesenchymal Stromal Cell-Mediated Immunomodulation. *PLoS One* **2016**, *11*, e0147868, doi:10.1371/journal.pone.0147868.

283. Yang, C.; Cao, M.; Liu, H.; He, Y.; Xu, J.; Du, Y.; Liu, Y.; Wang, W.; Cui, L.; Hu, J.; Gao, F. The high and low molecular weight forms of hyaluronan have distinct effects on CD44 clustering. *J Biol Chem* **2012**, *287*, 43094-43107, doi:10.1074/jbc.M112.349209.

284. Sohr, S.; Engeland, K. RHAMM is differentially expressed in the cell cycle and downregulated by the tumor suppressor p53. *Cell Cycle* **2008**, *7*, 3448-3460, doi:10.4161/cc.7.21.7014.

285. Lee, Y.; Arai, Y.; Ahn, J.; Kim, D.; Oh, S.; Kang, D.; Lee, H.; Moon, J.J.; Choi, B.; Lee, S.-H. Three-dimensional microenvironmental priming of human mesenchymal stem cells in hydrogels facilitates efficient and rapid retroviral gene transduction via accelerated cell cycle synchronization. *NPG Asia Materials* **2019**, *11*, 27, doi:10.1038/s41427-019-0127-9.

286. Bonab, M.M.; Alimoghaddam, K.; Talebian, F.; Ghaffari, S.H.; Ghavamzadeh, A.; Nikbin, B. Aging of mesenchymal stem cell in vitro. *BMC Cell Biol* **2006**, *7*, 14, doi:10.1186/1471-2121-7-14.

287. Kretlow, J.D.; Jin, Y.Q.; Liu, W.; Zhang, W.J.; Hong, T.H.; Zhou, G.; Baggett, L.S.; Mikos, A.G.; Cao, Y. Donor age and cell passage affects differentiation potential of

murine bone marrow-derived stem cells. *BMC Cell Biol* **2008**, *9*, 60, doi:10.1186/1471-2121-9-60.

288. Ksiazek, K. A comprehensive review on mesenchymal stem cell growth and senescence. *Rejuvenation Res* **2009**, *12*, 105-116, doi:10.1089/rej.2009.0830.

289. Melton, D.A.; Cowen, C. "Stemness": Definitions, Criteria, and Standards. In *Essentials of Stem Cell Biology (Second Edition)*, Lanza, R., Gearhart, J., Hogan, B., Melton, D., Pedersen, R., Thomas, E.D., Thomson, J., Wilmut, I., Eds. Academic Press: San Diego, **2009**; doi:10.1016/B978-0-12-374729-7.00083-4pp. xxiii-xxix.

290. Novak, D.; Hüser, L.; Elton, J.J.; Umansky, V.; Altevogt, P.; Utikal, J. SOX2 in development and cancer biology. *Semin Cancer Biol* **2020**, *67*, 74-82, doi:10.1016/j.semcancer.2019.08.007.

291. Riekstina, U.; Cakstina, I.; Parfejevs, V.; Hoogduijn, M.; Jankovskis, G.; Muiznieks, I.; Muceniece, R.; Ancans, J. Embryonic stem cell marker expression pattern in human mesenchymal stem cells derived from bone marrow, adipose tissue, heart and dermis. *Stem Cell Rev Rep* **2009**, *5*, 378-386, doi:10.1007/s12015-009-9094-9.

292. Boyer, L.A.; Lee, T.I.; Cole, M.F.; Johnstone, S.E.; Levine, S.S.; Zucker, J.P.; Guenther, M.G.; Kumar, R.M.; Murray, H.L.; Jenner, R.G.; Gifford, D.K.; Melton, D.A.; Jaenisch, R.; Young, R.A. Core transcriptional regulatory circuitry in human embryonic stem cells. *Cell* **2005**, *122*, 947-956, doi:10.1016/j.cell.2005.08.020.

293. Go, M.J.; Takenaka, C.; Ohgushi, H. Forced expression of Sox2 or Nanog in human bone marrow derived mesenchymal stem cells maintains their expansion and differentiation capabilities. *Exp Cell Res* **2008**, *314*, 1147-1154, doi:10.1016/j.yexcr.2007.11.021.

294. Han, S.-M.; Han, S.-H.; Coh, Y.-R.; Jang, G.; Chan Ra, J.; Kang, S.-K.; Lee, H.-W.; Youn, H.-Y. Enhanced proliferation and differentiation of Oct4- and Sox2-overexpressing human adipose tissue mesenchymal stem cells. *Exp Mol Med* **2014**, *46*, e101-e101, doi:10.1038/emm.2014.28.

295. Liu, T.M.; Wu, Y.N.; Guo, X.M.; Hui, J.H.; Lee, E.H.; Lim, B. Effects of ectopic Nanog and Oct4 overexpression on mesenchymal stem cells. *Stem Cells Dev* **2009**, *18*, 1013-1022, doi:10.1089/scd.2008.0335.

296. Asparuhova, M.B.; Chappuis, V.; Stähli, A.; Buser, D.; Sculean, A. Role of hyaluronan in regulating self-renewal and osteogenic differentiation of mesenchymal stromal cells and pre-osteoblasts. *Clin Oral Investig* **2020**, *24*, 3923-3937, doi:10.1007/s00784-020-03259-8.

297. Sakai, S.; Ohi, H.; Taya, M. Gelatin/Hyaluronic Acid Content in Hydrogels Obtained through Blue Light-Induced Gelation Affects Hydrogel Properties and Adipose Stem Cell Behaviors. *Biomolecules* **2019**, *9*, 342, doi:10.3390/biom9080342.

298. Kozhemyakina, E.; Lassar, A.B.; Zelzer, E. A pathway to bone: signaling molecules and transcription factors involved in chondrocyte development and maturation. *Development* **2015**, *142*, 817-831, doi:10.1242/dev.105536.

299. Lefebvre, V. Roles and regulation of SOX transcription factors in skeletogenesis. *Curr Top Dev Biol* **2019**, *133*, 171-193, doi:10.1016/bs.ctdb.2019.01.007.

300. Lefebvre, V.; Dvir-Ginzberg, M. SOX9 and the many facets of its regulation in the chondrocyte lineage. *Connect Tissue Res* **2017**, *58*, 2-14, doi:10.1080/03008207.2016.1183667.

301. Lefebvre, V.; Li, P.; de Crombrugghe, B. A new long form of Sox5 (L-Sox5), Sox6 and Sox9 are coexpressed in chondrogenesis and cooperatively activate the type II collagen gene. *EMBO J* **1998**, *17*, 5718-5733, doi:10.1093/emboj/17.19.5718.

302. Akiyama, H.; Chaboissier, M.C.; Martin, J.F.; Schedl, A.; de Crombrugghe, B. The transcription factor Sox9 has essential roles in successive steps of the chondrocyte

differentiation pathway and is required for expression of Sox5 and Sox6. *Genes Dev* **2002**, *16*, 2813-2828, doi:10.1101/gad.1017802.

303. Smits, P.; Li, P.; Mandel, J.; Zhang, Z.; Deng, J.M.; Behringer, R.R.; de Crombrugghe, B.; Lefebvre, V. The transcription factors L-Sox5 and Sox6 are essential for cartilage formation. *Dev Cell* **2001**, *1*, 277-290, doi:10.1016/s1534-5807(01)00003-x.

304. Ogawa, Y.; Takahashi, N.; Takemoto, T.; Nishiume, T.; Suzuki, M.; Ishiguro, N.; Kojima, T. Hyaluronan promotes TRPV4-induced chondrogenesis in ATDC5 cells. *PLoS One* **2019**, *14*, e0219492, doi:10.1371/journal.pone.0219492.

305. Wu, S.C.; Chen, C.H.; Wang, J.Y.; Lin, Y.S.; Chang, J.K.; Ho, M.L. Hyaluronan size alters chondrogenesis of adipose-derived stem cells via the CD44/ERK/SOX-9 pathway. *Acta Biomater* **2018**, *66*, 224-237, doi:10.1016/j.actbio.2017.11.025.

306. Liu, C.F.; Angelozzi, M.; Haseeb, A.; Lefebvre, V. SOX9 is dispensable for the initiation of epigenetic remodeling and the activation of marker genes at the onset of chondrogenesis. *Development* **2018**, *145*, doi:10.1242/dev.164459.

307. Amorim, S.; Martins, A.; Neves, N.M.; Reis, R.L.; Pires, R.A. Hyaluronic acid/poly-l-lysine bilayered silica nanoparticles enhance the osteogenic differentiation of human mesenchymal stem cells. *J Mater Chem B* **2014**, *2*, 6939-6946, doi:10.1039/C4TB01071J.

308. Huang, L.; Cheng, Y.Y.; Koo, P.L.; Lee, K.M.; Qin, L.; Cheng, J.C.; Kumta, S.M. The effect of hyaluronan on osteoblast proliferation and differentiation in rat calvarial-derived cell cultures. *J Biomed Mater Res A* **2003**, *66*, 880-884, doi:10.1002/jbm.a.10535.

309. Kawano, M.; Ariyoshi, W.; Iwanaga, K.; Okinaga, T.; Habu, M.; Yoshioka, I.; Tominaga, K.; Nishihara, T. Mechanism involved in enhancement of osteoblast differentiation by hyaluronic acid. *Biochemical and Biophysical Research Communications* **2011**, *405*, 575-580, doi:10.1016/j.bbrc.2011.01.071.

310. Zhao, N.; Wang, X.; Qin, L.; Guo, Z.; Li, D. Effect of molecular weight and concentration of hyaluronan on cell proliferation and osteogenic differentiation in vitro. *Biochem Biophys Res Commun* **2015**, *465*, 569-574, doi:10.1016/j.bbrc.2015.08.061.

311. Kaneko, K.; Higuchi, C.; Kunugiza, Y.; Yoshida, K.; Sakai, T.; Yoshikawa, H.; Nakata, K. Hyaluronan inhibits BMP-induced osteoblast differentiation. *FEBS Lett* **2015**, *589*, 447-454, doi:10.1016/j.febslet.2014.12.031.

312. Zou, L.; Zou, X.; Chen, L.; Li, H.; Mygind, T.; Kassem, M.; Bünger, C. Effect of hyaluronan on osteogenic differentiation of porcine bone marrow stromal cells in vitro. *J Orthop Res* **2008**, *26*, 713-720, doi:10.1002/jor.20539.

313. Zhai, P.; Peng, X.; Li, B.; Liu, Y.; Sun, H.; Li, X. The application of hyaluronic acid in bone regeneration. *Int J Biol Macromol* **2020**, *151*, 1224-1239, doi:10.1016/j.ijbiomac.2019.10.169.

314. Zhao, N.; Wang, X.; Qin, L.; Zhai, M.; Yuan, J.; Chen, J.; Li, D. Effect of hyaluronic acid in bone formation and its applications in dentistry. *J Biomed Mater Res A* **2016**, *104*, 1560-1569, doi:10.1002/jbm.a.35681.

315. Park, B.G.; Lee, C.W.; Park, J.W.; Cui, Y.; Park, Y.S.; Shin, W.S. Enzymatic fragments of hyaluronan inhibit adipocyte differentiation in 3T3-L1 pre-adipocytes. *Biochem Biophys Res Commun* **2015**, *467*, 623-628, doi:10.1016/j.bbrc.2015.10.104.

316. Park, B.G.; Park, Y.S.; Park, J.W.; Shin, E.; Shin, W.S. Anti-obesity potential of enzymatic fragments of hyaluronan on high-fat diet-induced obesity in C57BL/6 mice. *Biochem Biophys Res Commun* **2016**, *473*, 290-295, doi:10.1016/j.bbrc.2016.03.098.

317. Wilson, N.; Steadman, R.; Muller, I.; Draman, M.; Rees, D.A.; Taylor, P.; Dayan, C.M.; Ludgate, M.; Zhang, L. Role of Hyaluronan in Human Adipogenesis: Evidence from in-Vitro and in-Vivo Studies. *Int J Mol Sci* **2019**, *20*, 2675, doi:10.3390/ijms20112675.

318. Ji, E.; Jung, M.Y.; Park, J.H.; Kim, S.; Seo, C.R.; Park, K.W.; Lee, E.K.; Yeom, C.H.; Lee, S. Inhibition of adipogenesis in 3T3-L1 cells and suppression of abdominal fat accumulation in high-fat diet-feeding C57BL/6J mice after downregulation of hyaluronic acid. *Int J Obes (Lond)* **2014**, *38*, 1035-1043, doi:10.1038/ijo.2013.202.

319. Zhu, Y.; Kruglikov, I.L.; Akgul, Y.; Scherer, P.E. Hyaluronan in adipogenesis, adipose tissue physiology and systemic metabolism. *Matrix Biol* **2019**, *78-79*, 284-291, doi:10.1016/j.matbio.2018.02.012.

320. Bahrami, S.B.; Tolg, C.; Peart, T.; Symonette, C.; Veiseh, M.; Umoh, J.U.; Holdsworth, D.W.; McCarthy, J.B.; Luyt, L.G.; Bissell, M.J.; Yazdani, A.; Turley, E.A. Receptor for hyaluronan mediated motility (RHAMM/HMMR) is a novel target for promoting subcutaneous adipogenesis. *Integr Biol (Camb)* **2017**, *9*, 223-237, doi:10.1039/c7ib00002b.

321. Jensen, C.; Teng, Y. Is It Time to Start Transitioning From 2D to 3D Cell Culture? *Front Mol Biosci* **2020**, *7*, 33, doi:10.3389/fmolb.2020.00033.

322. Flynn, L.E.; Prestwich, G.D.; Semple, J.L.; Woodhouse, K.A. Proliferation and differentiation of adipose-derived stem cells on naturally derived scaffolds. *Biomaterials* **2008**, *29*, 1862-1871, doi:10.1016/j.biomaterials.2007.12.028.

323. Hemmrich, K.; Van de Sijpe, K.; Rhodes, N.P.; Hunt, J.A.; Di Bartolo, C.; Pallua, N.; Blondeel, P.; von Heimburg, D. Autologous in vivo adipose tissue engineering in hyaluronan-based gels--a pilot study. *J Surg Res* **2008**, *144*, 82-88, doi:10.1016/j.jss.2007.03.017.

Annex

A.1 List of Figures

A.2 List of Tables

A.3 List of Abbreviations

°C	Degree Celsius
2D	Two-dimensional
3D	Three-dimensional
ACAN	Gene of aggrecan
ACI	Autologous chondrocyte implantation
ACPC	Articular cartilage progenitor cell
Akt	Protein kinase B
ALP	Alkaline phosphatase
ANOVA	Analysis of variance
bFGF	Basic fibroblast growth factor
BMP	Bone morphogenic protein
BMSC	Bone marrow-derived stem/stromal cells
BSA	Bovine serum albumin
Ca^{2+}	Calcium/calcium ion
$CaCl_2$	Calcium chloride
Calcein-AM	Calcein acetoxymethyl ester
CD	Cluster of differentiation
CD44	Cluster of differentiation 44
CD168	Cluster of differentiation 168; see also HMMR or RHAMM
cDNA	Complementary deoxyribonucleic acid
CIAP	Calf intestinal alkaline phosphatase
cm	Centimetre
CO_2	Carbon dioxide
COL1A1	Gene of α1 chain of type I collagen
COL10A1	Gene of α1 chain of type X collagen
COL2A1	Gene of α1 chain of type II collagen
c-src	Cellular sarcoma tyrosine protein kinase
d	Day
dd	double distilled
DAB	Para-dimethylaminobenzaldehyde
DAPI	4′,6-diamidino-2-phenylindole
DMEM	Dulbecco's Modified Eagle´s Medium
DMEM/F12	Dulbecco's Modified Eagle´s Medium: Nutrient Mixture F-12
DMMB	Dimethylmethylene blue
DMSO	Dimethyl sulfoxide
DNA	Deoxyribonucleic acid
DPBS	Dulbecco´s phosphate buffered saline
ECM	Extracellular matrix
EDTA	Ethylenediaminetetraacetic acid
ErbB1,2	Erythroblastic leukemia viral oncogene B1,2; ErbB1: Epidermal growth factor receptor 1; ErbB2: Human epidermal growth factor receptor 2
ERK1/2	Extracellular signal-regulated kinase 1/2
ESC	Embryonic stem cell
FACS	Fluorescence activated cell sorting/scanning; flow cytometry
FAK	Focal adhesion kinase
FCS	Fetal calf serum
FITC	Fluorescein isothiocyanate
FMZ	Department for Functional Materials in Medicine and Dentistry

g	Gram
GAG	Glycosaminoglycan
GAPDH	Glyceraldehyde 3-phosphate dehydrogenase
GelMA	Gelatin methacryloyl
GLUT1	Glucose transporter 1
GPI	Glycosylphosphatidylinositol
h	Hour
HA	Hyaluronic acid
HAMA	Hyaluronic acid methacrylate
HARE	Hyaluronan receptor for endocytosis
HAS	Hyaluronan synthase
HA-SH	Thiol-modified hyaluronic acid
HCl	Hydrogen chloride
HEPES	4-(2-hydroxyethyl)-1-piperazineethanesulfonic acid
HIF	Hypoxia inducible factor
HLA-DR	Human leukocyte antigen-DR isotype
HMMR	Hyaluronan mediated motility receptor; see also CD168 or RHAMM
HPRT1	Hypoxanthine-guanine phosphoribosyltransferase
HRE	Hypoxia inducible factor responsive element
HRP	Horseradish peroxidase
Hsp90	Heat shock protein 90
HYAL	Hyaluronidase
Hz	Hertz
IHC	Immunohistochemistry
iPSC	Induced pluripotent stem cell
ITS	Insulin-Transferrin-Selenium
kDa	Kilodalton
kPa	Kilopascal
LYVE-1	Lymphatic vessel endothelial hyaluronan receptor 1
MACT	Matrix assisted chondrocyte transplantation
MAPK	Mitogen-activated protein kinase
MDa	Megadalton
MEK	Mitogen-activated protein kinase kinase; MAPKK
mg	Milligram
$MgCl_2$	Magnesium chloride
min	Minute
ml	Millilitre
mm	Millimetre
mM	Millimolar
MMP13	Matrix metalloproteinase 13
MPER	Mammalian protein extraction reagent
mRNA	Messenger ribonucleic acid
MSC	Mesenchymal stromal cells
MW	Molecular weight
µg	Microgram
µm	Micrometre
µM	Micromolar
NaCl	Sodium chloride
NEAA	Non-essential amino acids
NF-κB	Nuclear factor kappa-light-chain-enhancer of activated B cells
ng	Nanogram

nm	Nanometre
O_2	Oxygen
OA	Osteoarthritis
OAT	Osteochondral autograft transfer
OCA	Osteochondral allograft transfer
OCT4	Octamer binding transcription factor 4; see POU5F1
CXCL-12	C-X-C motif chemokine ligand 12
P	Passage
p.	Page
PACI	Particulate articular cartilage implantation
P(AGE-co-G)	Allyl-modified polyglycidol
PBE	Phosphate buffered extraction
PBS	Phosphate buffered saline
PCL	Polycaprolactone
PCR	Polymerase chain reaction
PDGFR	Platelet-derived growth factor receptor
PDK1	3-phosphoinositide-dependent protein kinase 1
PEG	Polyethylene glycol
PEGDA	Polyethylene glycol diacrylate
PG	Polyglycidol
PGK1	Phosphoglycerate kinase 1
pH	Potential of hydrogen
PI3K	Phosphatidylinositol 3-kinase
PKC	Protein kinase C
PLA	Polylactic acid
PLCε	Phospholipase C-ε
pNPP	p-nitrophenyl phosphate
POU5F1	POU class 5 homeobox 1; see OCT4
pp.	Pages
PPARG	Peroxisome proliferator-activated receptor gamma
PRG4	Proteoglycan 4
PS	Penicillin/streptomycin
qRT-PCR	Quantitative real-time polymerase chain reaction
Ras	Rat sarcoma
RAF1	Rapidly accelerated fibrosarcoma 1
RHAMM	Receptor for hyaluronan mediated motility; see also CD168 or HMMR
RNA	Ribonucleic acid
ROS	Reactive oxygen species
Rpm	Rounds per minute
RT	Room temperature
RUNX2	Runt-related transcription factor 2
sec	Second
SOX2	Sex determining region Y-box 2
SOX5	Sex determining region Y-box 5
SOX6	Sex determining region Y-box 6
SOX9	Sex determining region Y-box 9
SP7	SP7 transcription factor; osterix
STC1	Stanniocalcin 1
TEN	Tris-EDTA-NaCl
TGFβ	Transforming growth factor β
TLR2,4	Toll-like-receptor 2,4

TSG-6	Tumor necrosis factor-stimulated gene 6
U	Unit
UV	Ultraviolet
wt%	Weight percent
x g	Times gravity

A.4 Statement on Copyright and Self-plagiarism

The data presented in this thesis have been partially published in the International Journal for Molecular Sciences (IJMS) as an original article entitled "Differential Production of Cartilage ECM in 3D Agarose Constructs by Equine Articular Cartilage Progenitor Cells and Mesenchymal Stromal Cells" and in the journal Biofabrication as an original article entitled "A composite hydrogel-3D printed thermoplast osteochondral anchor as example for a zonal approach to cartilage repair: in vivo performance in a long-term equine model".

The original article "Differential Production of Cartilage ECM in 3D Agarose Constructs by Equine Articular Cartilage Progenitor Cells and Mesenchymal Stromal Cells" was published by MDPI (parent publisher of IJMS) under an open access Creative Commons CC BY 4.0 license and copyright was retained by the authors. Data and illustrations from this article were used in identical or modified form. I, Stefanie Schmidt, was mainly responsible for the production of all data and the preparation of all Figures that were reused from this original article.

In accordance with the regulations of the parent publisher of the journal Biofabrication, IOP Publishing, several Figures from the original article "A composite hydrogel-3D printed thermoplast osteochondral anchor as example for a zonal approach to cartilage repair: in vivo performance in a long-term equine model" were used in unmodified form. I, Stefanie Schmidt, was mainly responsible for the production of all data and the preparation of all Figures that were reused from this original article.

Schmidt, S.; Abinzano, F.; Mensinga, A.; Teßmar, J.; Groll, J.; Malda, J.; Levato, R.; Blunk, T. Differential Production of Cartilage ECM in 3D Agarose Constructs by Equine Articular Cartilage Progenitor Cells and Mesenchymal Stromal Cells. *Int J Mol Sci* **2020**, *21*, 7071, doi:10.3390/ijms21197071.

Mancini, I.A.D.; Schmidt, S.; Brommer, H.; Pouran, B.; Schäfer, S.; Tessmar, J.; Mensinga, A.; van Rijen, M.H.P.; Groll, J.; Blunk, T.; Levato, R.; Malda, J.; van Weeren, P.R. A composite hydrogel-3D printed thermoplast osteochondral anchor as example for a zonal approach to cartilage repair: in vivo performance in a long-term equine model. *Biofabrication* **2020**, *12*, 035028, doi:10.1088/1758-5090/ab94ce.

A.5 Affidavit

Affidavit

I hereby confirm that my thesis entitled "Cartilage Tissue Engineering – Comparison of Articular Cartilage Progenitor Cells and Mesenchymal Stromal Cells in Agarose and Hyaluronic Acid-Based Hydrogels" is the result of my own work. I did not receive any help or support from commercial consultants. All sources and / or materials applied are listed and specified in the thesis.

Furthermore, I confirm that this thesis has not yet been submitted as part of another examination process neither in identical nor in similar form.

Place, Date   Signature

Eidesstattliche Erklärung

Hiermit erkläre ich an Eides statt, die Dissertation „Tissue Engineering von Knorpel – Vergleich von Gelenkknorpel-Vorläuferzellen und mesenchymalen Stromazellen in Agarose- und Hyaluronsäure-basierten Hydrogelen" eigenständig, d.h. insbesondere selbständig und ohne Hilfe eines kommerziellen Promotionsberaters, angefertigt und keine anderen als die von mir angegebenen Quellen und Hilfsmittel verwendet zu haben.

Ich erkläre außerdem, dass die Dissertation weder in gleicher noch in ähnlicher Form bereits in einem anderen Prüfungsverfahren vorgelegen hat.

Ort, Datum   Unterschrift

A.6 Acknowledgement

A.7 Curriculum Vitae